AD-A079 864 MAGNETIC ANALYSIS CORP MOUNT VERNON NY F/G 19/1
FEASIBILITY STUDY ON THE USE OF LEAKAGE FLUX NDT METHODS FOR AU--ETC(U)
1979 E SPIERER, D BUGDEN, M LUPERO

UNCLASSIFIED NL

1 OF 2
AD A079864

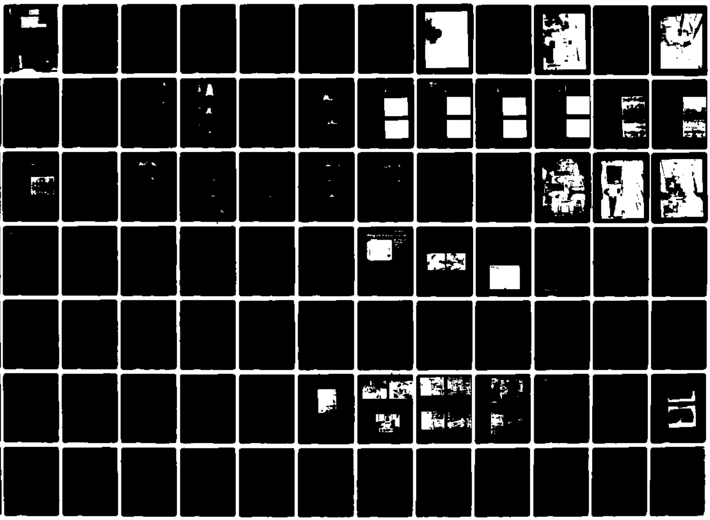

DISCLAIMER NOTICE

LEVEL II

11 1979 12 100

6

FEASIBILITY STUDY ON THE USE OF LEAKAGE FLUX NDT METHODS FOR AUTOMATIC INSPECTION OF M-42 GRENADE BODIES

By

10 Ed Spierer,
Donald Bugden
Mauro Lupero

Magnetic Analysis Corporation
Mt. Vernon, New York

"The view, opinions, and/or findings contained in this report are those of the authors and should not be construed as an official Department of the Army position, policy or decision, unless so designated by other documentation."

TABLE OF CONTENTS

		Page
List of Illustrations		iii
I.	Introduction	1
II.	Description of Method	2
III.	Description of Apparatus	4
	A. Instrumentation (Appendices II & III) and	4
	B. Mechanics	4
	1. Transverse Magnetization	6
	2. Longitudinal Magnetization	6
	C. Reference Specimens (Appendix V) and	6
IV.	Data Acquisition, Analysis and Results	10
	A. Experiments Conducted on Reference Specimens	11
	B. Tests Conducted on Natural Defects	25
V.	Discussion	25
VI.	Conceptual Design	31
VII.	Conclusions and Recommendations	36
	A. Summary of Results	36
	B. Conclusions	37
	C. Recommendations	37

LIST OF ILLUSTRATIONS

Figure		Page
1	M-42 Grenade Bodies	3
2	Instrumentation Used	5
3	Transverse Magnetization Mechanics	7
4	Rotoflux Signal Processing Diagram	8
5	Longitudinal Magnetization Mechanics	9
6	Oscillosgraph Recordings of Good Body Using Transverse Magnetization	12
7 - 16	System Response to Artificial Notches	13-24
17 - 21	System Response to Natural Defects	26-30
22	Rotoflux Machine	33
23	Heliflux Machine	34
24	Extruded Steel Part Being Tested Heliflux Machine	35

I. INTRODUCTION

The purpose of this program was to determine, by use of laboratory setups, the effectiveness of magnetic perturbation (leakage flux) techniques for locating and quantifying flaws in M-42 grenade bodies ~~(Figure 1)~~. Various magnetizing and scanning schemes were implemented in order to find surface and subsurface flaws with longitudinal or transverse orientations. Of special interest was the ability to find defects in the embossed area of the inner surface where there may be a higher probability of crack propogation. A side benefit is the possibility of ascertaining the presence and depth of the embossed area.

The evaluation setups were developed about a simple bench lathe, but the eventual design goal of providing an automatic, high speed nondestructive inspection system was an overriding consideration in the design of the experiments. Some of the conceptual options for developing a production machine are presented in a later section of this report.

The justification for these studies was based upon certain inherent advantages of the leakage flux method compared to options such as ultrasonic, eddy current, and magnetic particle inspection. These advantages are attractive for round, cylindrical parts fabricated of magnetic material, which must be interrogated over the various diameters of an irregular profile.

A. Although ultrasonic testing has better sensitivity than leakage flux to very small subsurface defects under ideal testing conditions, these advantages are obviated when problems such as unusual geometry, uneven surface conditions, and unpredictable defect location and orientation exist. There is also the limitation that the need to couple the ultrasound through a dense medium, and to provide proper transducer orientation and scanning, often renders ultrasonics a cumbersome method about which to build an automatic machine. Also, its dependence upon an intermittent (pulse-echo) format eventually limits scanning rates. In some cases, the need to work in a coupling medium (usually water) disqualifies the method because of the deleterious effect of the coupling medium upon the material being inspected.

B. In the case of the eddy current technique, the size and orientation of defects of interest in the M-42 grenade bodies, would dictate the use of probe type sensors. Encircling coils would not be able to find the defects of interest, especially considering the problem of separating them from the geometric variations in the part. On the other hand, state of the art eddy current probe coils are limited to detecting defects only in the surface close to them when applied to ferromagnetic material. They would not be able to find defects which did not extend to the inner or outer surface. In the case of loaded grenades, this limitation would prevent inspection of the inner surfaces to which there is no access. Furthermore, in the case of unloaded bodies the need to inspect the inner surfaces from the inside would impose difficult requirements on the design of an automatic machine. Finally, the influence of the embossing would prevent reliable crack detection in that area because of the superficial penetration of eddy currents generated by probe coils.

C. Although the magnetic particle technique depends upon the same basic phenomena, magnetic perturbation, as the leakage flux methods explored in this study, there are significant differences. Magnetic particle inspection basically assumes human intervention and is not easily adapted to an automatic machine. Of greater importance is the fact that electronic sensors and signal processing will detect defects which are not discerned with the particle method. This is especially true of internal defects. In fact, three grenade bodies which had been judged to be acceptable on the basis of magnetic particle inspection were found to have significant defects by the experimental leakage flux system described here. The magnetic particle technique is also weak in its inability to quantify defects.

The data which will be presented here seems to support the original premise that an automatic leakage flux inspection system would be well suited for the task of inspecting M-42 grenade bodies. It is also reasonable to broaden this judgment to include other components of artillery systems where the needs and circumstances of the inspection process are similar.

II. DESCRIPTION OF METHOD

The literature contains a great deal of theoretical and practical information on the subject of leakage flux, and an extensive bibliography is included in this report. A good portion of those efforts, and the successes derived, address the problems of inspection of components for artillery systems. A good basic description of the method is excerpted here from a previous study on the problem of inspecting 155 MM projectiles.

> The magnetic perturbation inspection method essentially consists of establishing a magnetic flux in a ferromagnetic material and then scanning the surface of the material with a sensitive magnetic probe to detect anomalies or perturbations caused in the flux by nonhomogeneities in ferromagnetic material. Figure 3 (see Appendix I) schematically illustrates this concept. Physically, this is a problem in magnetostatics and analyses of solutions have provided guidance for optimizing conditions and forecasting results. In the upper illustrations, flux is assumed to be directed from right to left, and computer plots of signatures obtained under these conditions from nonferromagnetic regions or flaws are shown in the two lower illustrations. The characteristic shape of the signatures are dependent on the magnetic field component which is sensed by the probe. For the upper signatures the probe is oriented to sense the component normal to the applied field and the scan is in the direction of the applied field. For the lower signatures the probe is oriented to sense the component in the direction of the applied field and the scan is in a direction

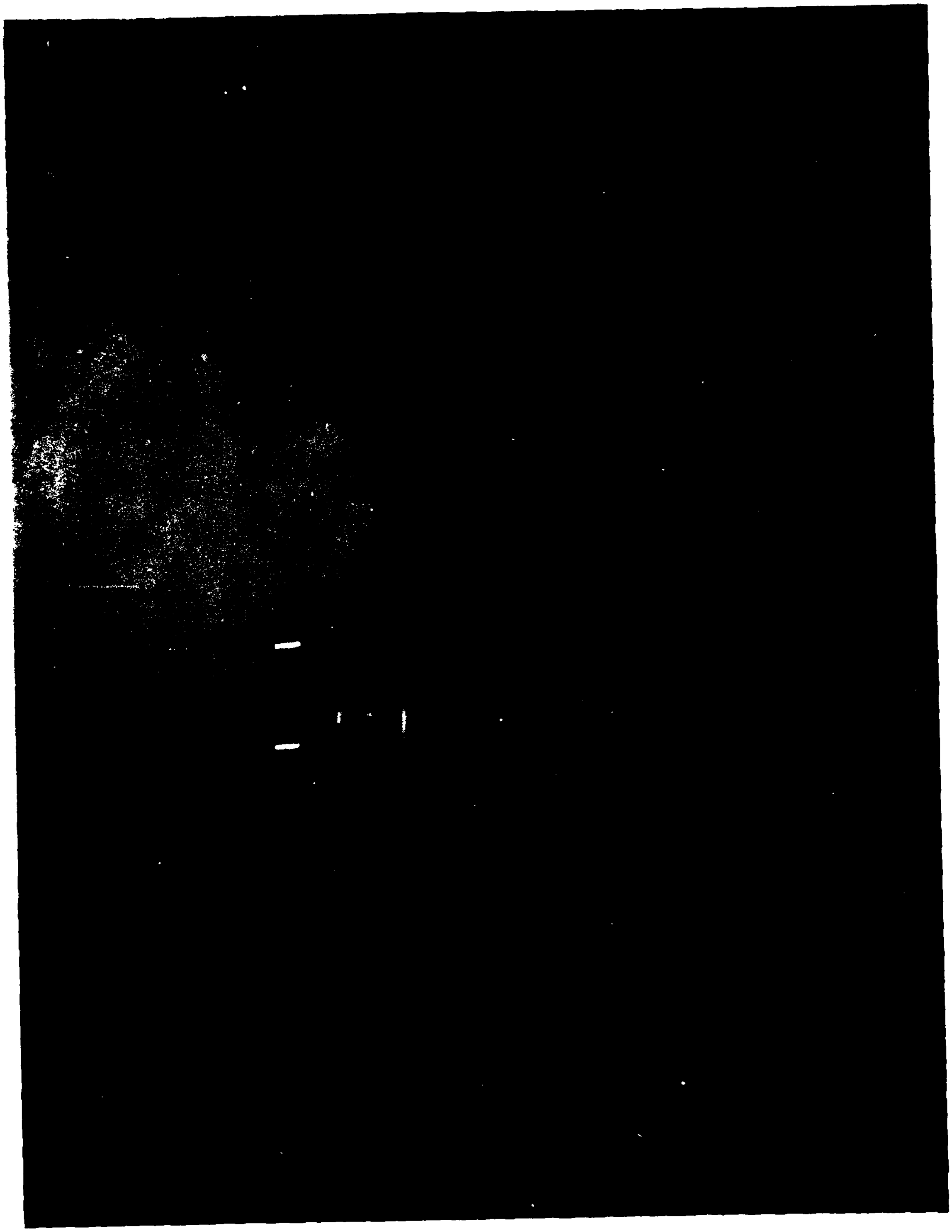

Figure 1

normal to the applied field. Other configurations are possible and selection is based on analysis of the specific inspection of interest.

Analysis of characteristic signatures provides considerable quantitative information concerning the perturbation source. For example, (in the upper signature of Figure 3 [Appendix I]), quantities that can be derived include:

a) flaw location - coincides with the zero crossing

b) flaw volume - indicated by peak-to-peak amplitude

c) flaw depth from surface - related to the peak-to-peak separation measured in the direction of the applied field

Extensive experimental results show general agreement with many details predicted by theory and also have confirmed that the method provides excellent qualitative and, after calibration, quantitative results.[1]

One important additional technique applied in this current study on the M-42 grenade bodies is separating defect signals on the basis of flaw signal frequency, which permits some degree of equalization of signals for defects of equal size located at different material depths.

III. DESCRIPTION OF APPARATUS

The apparatus used in this experiment can be divided into two general categories: instrumentation and mechanics.

A. Instrumentation

The instrumentation used was a stock item which is supplied by Magnetic Analysis as part of the Rotoflux and Heliflux Systems (see Figure 2). A brief description is provided in Appendix II while considerable detail is found in Appendix III. The reader is urged to study those two appendices. Recordings of the outputs of the O.D. and I.D. channels were made on a Sanborn Model 127 Oscillograph and are presented as part of the data.

B. Mechanics

The mechanical portions of the experimental set-ups were adapted specifically to the task of finding longitudinal and transverse notches or defects in the grenade bodies.

---

[1]Russell D. Williams and John R. Barton, Magnetic Perturbation Inspection of Artillery Projectiles, Report No. AMMRC CTR 77-23, Army Materials and Mechanics Research Center, Massachusetts, September 1977, p. 4.

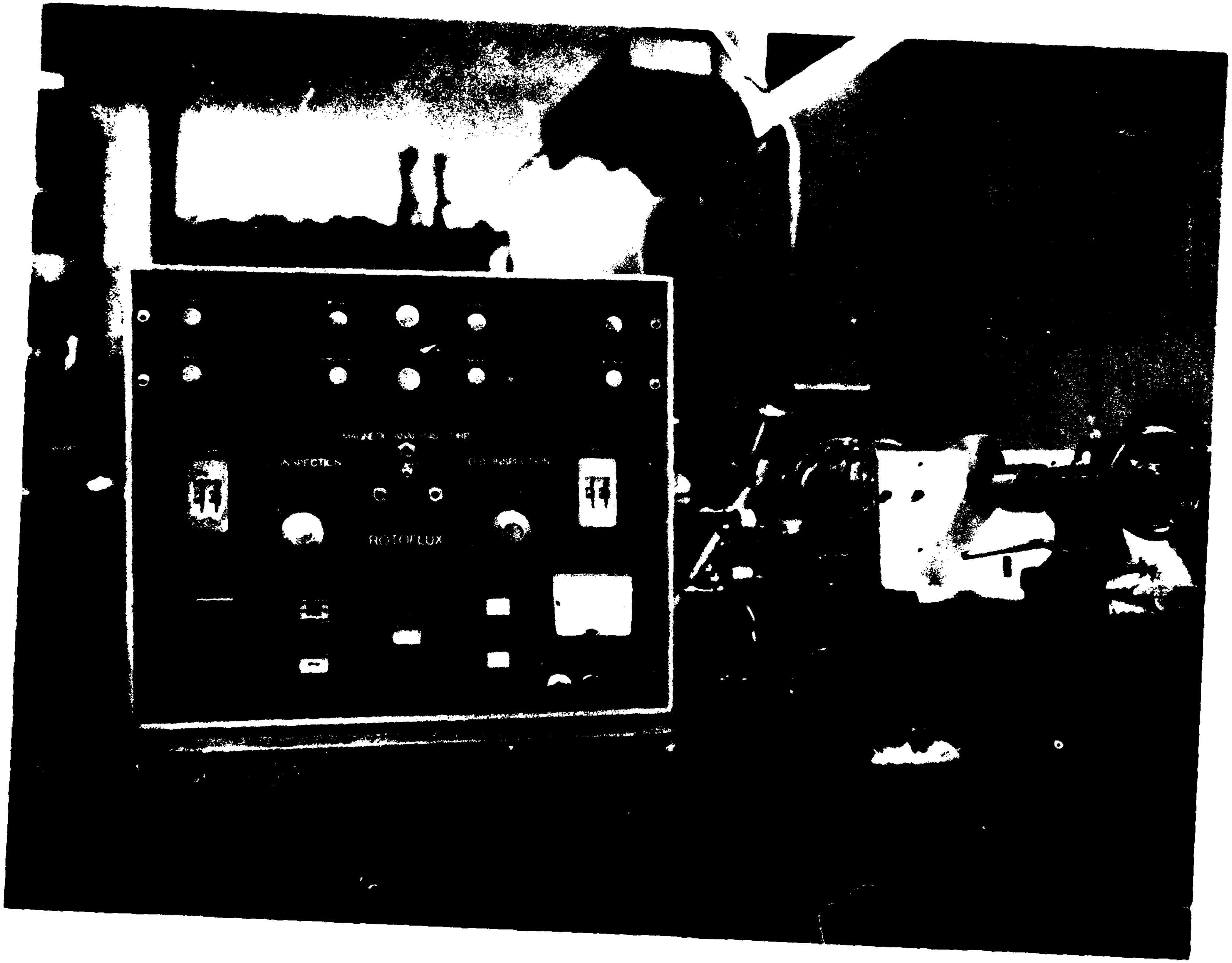

Figure 2

1. Transverse Magnetization - The detection of flaws or artificial notches which are generally in the longitudinal direction (parallel to the axis of the grenade body) was accomplished using transverse magnetization. Figure 3 shows the rig used for this evaluation.

Two horseshoe type permanent magnets are mounted in the lathe carriage. The fields of the two magnets are in opposition so that a resultant field is forced through the pole pieces across the cross-section of the grenade body. A wire coil induction type probe 1/8" in diameter is placed between the two pole pieces .020" off the surface of the grenade body. This type of sensor relies on cutting the lines of the leakage flux field produced by a defect during the rotation of the magnets and the probe in relation to the test piece. In this case the piece is rotated, but the option of rotating the te mechanism (magnetizing source and sensor) should be considered for the production machine. The amplitude of voltage generated by this cutting action, at some given rate, provides defect signals which are proportional to the size, orientation, and location of the defect. The frequency components of this signal is influenced by the material depth of the defect, and this phenomena is used in the system evaluated here to equalize defects of equivalent size which occur at varying material depths. This signal processing technique is shown in Figure 4.

The test piece was chucked in the lathe between a specially fabricated arbor and the tail stock center, and spun as the carriage mounted magnet and probe assembly traversed the skirt (larger diameter) of the grenade body. This action provides a helical scan at a rate dependent upon factors which will be discussed in the section on conceptual machine design.

2. Longitudinal Magnetization - Detection of flaws or artificial notches which are generally in the transverse direction (perpendicular to the axis of the grenade body) utilizes longitudinal magnetization. The rig used for this evaluation can be seen in Figure 5. A circular (toroidal) magnet is mounted on the tool bed carriage with a fixed wire coil induction type probe. The probe is oriented so as to be responsive to leakage flux in the axial direction (parallel to the axis of the grenade body), as would be produced by defects which are generally transverse.

The scanning of the piece is accomplished in the manner described for circumferential magnetization; and again, there are options to be considered in optimizing a production system which will be discussed later.

C. Reference Specimens

In order to provide a basis for calibrating the test system, and to approximate its response to natural defects of various size, orientation and location, a number of artificial reference notches and holes were introduced into sample pieces. The pieces which were notched were selected from approximately 100 pieces which had been subjected to magnetic particle inspection and judged to be free of significant defects. The pieces selected for notching were ones which

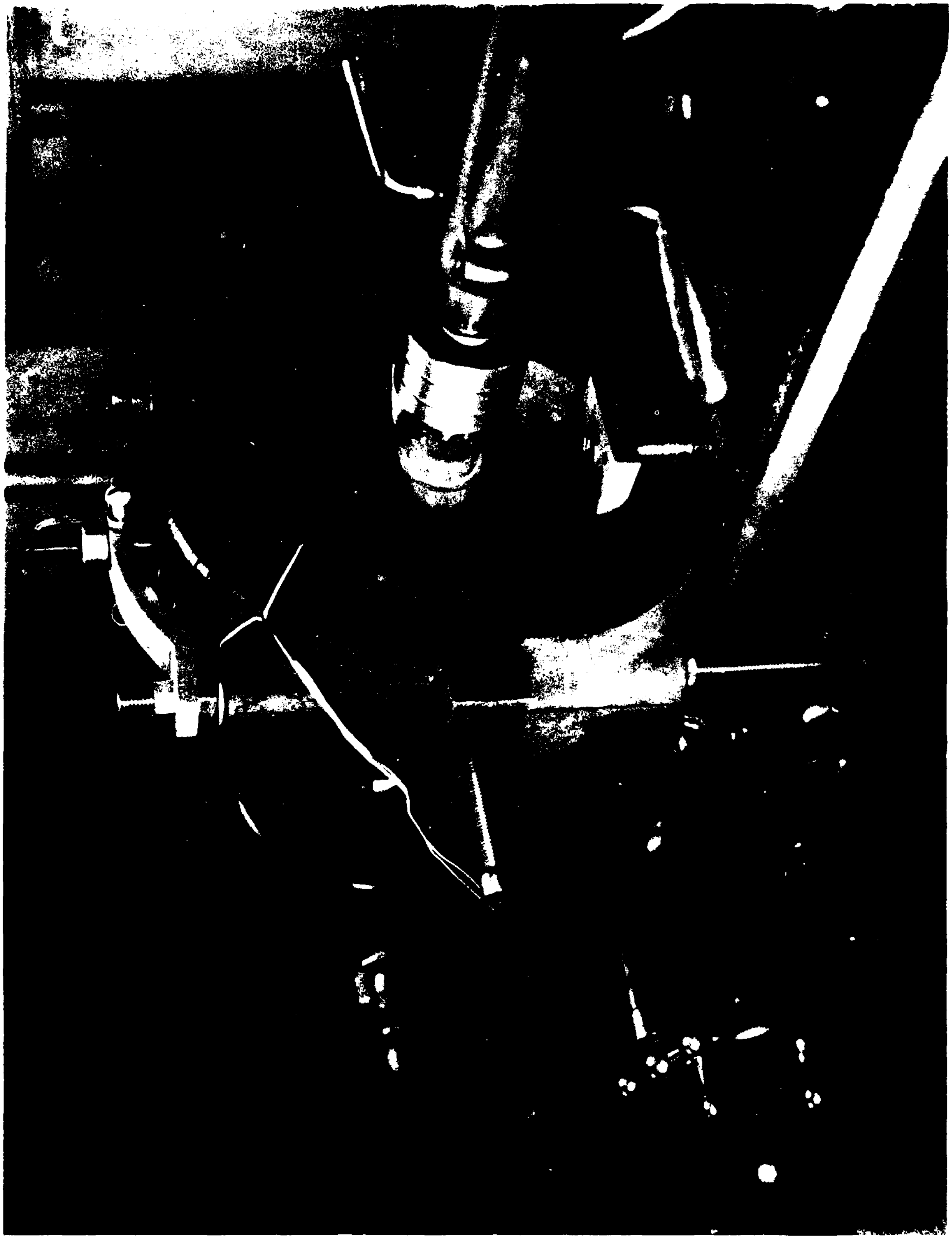

Figure 3

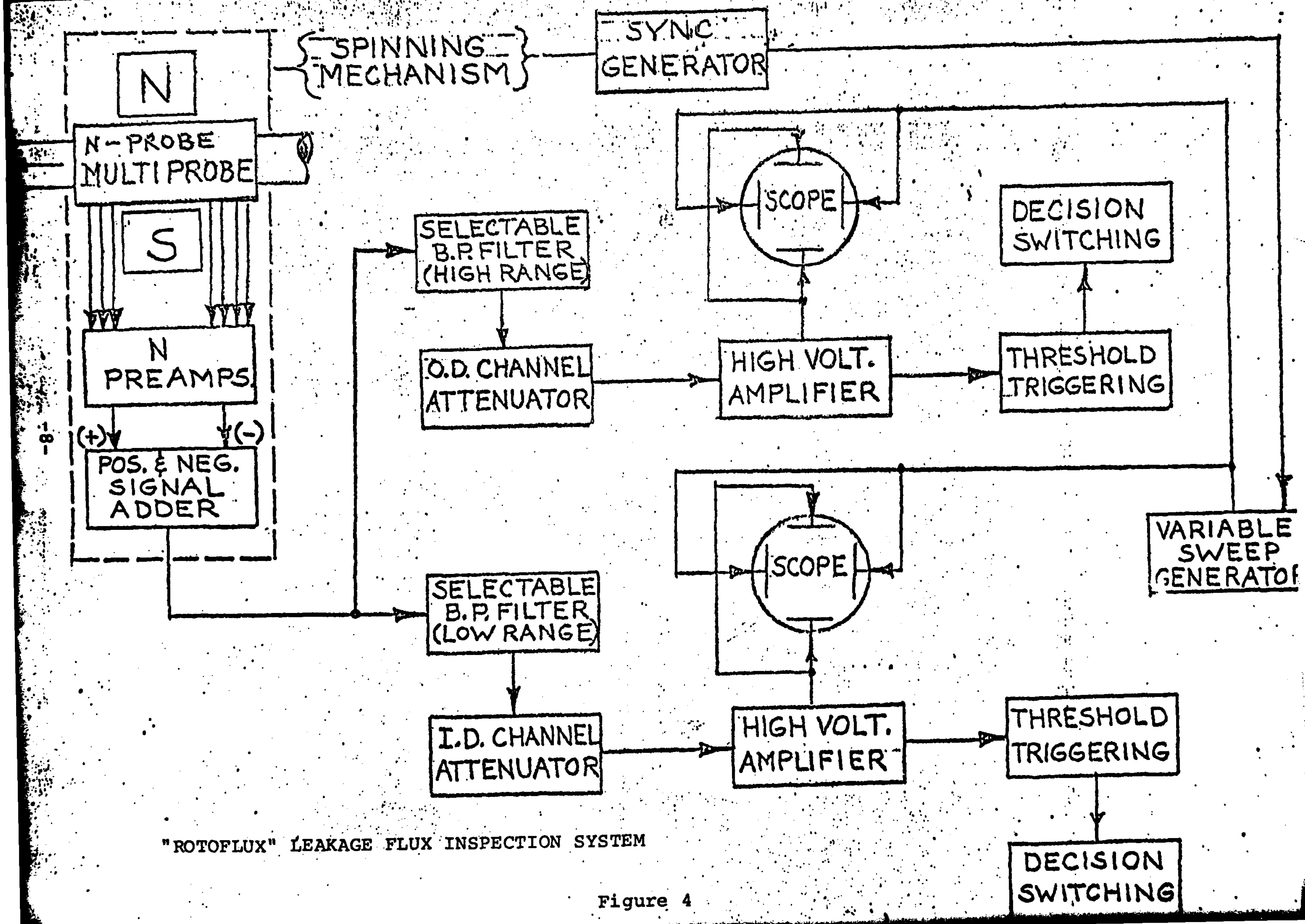

"ROTOFLUX" LEAKAGE FLUX INSPECTION SYSTEM

Figure 4

Figure 5

showed the lowest noise level on the apparatus described in Section III.B. One important development was the discovery of three bodies which showed significant indications during pre-screening but which had not been condemned by the magnetic particle inspection. These three pieces were subsequently shown to have significant defects during the metallurgical workup described in Appendix IV.

Selected pieces were then notched to provide calibration standards. Certified longitudinal and transverse notches of various depths were manufactured by Westpro Labs in Salem, Oregon by means of the Electric Discharge Method (E.D.M.). Through and partial holes were made by Magnetic Analysis Corporation. Two important considerations in placing the notches were to test the method's ability to separate notches from the embossed inner surface, and its ability to separate the notches from the edge of the open end. These reference standards are described in Appendix V.

IV. DATA ACQUISITION, ANALYSIS AND RESULTS

Tests were run on production pieces in various categories. The notches and holes which were described in the previous section were devised to test the detection capability of the system to separate significant defects from normal variations in the part. These test parameters covered the need to find longitudinal and transverse notches in the outer and inner surfaces, holes drilled normal to the outside surface and holes parallel to the axis of the grenade bodies. Reference notches were placed in the embossed area to test the capability to separate them from the indication caused by the embossing. Holes drilled from the open end of the body were used to evaluate the capability to test to the end of the piece. Also covered was the question of equalizing the amplitude of the response to O.D. and I.D. notches of equal magnitude. This is an important consideration on loaded grenades where testing needs to be done from the outer surfaces. The reasons this presents problems, and the remedies for them, are well covered in Appendix III, pp 2-4. Tests were conducted on both unloaded and loaded grenade bodies. <u>It is important to be aware that in all cases data presented here was taken from the outside of the grenade body</u>.

After preliminary trials with various magnetizing and scanning combinations, the apparatus described in Section III was employed for testing parts with artificial notches and natural defects. As the pieces were rotated at 345 rpm the skirts were scanned helically as the carriage mounted magnet and 1/8" diameter probe assembly traversed the skirt in approximately 40 seconds. Strip chart recordings were produced representing the total length of the skirt of each part, so that a profile of the notch or defect can be easily seen. At the same time, photographs were made of the Heliflux/Rotoflux[2] oscilloscope

---

[2] Magnetic Analysis uses the name Heliflux in systems where scanning is achieved by rotating the part to be inspected. Rotoflux systems depend on rotating the magnet probe assembly. Either technique utilizes the same standard instrumentation.

presentation at a particular cross-section. The scope presentation represents the signals detected in one revolution of the part relative to the magnet and probe assembly. It should be noted that the standard HFX/RFX instrument includes the signal processing and switching logic which would be required to evolve an automatic system from the laboratory apparatus.

Because of the limitations of time and money placed upon this study, it was not possible to extend the test to the shoulder area. Past experience on parts of similar configuration, however, pursuades the writers that with proper fixturing and probe design, results comparable to those realized on the skirt would be obtained on the shoulder.

A. Experiments Conducted on Reference Specimens

Figure 6 shows strip chart recordings of two typical grenade bodies which produced no significant defect indications in the transverse magnetization apparatus. Figure 7 shows the response of the transverse magnetization technique to 1/4" long longitudinal O.D. notches in unloaded bodies with depths of 50%, 25%, and 10% of the wall thickness. Figure 8a shows the equal response of this same apparatus to equal 25% longitudinal O.D. and I.D. notches, which is accomplished by dividing the O.D. and I.D. indications on the basis of frequency and equalizing their amplitudes by individually adjusting the gains in the respective instrument channels.

In Figure 8b it can be seen that without this capability, there is a disparity of about 3:1 between O.D. and I.D. notches of equal size. Figure 9 shows the 25% I.D. notch before and after loading as detected by the transverse magnetization system. The alert reader is certain to notice that the I.D. defects in Figure 9 are presented as outputs of the O.D. channel which is a seeming inconsistency in procedure which requires explanation.

In normal practice the O.D. and I.D. channel outputs would be recorded simultaneously on a dual channel recorder. In this experiment, however, because of equipment availability, the outputs were recorded alternately on a single channel recorder; and the 25% I.D. longitudinal notch was not recorded from the I.D. channel after loading.

The reader should be assured, however, that the designations of O.D. and I.D. channel are, on a particular test piece, relative to each other and dependent upon optimizing the filter and sensitivity settings in the two channels. There is no question that identical indications for an I.D. notch before and after loading can be obtained from the I.D. channel.

Going to the response of the longitudinal magnetization system to transverse notches, Figure 10 shows the response to a transverse O.D. notch with a depth of 25% of the wall thickness. To further illustrate the features of the instrumentation used, photographs were made of the oscilloscope display of these notches. Again,

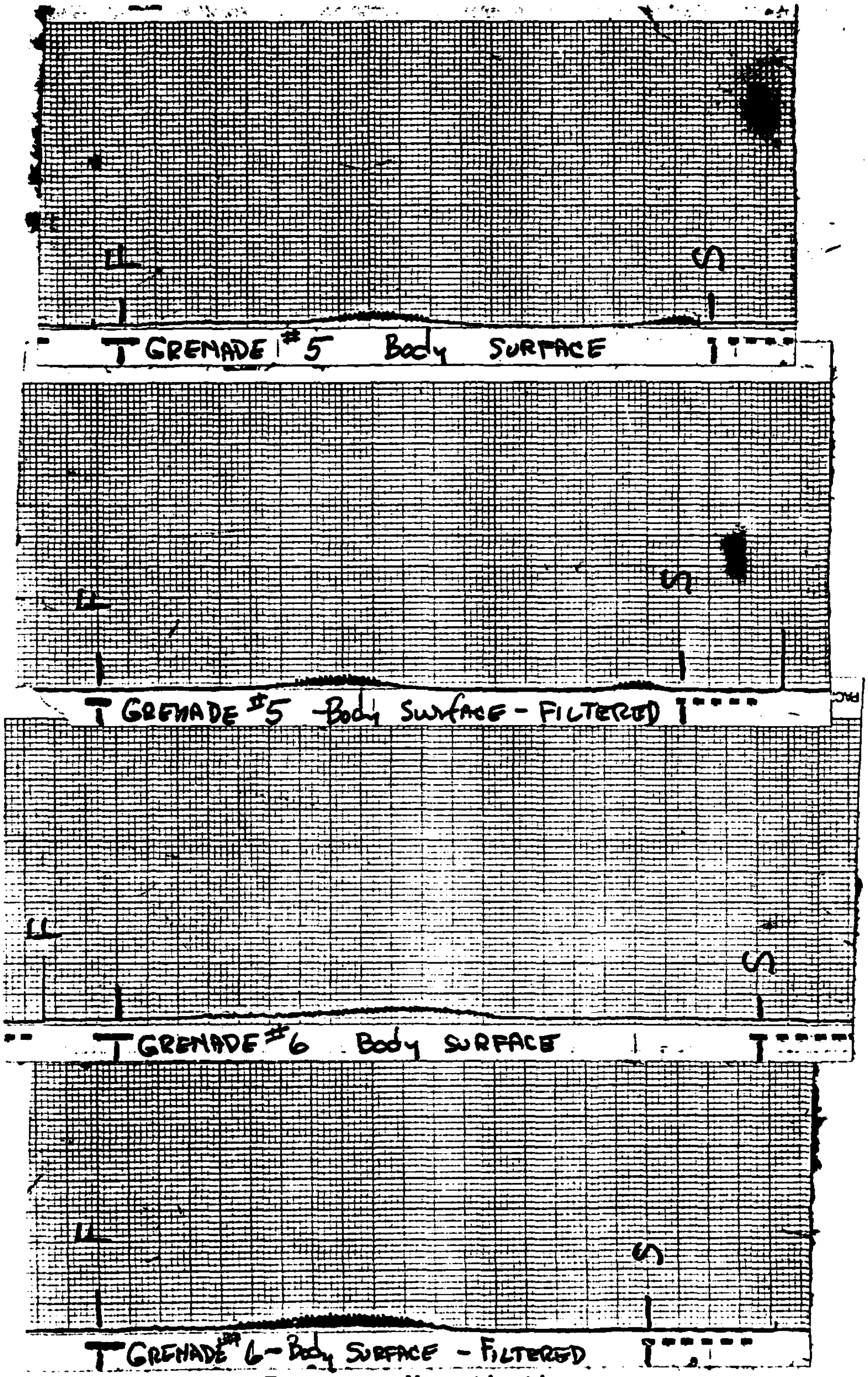

Transverse Magnetization

Figure 6

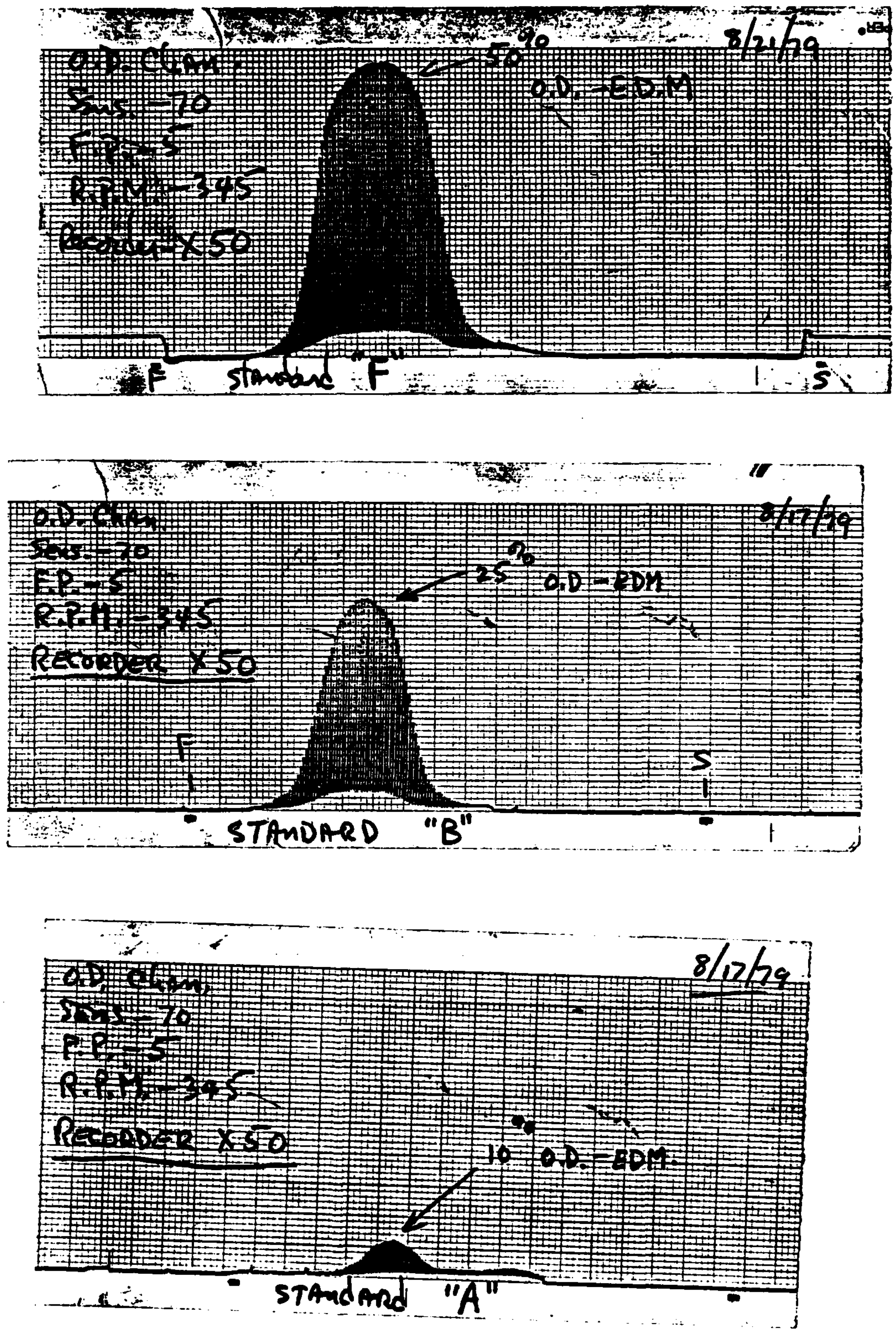

Transverse Magnetization

Figure 7

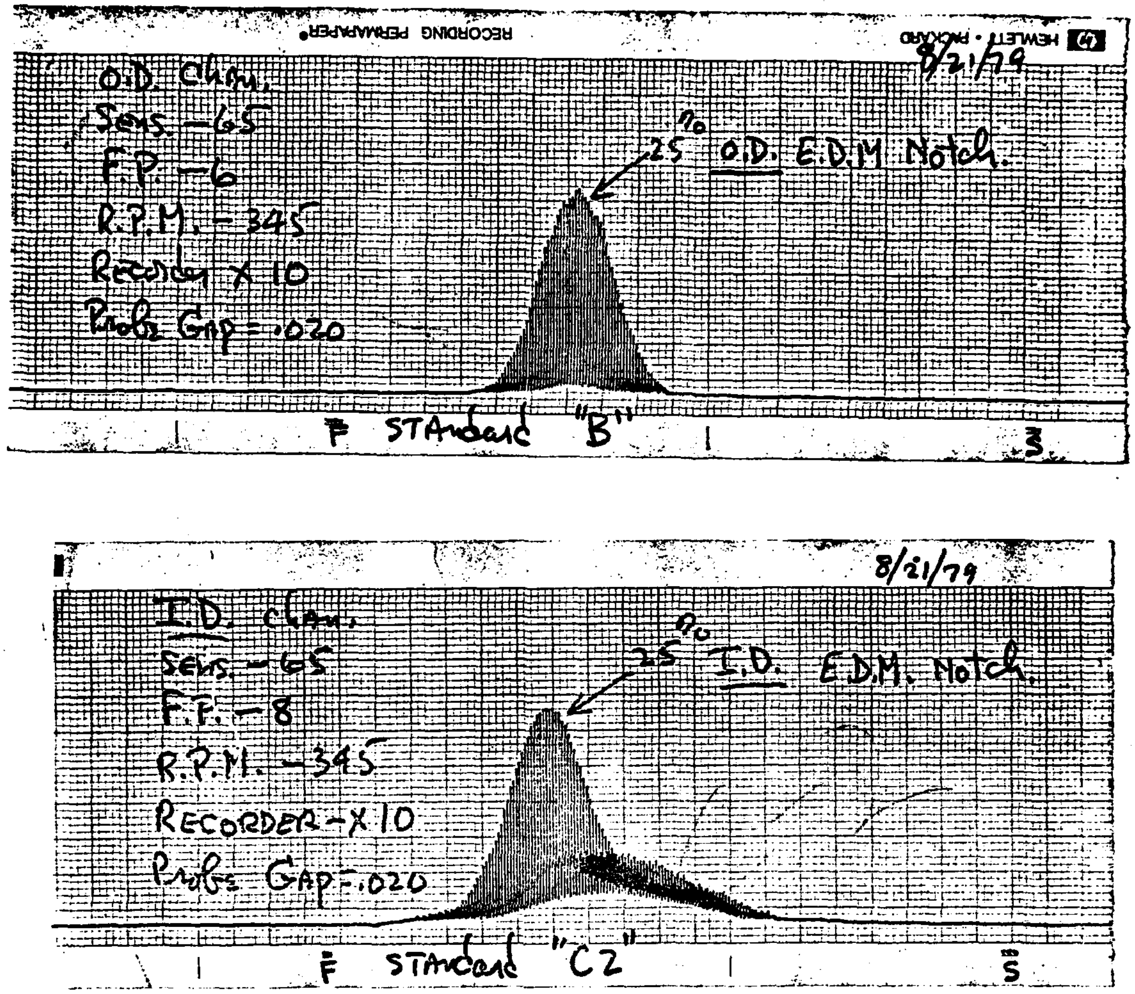

Figure 8a

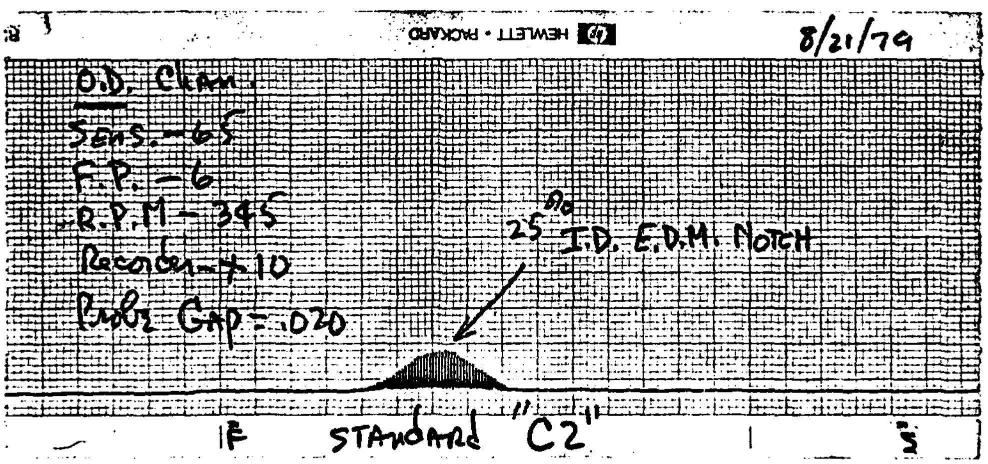

Transverse Magnetization

Figure 8b

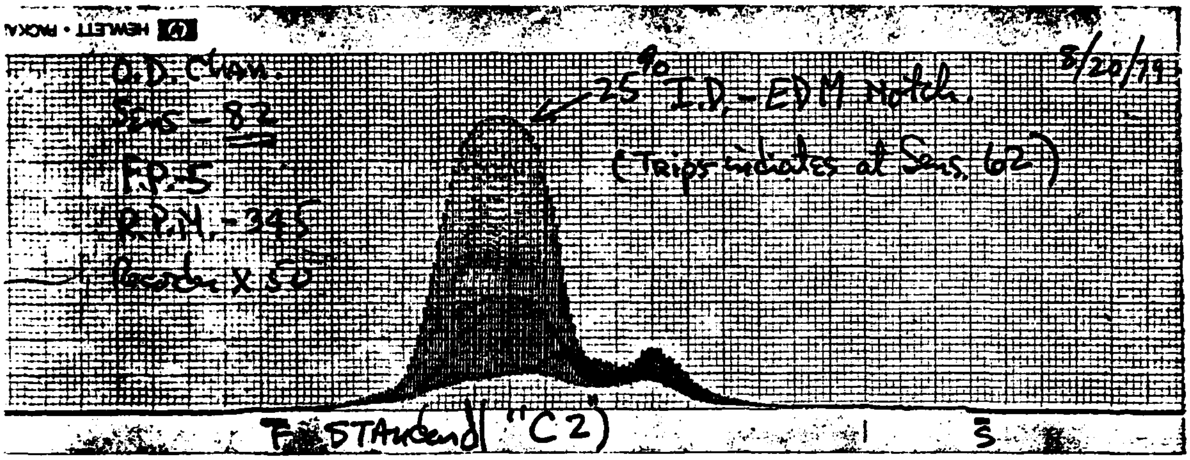

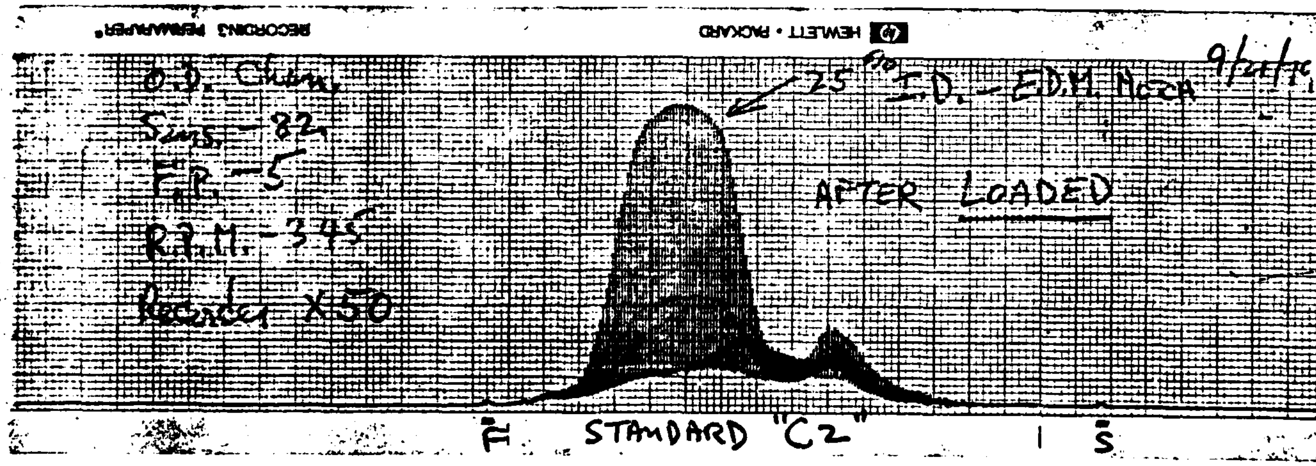

Transverse Magnetization

Figure 9

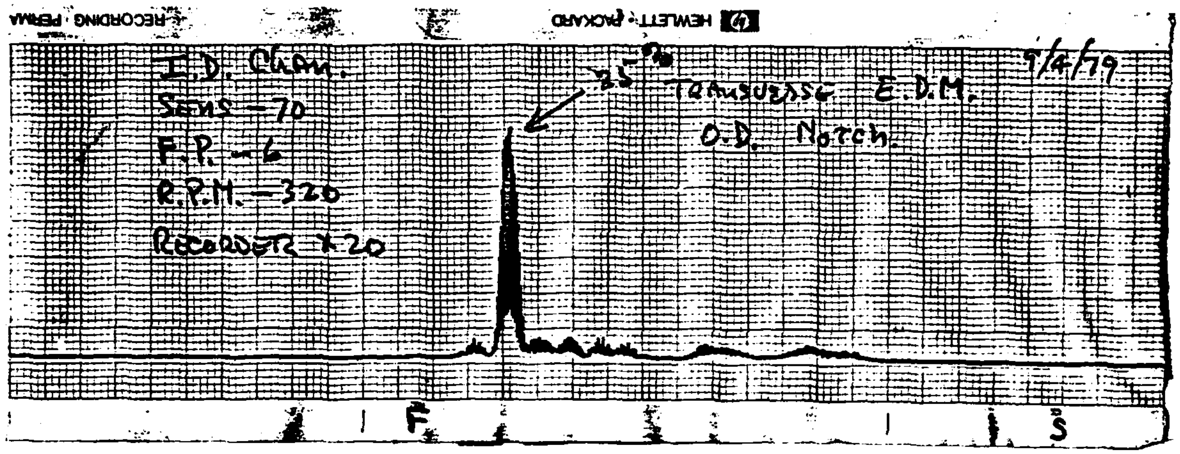

25% Transverse
EDM O.D. Notch
I.D. Channel
Sensitivity = 70
Filter = 6
Rotational Speed = 320 RPM

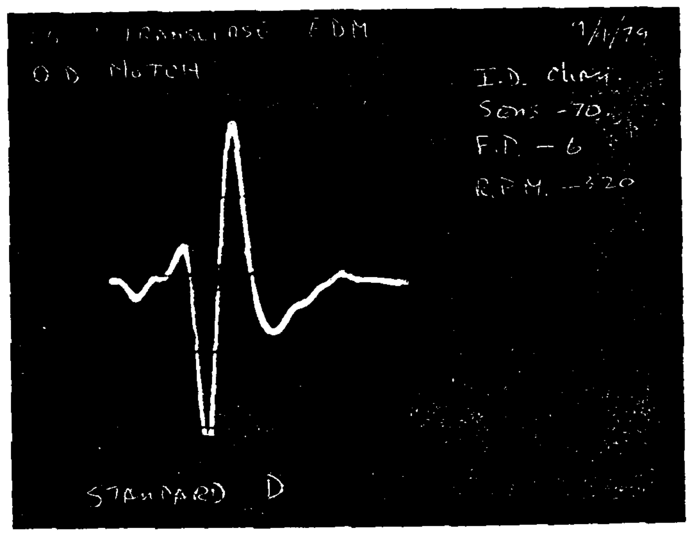

Standard D

25% Transverse
EDM O.D. Notch
O.D. Channel
Sensitivity = 74
Unfiltered
Rotational Speed = 320 RPM

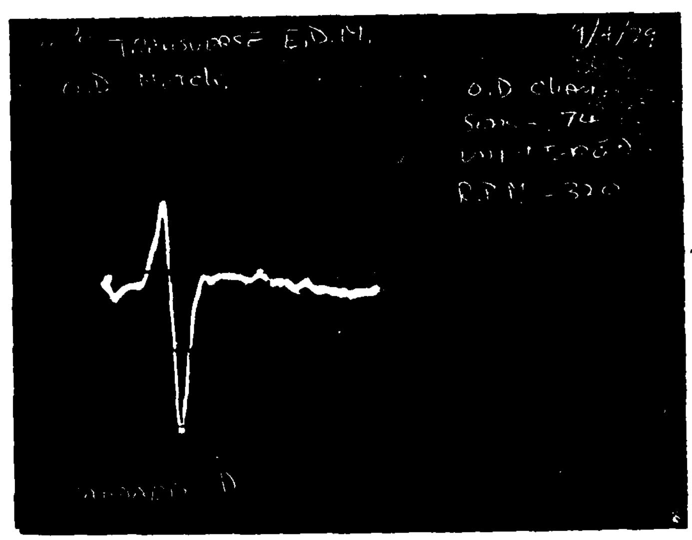

Standard D

Longitudinal Magnetization

Figure 10

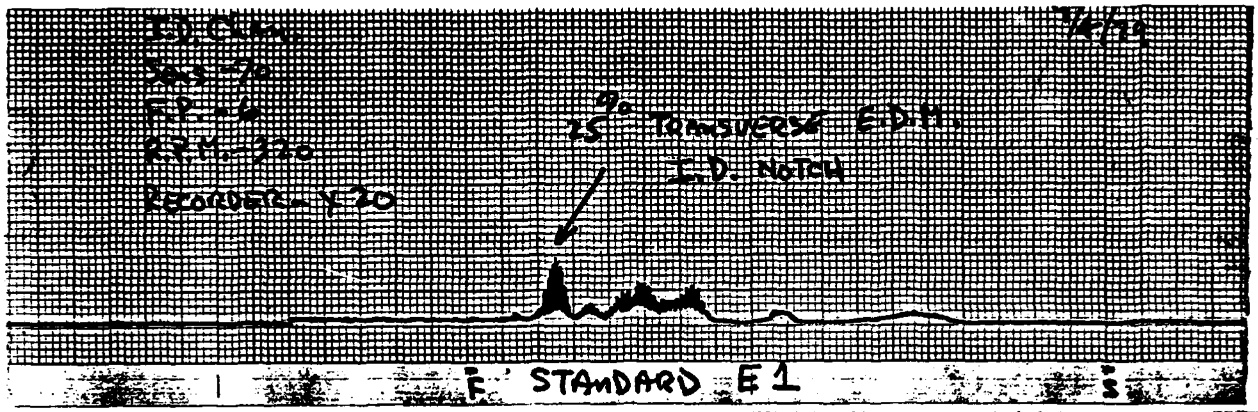

25% Transverse
EDM I.D. Notch
I.D. Channel
Sensitivity = 70
Filter = 6
Rotational Speed = 320 RPM

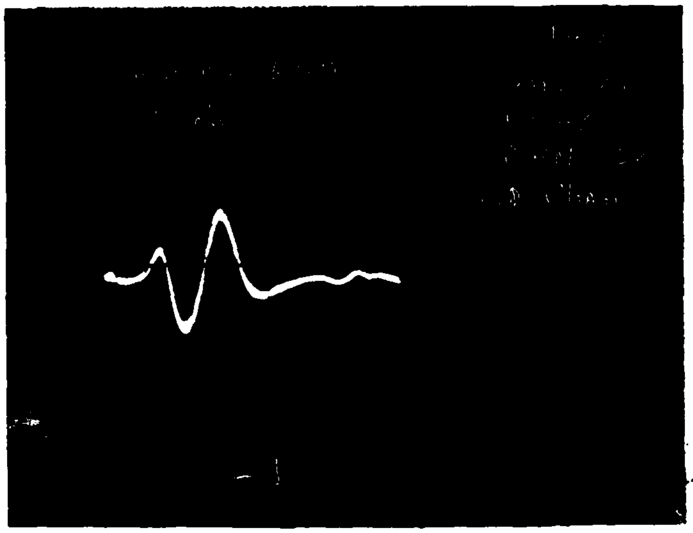

Standard E-1

25% Transverse
EDM I.D. Notch
O.D. Channel
Sensitivity = 74
Unfiltered
Rotational Speed = 320 RPM

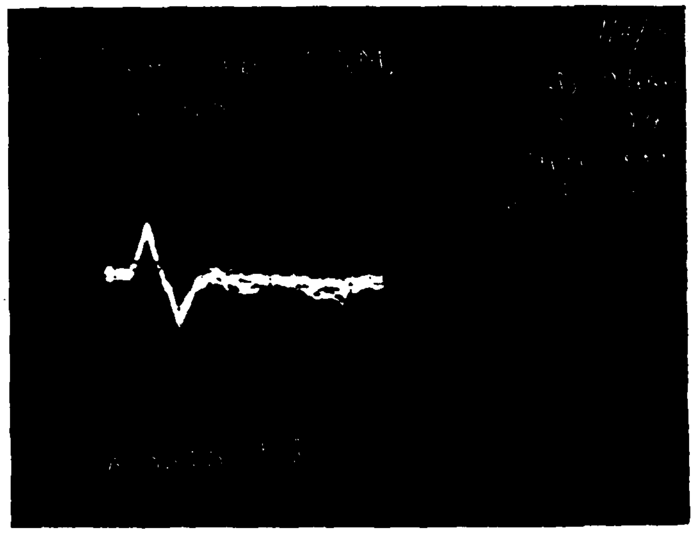

Standard E-1

Longitudinal Magnetization

Figure 11

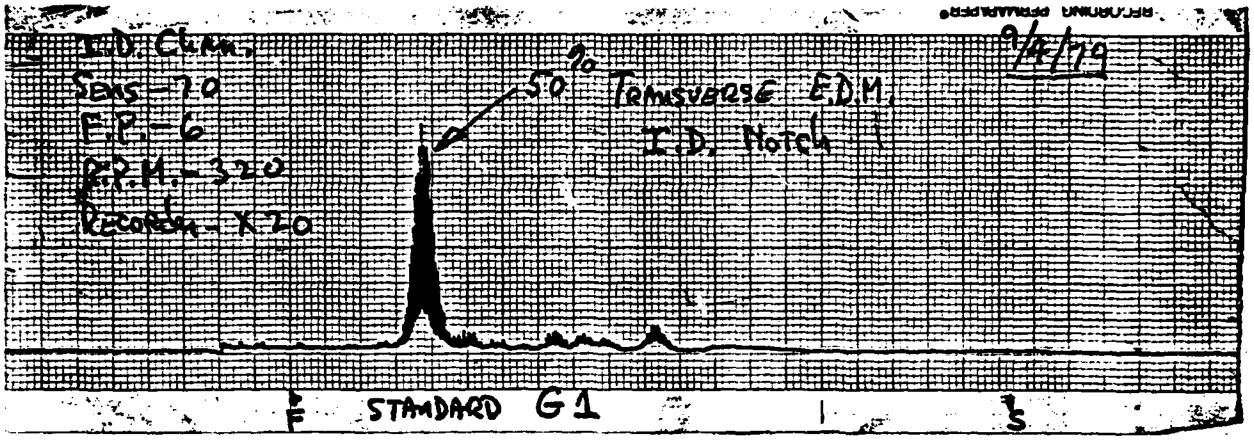

50% Transverse
EDM I.D. Notch
I.D. Channel
Sensitivity = 70
Filter = 6
Rotational Speed = 320 RPM

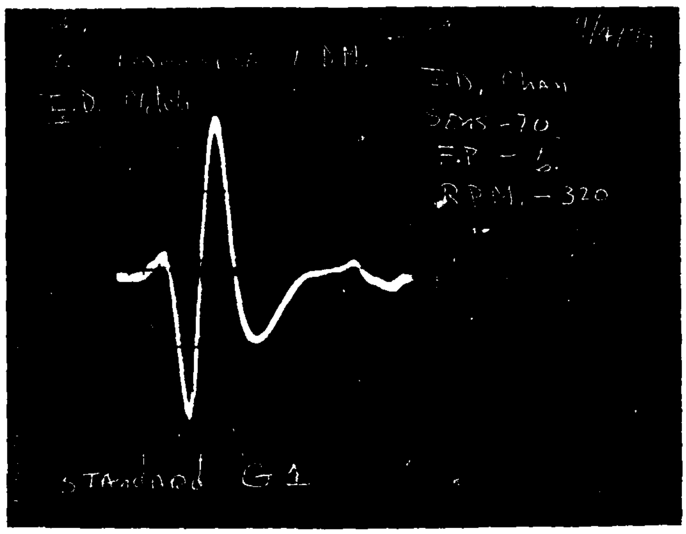

Standard G-1

50% Transverse
EDM I.D. Notch
O.D. Channel
Sensitivity = 74
Unfiltered
Rotational Speed = 320 RPM

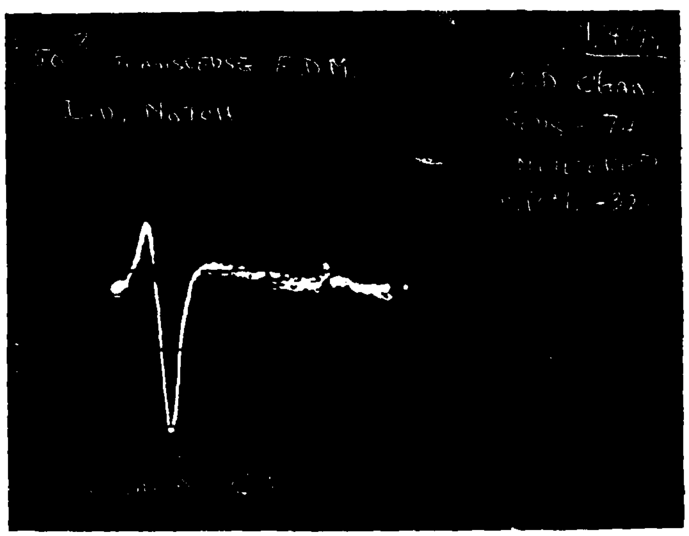

Standard G-1

Longitudinal Magnetization

Figure 12

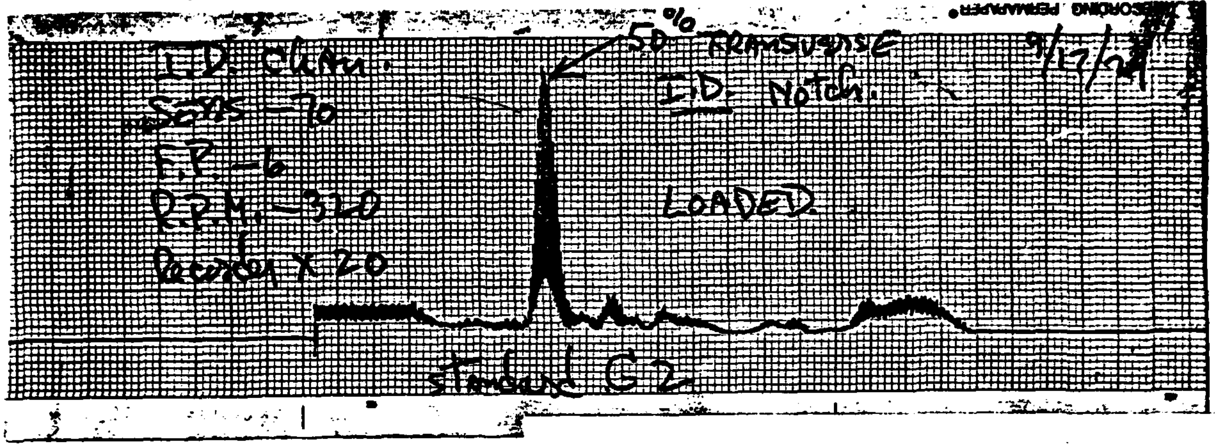

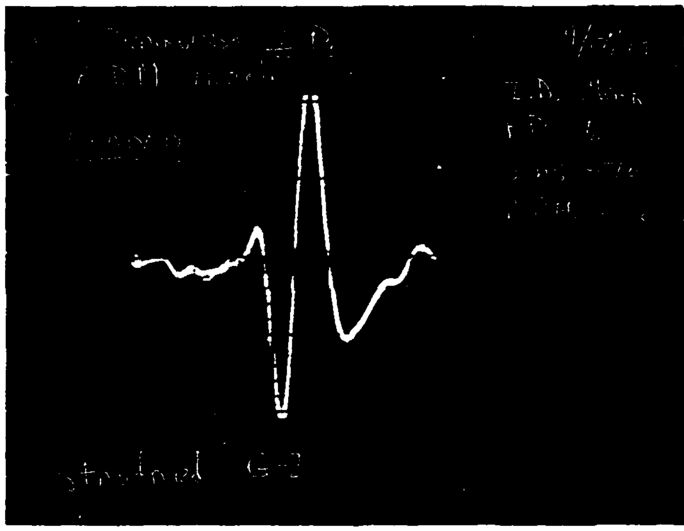

50% Transverse
EDM I.D. Notch
I.D. Channel
Sensitivity = 70
Filter = 6
Rotational Speed = 320 RPM

Standard G-2 Loaded

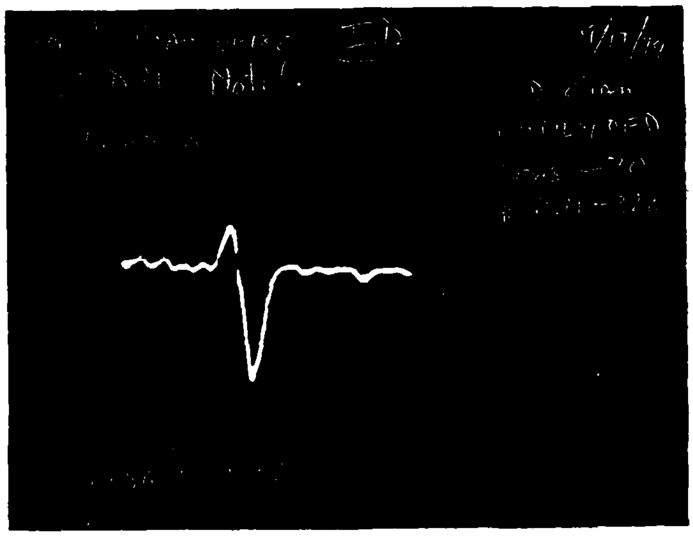

50% Transverse
EDM I.D. Notch
O.D. Channel
Sensitivity = 74
Unfiltered
Rotational Speed = 320 RPM

Standard G-2 Loaded

Longitudinal Magnetization

Figure 13

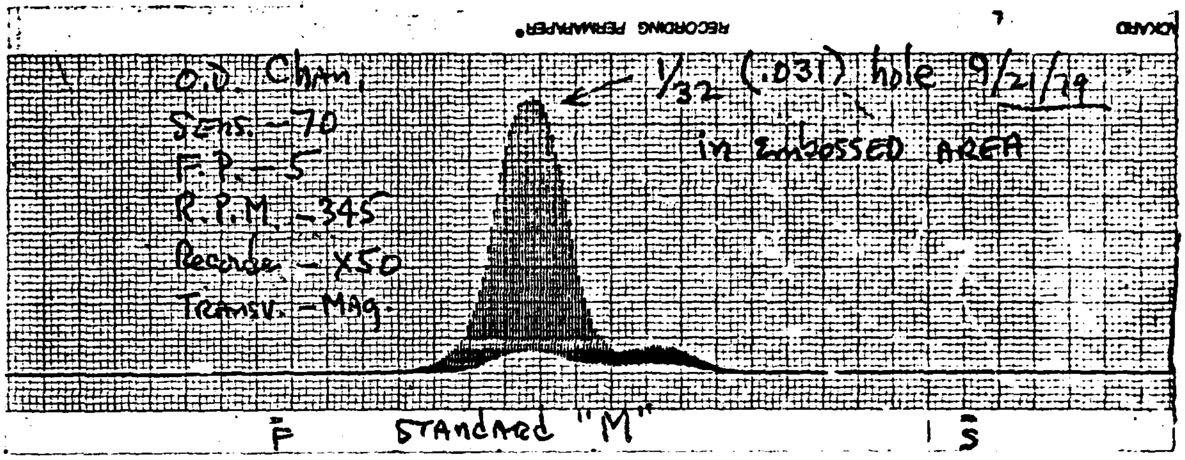

.031 Hole Through
Embossed Area
I.D. Channel
Sensitivity = 70
Unfiltered
Rotational Speed = 345 RPM

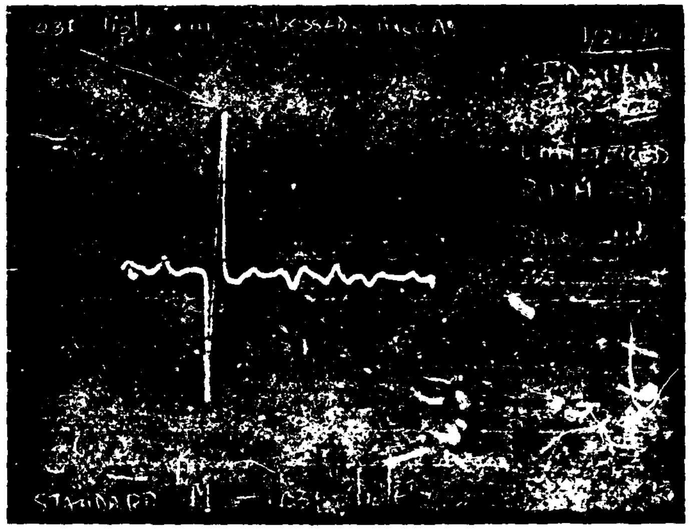

Standard M

.031" Hole Through
Embossed Area
O.D. Channel
Sensitivity = 60
Filter = 5
Rotational Speed = 345 RPM

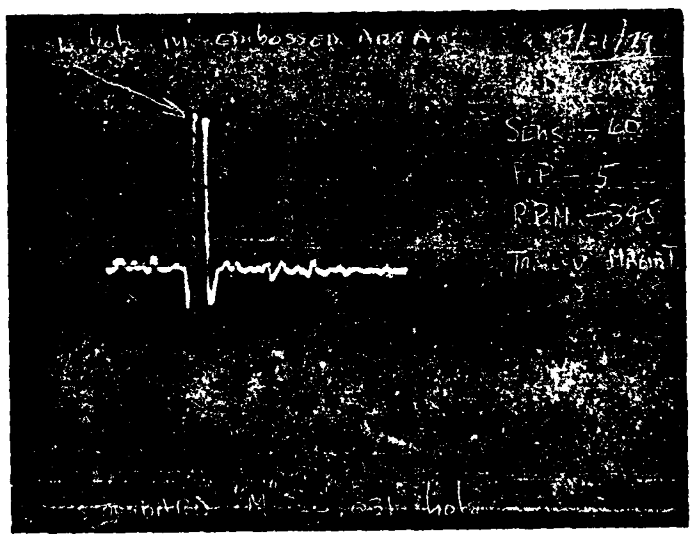

Standard M

Transverse Magnetization

Figure 14a

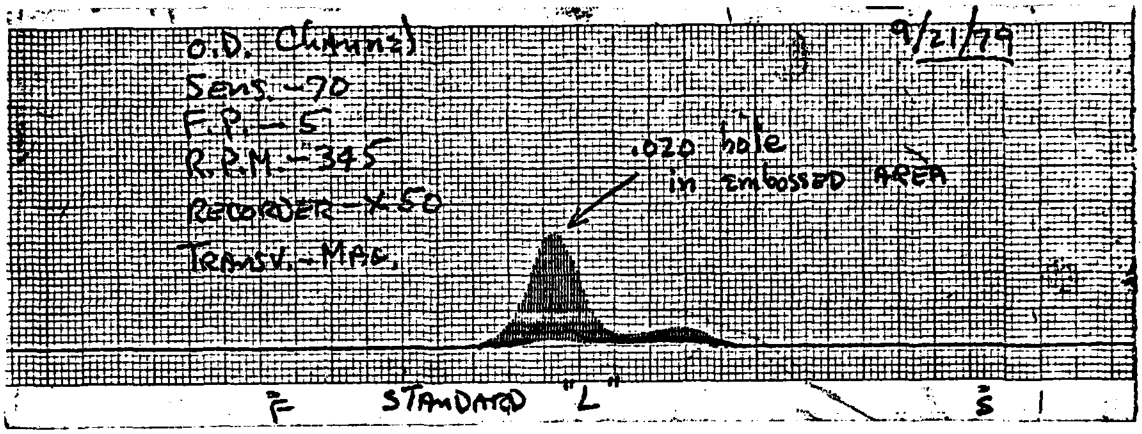

.020" Hole Through
Embossed Area
I.D. Channel
Sensitivity = 60
Unfiltered
Rotational Speed = 345 RPM

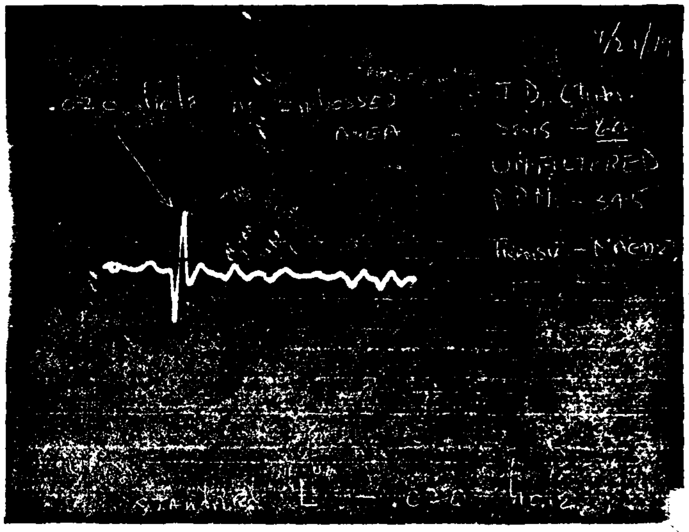

Standard L

.020" Hole Through
Embossed Area
O.D. Channel
Sensitivity = 60
Filter = 5
Rotational Speed = 345 RPM

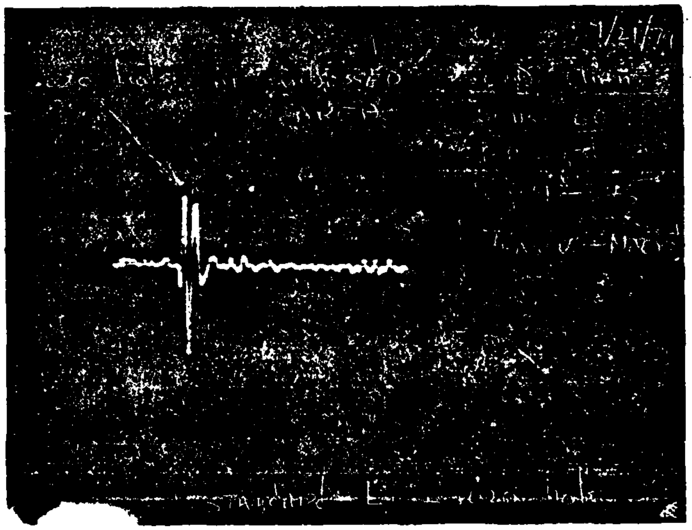

Standard L

Transverse Magnetization

Figure 14b

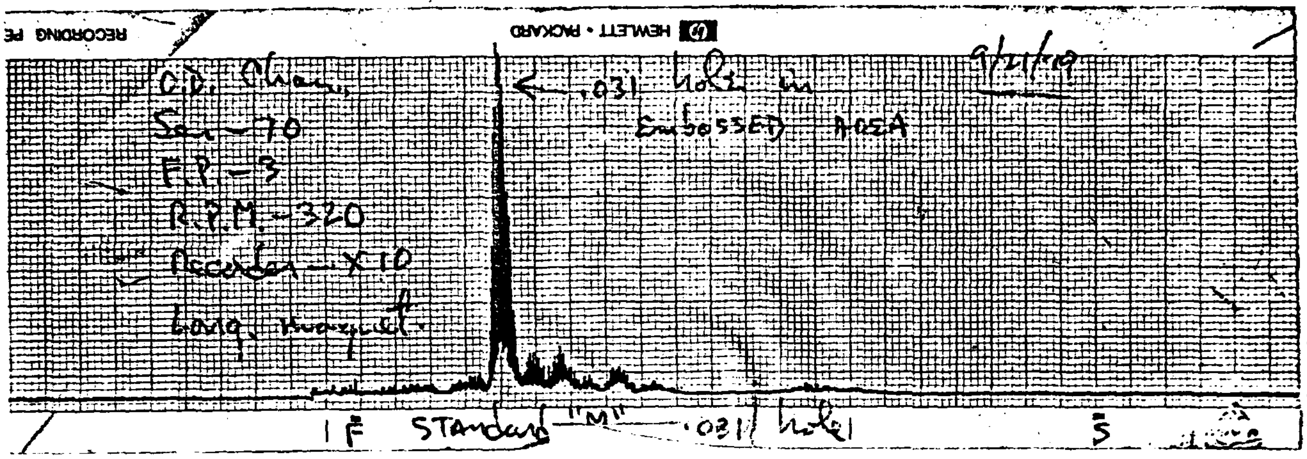

.031 Hole Through
Embossed Area
I.D. Channel
Sensitivity = 70
Unfiltered
Rotational Speed = 320 RPM

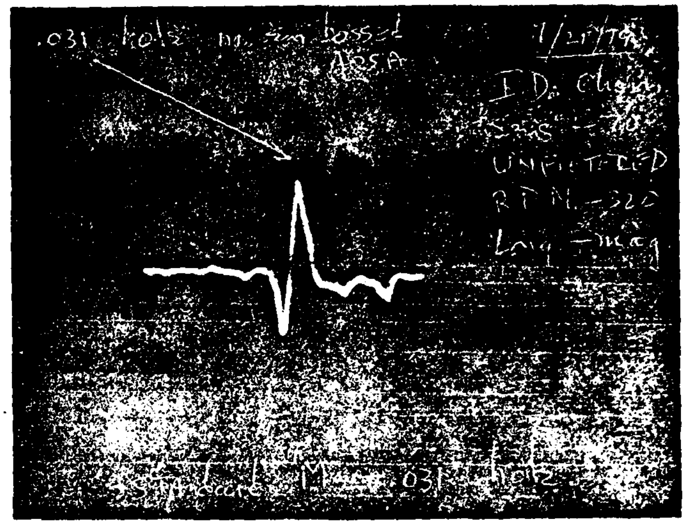

Standard M

.031 Hole Through
Embossed Area
O.D. Channel
Sensitivity = 70
Filter = 3
Rotational Speed = 320 RPM

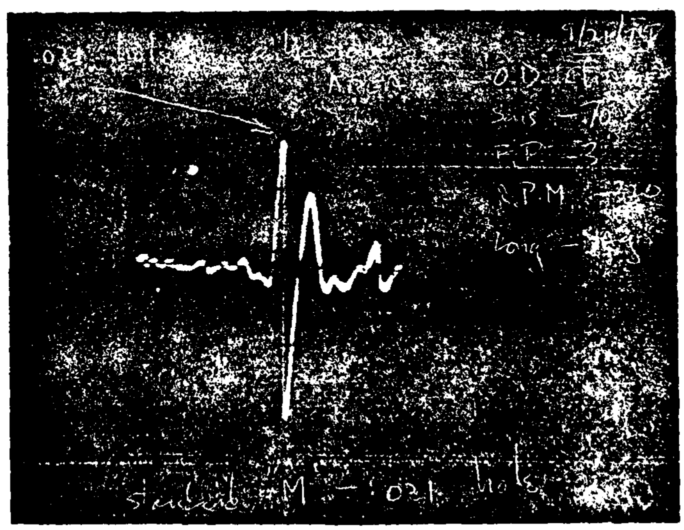

Standard M

Longitudinal Magnetization

Figure 15a

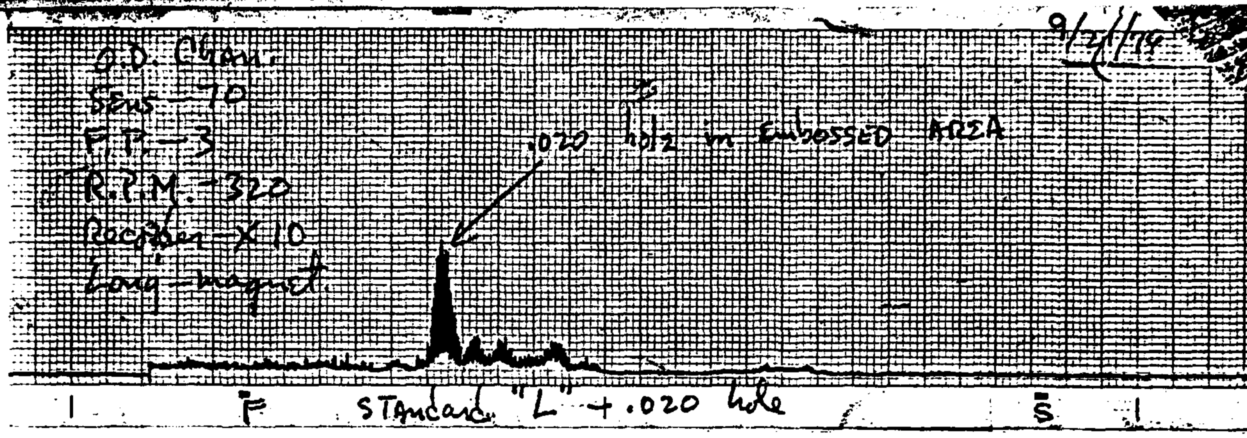

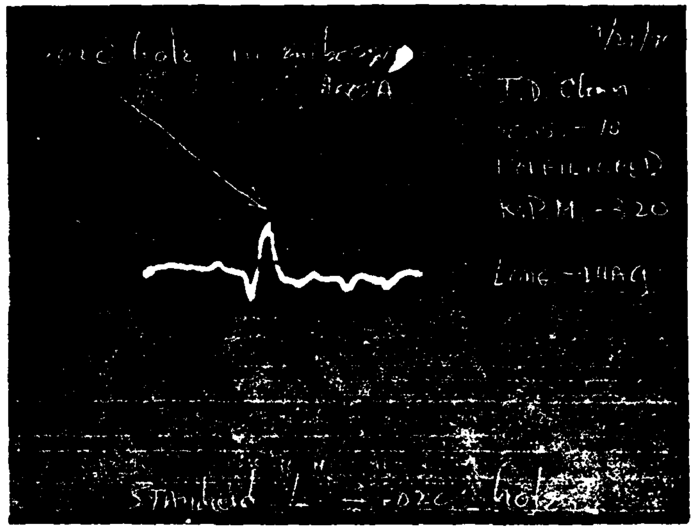

.020 Hole Through
Embossed Area
I.D. Channel
Sensitivity = 70
Unfiltered
Rotational Speed = 320 RPM

Standard L

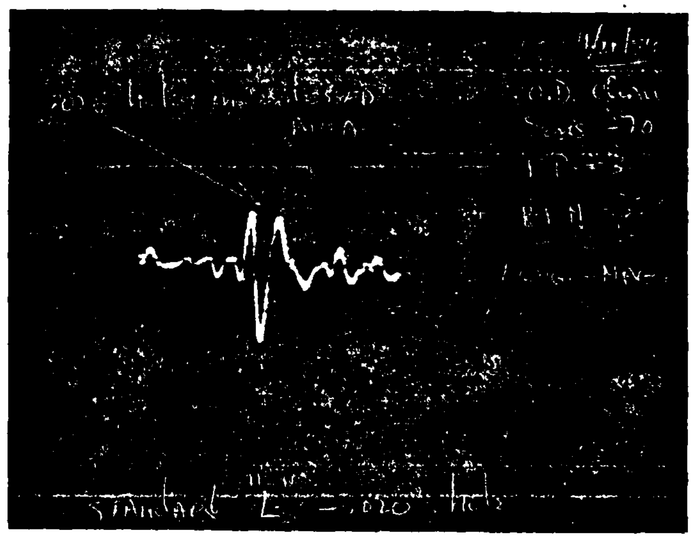

.020 Hole Through
Embossed Area
O.D. Channel
Sensitivity = 70
Filter = 3
Rotational Speed = 320 RPM

Standard L

Longitudinal Magnetization

Figure 15b

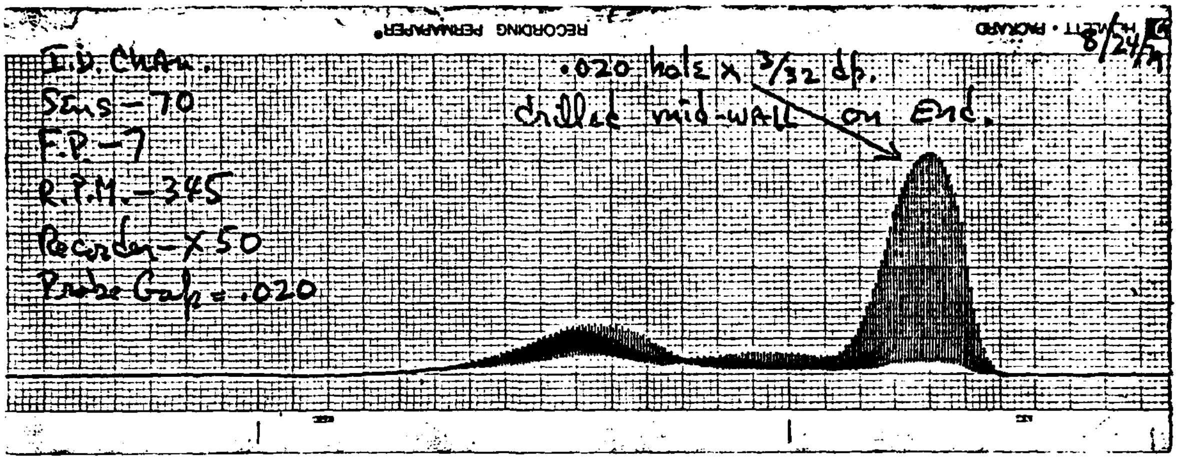

I.D. Channel
.020 Diameter Hole
3/32" Deep Drilled
Longitudinally into
Grenade Wall at Open End
I.D. Channel
Sensitivity = 58
Filter = 7
Rotational Speed = 345 RPM

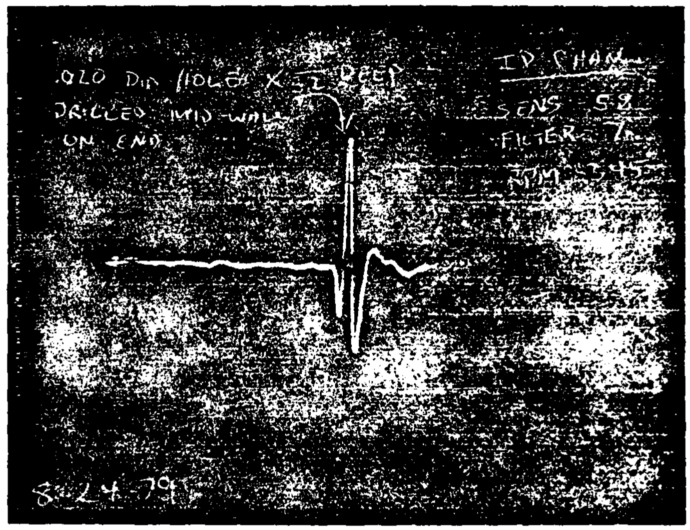

Transverse Magnetization

Figure 16

the oscilloscope displays one circumferential rotation in a notched cross-section.

Figure 11 shows the response to a 25% transverse I.D. notch. The signal-to-noise ratio, in this instance, should be derived by comparison to the unembossed area, since the depth of embossing can be nearly 20% and still be within dimensional specifications.

Figure 12 and 13 show a transverse I.D. notch which is of a depth approximately 50% of the wall thickness, before and after loading.

Figure 14 and 15 show the responses to .031 and .020 diameter holes drilled through the wall in the embossed area. Figure 14a and 14b were made with transverse magnetization, and 15a and 15b with longitudinal magnetization. The hole shown in Figure 16 was devised to test the ability of the system to find defects close to the open end of the grenade body.

B. Tests Conducted on Natural Defects

Figures 17 through 21 depict the profiles of a series of loaded bodies which have a wide variety of defect indications from none at all to large indications over the whole skirt. These tests were conducted with transverse magnetization and the readouts taken from the O.D. channel. The sensitivity has been increased, and the embossed area is well defined as can be seen in the recording for sample 22. Except for the three pieces treated in Appendix III, no metallurgical examination has been conducted; but the pieces are cataloged and this could be done in the future.

V. DISCUSSION

An important outcome of these experiments was the ability of the transverse magnetization system to find notches with even very short longitudinal components, such as the .020" diameter hole. However, on transverse E.D.M. notches, where the longitudinal component is only .005", it would be necessary to provide a separate technique based upon longitudinal magnetization which could approximately double the cost of an automatic machine.

Whether the added cost is warranted by the probability of significant natural defects occurring which have very short longitudinal components is beyond the purview of these reporters, but it is an important question to be asked. It may be worth noting that the shortest longitudinal component in reference notches used for calibrating the ultrasonic test which is presently used to inspect the part is .035", which is the width of the transverse notches described in the applicable documents. Although it was not demonstrated within the scope of the present study, it is likely that the transverse notches presently used as U.T. references could be detected with a transverse magnetization leakage flux system.

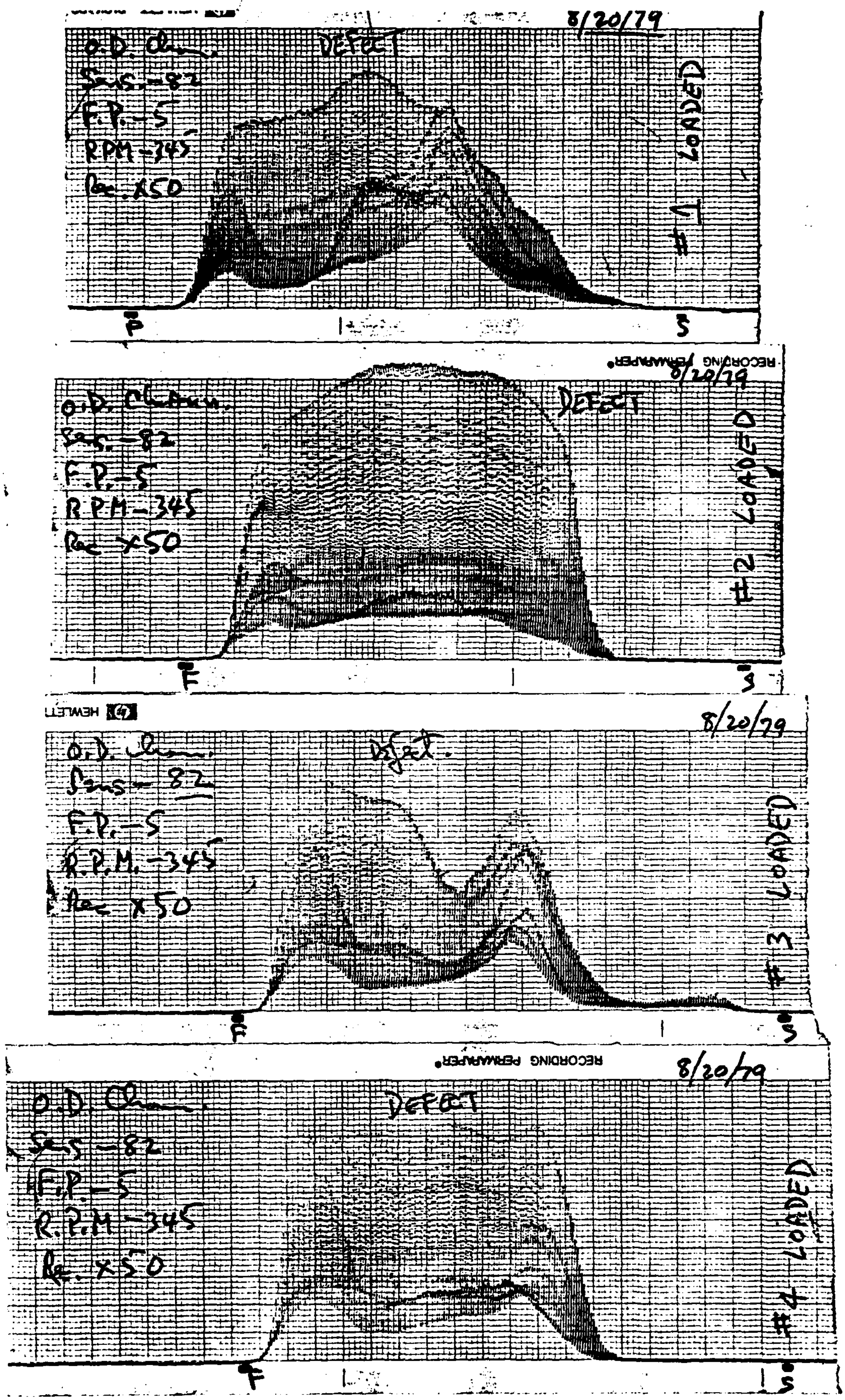

Transverse Magnetization

Figure 17

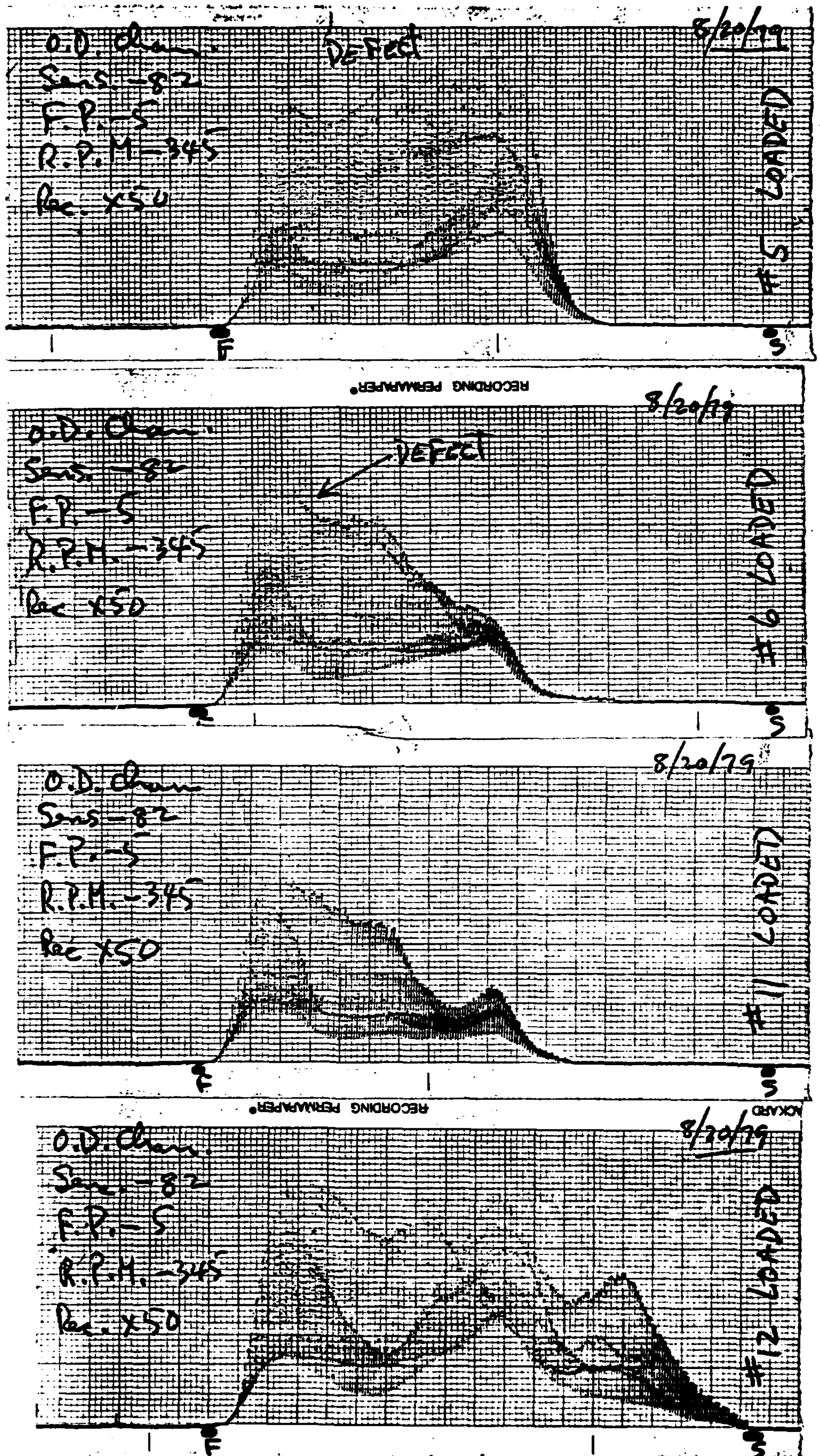

Transverse Magnetization

Figure 18

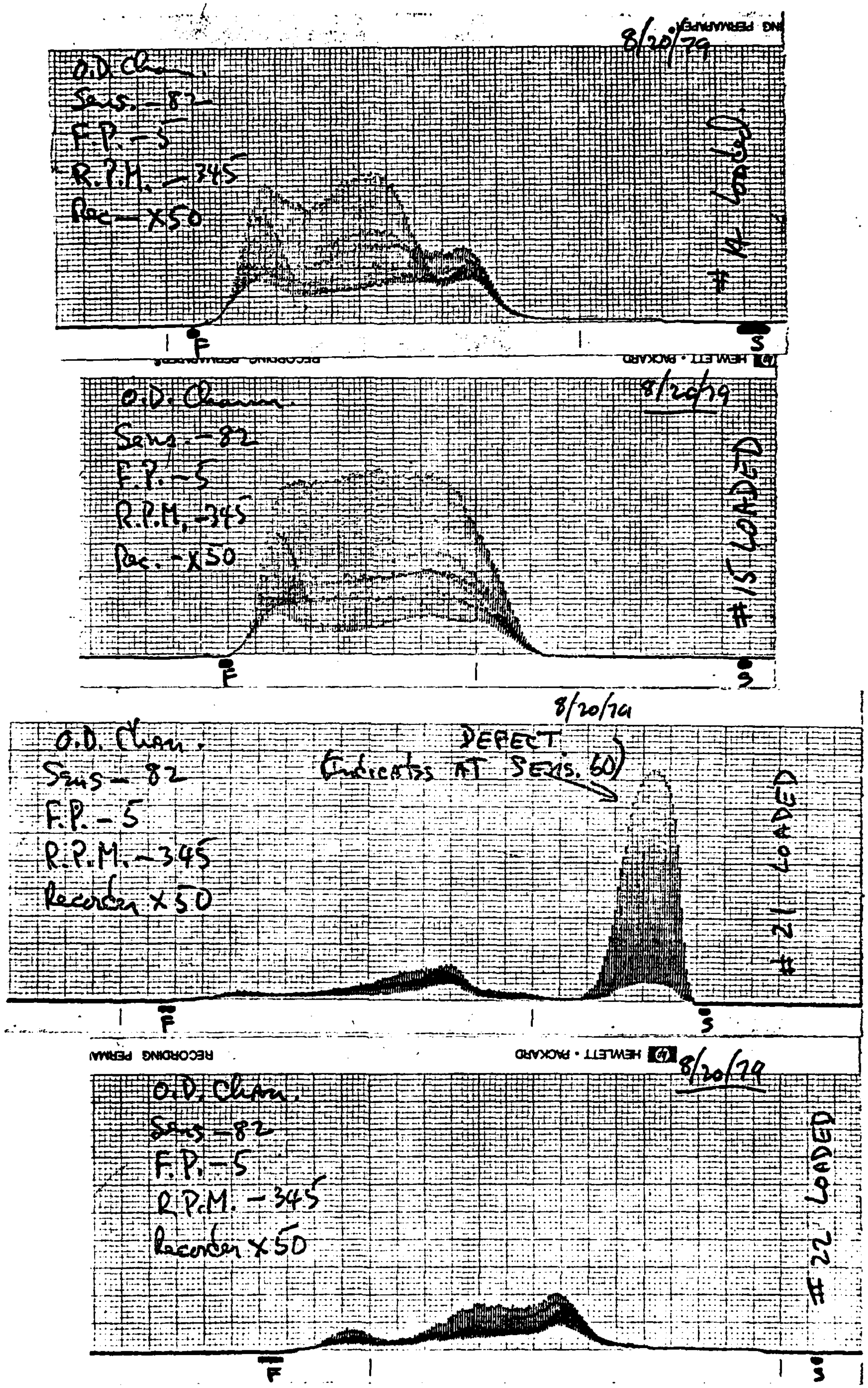

Transverse Magnetization

Figure 19

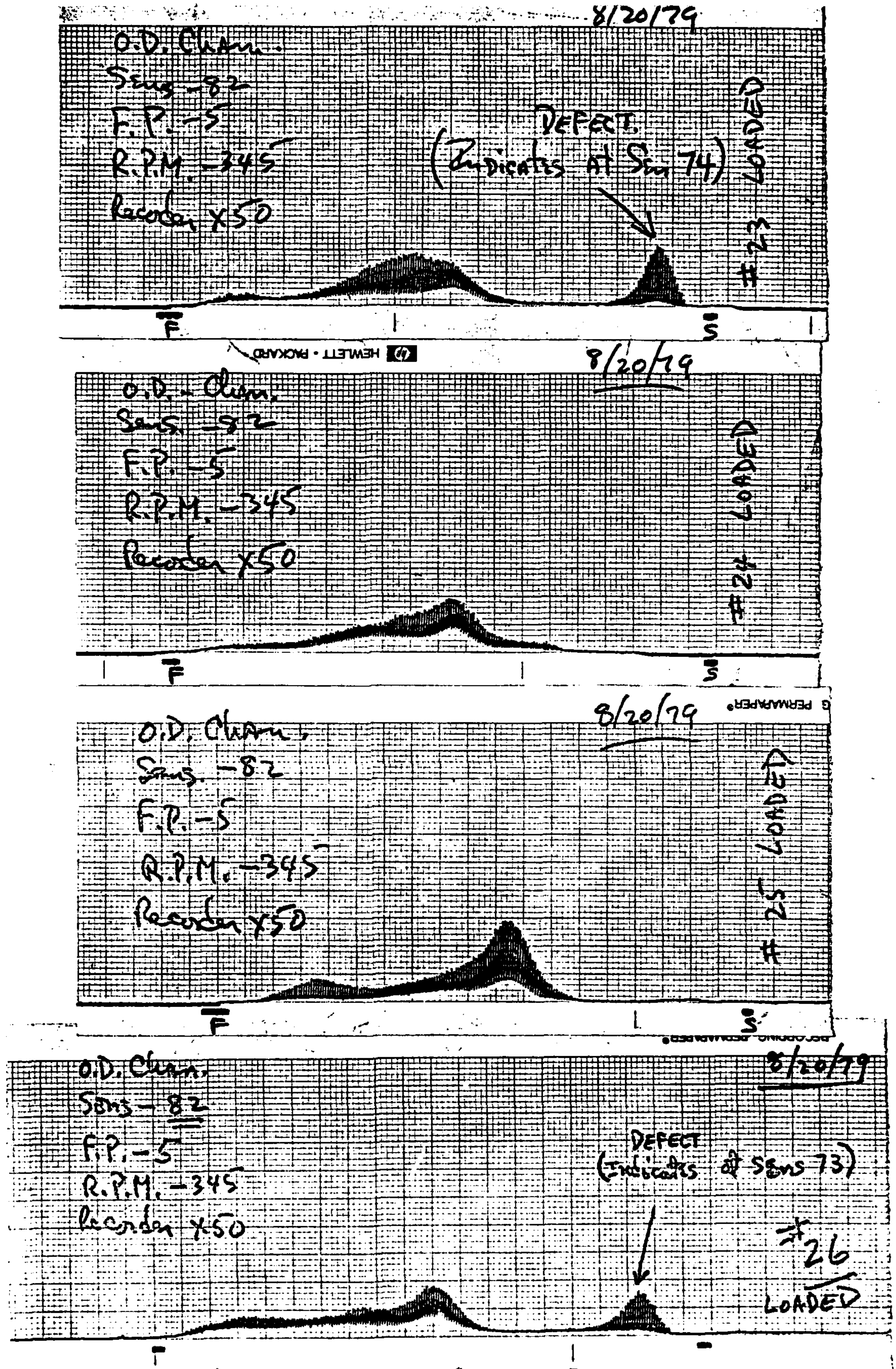

Transverse Magnetization

Figure 20

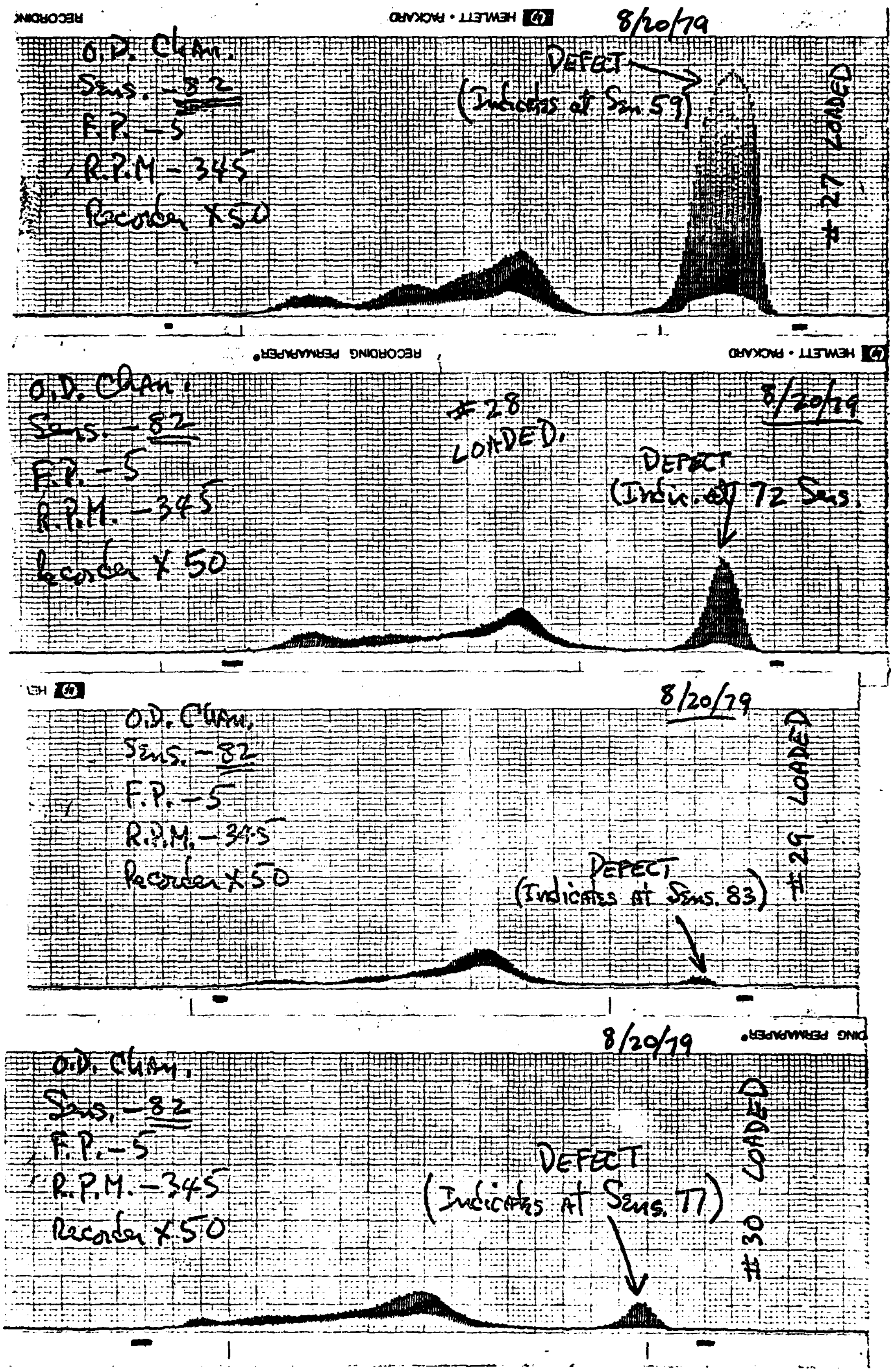

Transverse Magnetization

Figure 21

It should be noted that a great deal of "off the shelf" technology exists which is based upon transverse magnetization. Systems such as these have been used extensively for the inspection of tubular steel products such as those used in the oil and gas drilling and distribution industries. These existing systems address the basic problems of reliable detection of detrimental defects and the need to economically match testing speeds to production rates. The writers do not mean to advocate a system which does not find defects which are exclusively transverse, but wish to point out that this requires a considerable investment to add a provision for longitudinal magnetization. Again, this point is submitted in the form of a question to be answered by those ultimately responsible for the products performance.

Also to be considered is the impact of the size of reject reference notches upon the validity of the test system, as well as its complexity. This is a difficult question to answer, especially in relation to the embossed area which is intended to facilitate fragmentation, and which can penetrate to 20% of the wall. Ancillary to this question is whether the system should be able to detect the presence of and depth of the embossing. There is the possibility of sorting out M-46 bodies which do not have embossed I.D.'s from M-42 bodies. It is also necessary to decide whether the shoulder and/or other portions of the body require inspection and to what defect level.

The trade off decisions between thoroughness and efficiency produce options which are too numerous to be discussed here. These options should be discussed by the involved parties in order to reach an adequate solution which is practical in terms of physical and economical realities.

VI. CONCEPTUAL DESIGN

Since the test parameters have not been finalized, in terms of type, size, and location of notches in notched reject standards, it would be premature to describe a detailed production machine for this task. Also to be determined is at what stages of production the testing should take place. On the other hand, past experience with the method and the evidence gathered in this study indicate that any reasonable combination of testing requirements could be accommodated by fairly straightforward adaptations of existing systems. Systems which have been provided in the past fall roughly into two categories for which Magnetic Analysis Corporation uses the names Rotoflux and Heliflux. The major difference between the two is that the Rotoflux system provides a rotating magnet and probe assembly, and the items to be tested are transported through the center of the scanning mechanism. In Heliflux systems, the part is picked up, rotated, and presented to a stationary magnet and probe assembly in a manner which allows the designated portions of the part to be interrogated. Usually the Rotoflux is used to inspect long lengths of material with a constant cross-section, such as steel pipe or tubing, while the Heliflux is used for inspection of formed parts. In the case of each new application, both of these techniques should be considered.

An important consideration in assessing these two optional techniques is that the Rotoflux is inherently much faster, since the material is presented to the test assembly in a continuous stream. By use of multiprobe detectors, a wide swath of the material can be tested during each rotation, which allows fast thruput speeds. With the use of specially designed pole pieces and multiprobes, this broad coverage per revolution can be also achieved in a Heliflux type machine, but the task of positioning a piece for the test, and disposing of it after the test, can be quite time consuming contrasted to the continuous stream of the Rotoflux method.

Figure 22 shows a Rotoflux test system prior to installation at a steel tube manufacturing plant. The system shown can handle material up to 16" in diameter but smaller versions have also been supplied for this type of application. The test station shown is simply positioned between two roller conveyors and the product to be tested is passed through the rotating test assembly, and the total cross-section is thus inspected.

Figure 23 is a photograph of a Heliflux machine which tests a bottle shaped, heavy wall, steel extrusion which eventually become a critical automotive component. The smallest of these machines tests a part which is roughly comparable in shape to the M-42 grenade bodies and about twice the size. This kind of part can be seen positioned in the Heliflux test assembly in Figure 24. The essential mechanical scheme of these machines utilizes a walking beam lateral transfer which moves each piece into a special arbor mechanism which clamps the piece between two centers. Once clamped, the arbor spins the piece and moves it longitudinally into the test mechanism. At the end of the stroke, the shoulder portion is scanned all at once by a specially shaped multiprobe. While it is still rotating, the piece is withdrawn back past fixed probe assemblies which inspect the straight portions. Any signal exceeding the threshold levels is registered as the part is brought back to the walking beam and released. The walking beam moves the tested part to the next downstream station, and simultaneously positions the next part to be tested in the arbor mechanism. At a convenient downstream station, parts which have registered as defective are separated from acceptable parts. A conservative estimate of the production rate of this type of Heliflux machine is 1800 parts/hour.

Both the Rotoflux and Heliflux machines described use transverse magnetization only. A conservative prospect is that the use of longitudinal magnetization would require additional test stations. Although there may be a future possibility of combining the techniques, methods have not been developed or tried at this time.

Since the form of a final testing machine is so dependent upon the final determination of test parameters, it is not prudent to suggest firm costs which, at this time, would be based upon a considerable amount of conjecture. This is especially true in the case of testing loaded grenades where safety considerations may disqualify the most attractive conventional solutions for handling nonexplosive parts. In order to roughly establish an order of magnitude,

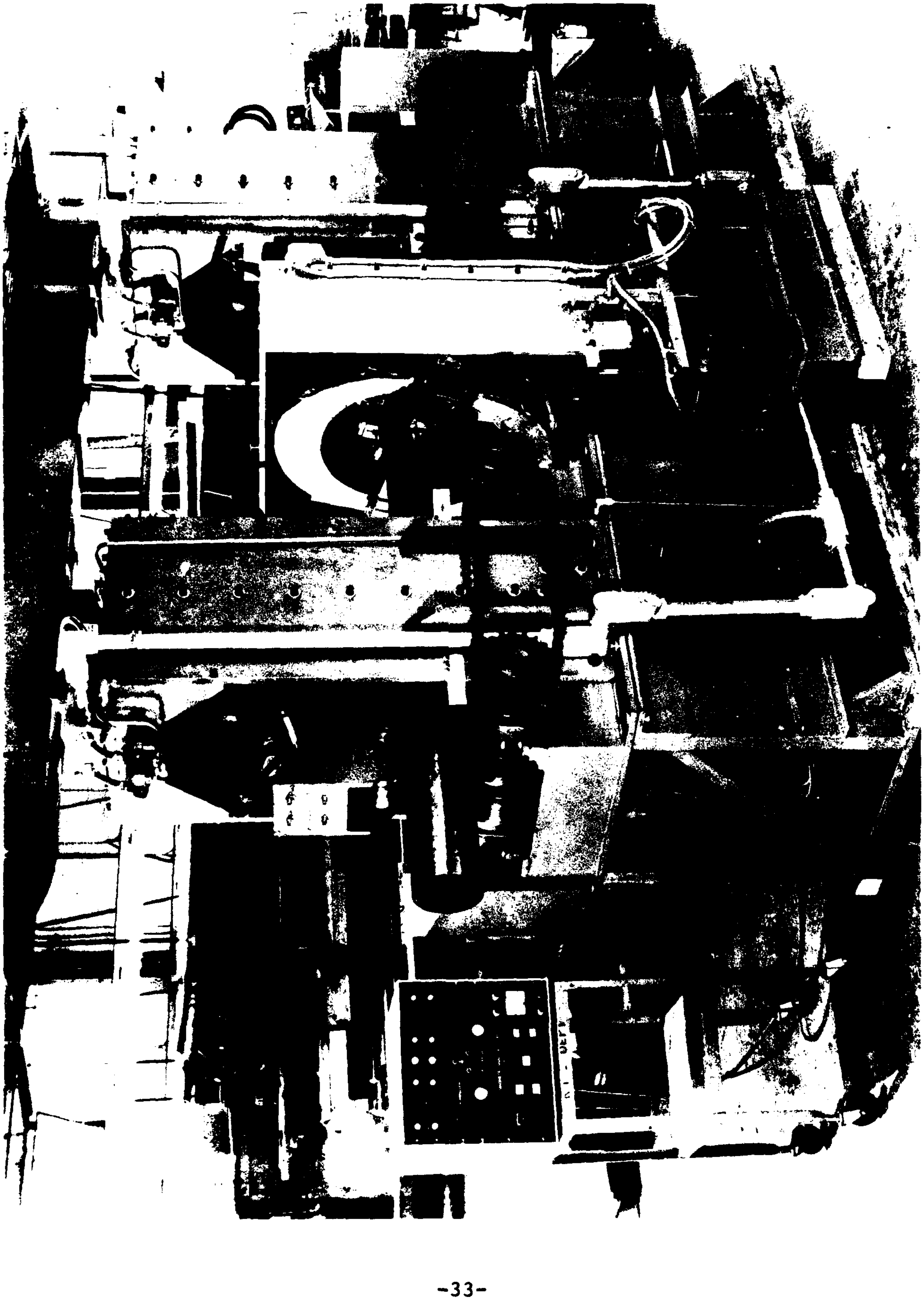

Figure 22

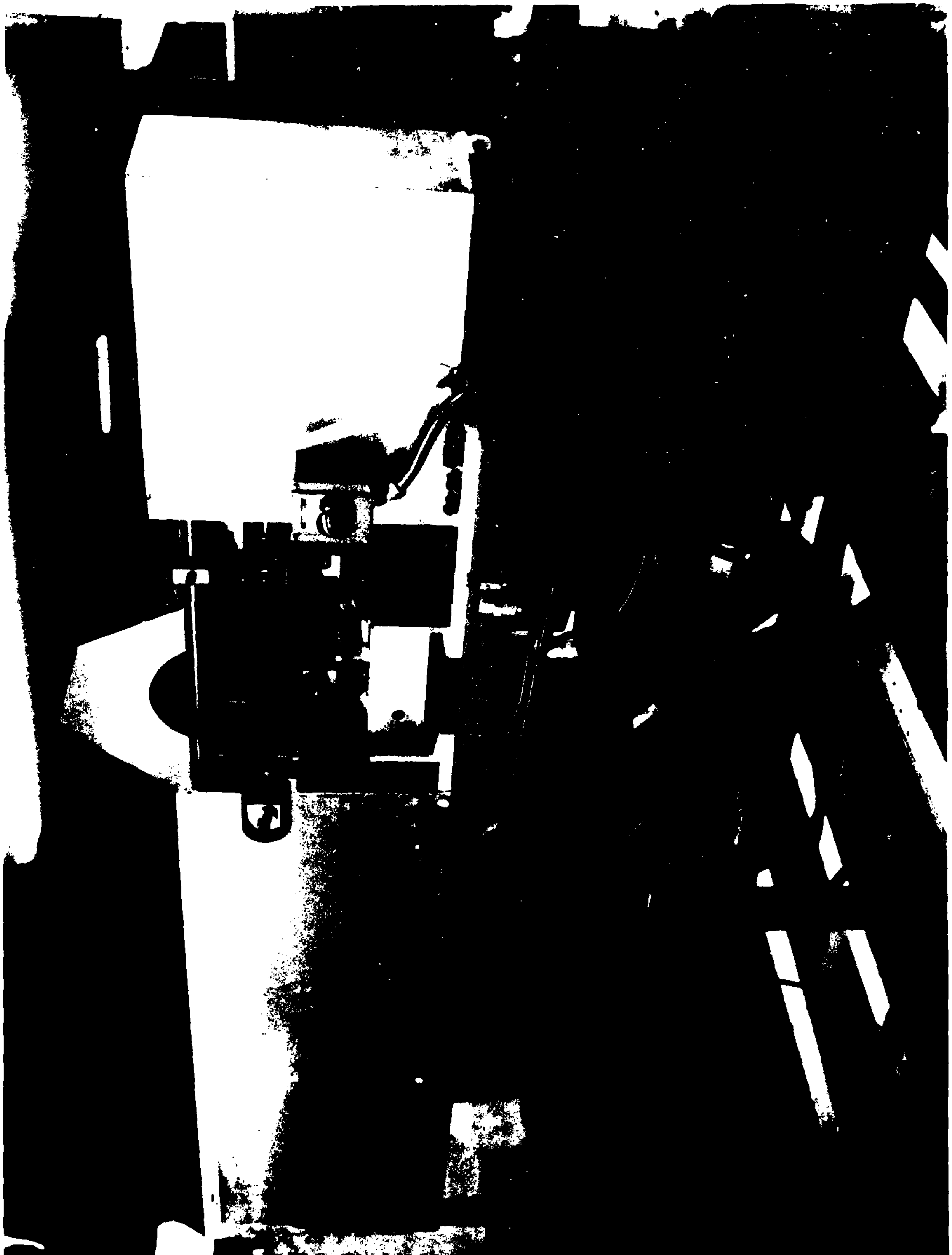

Figure 23

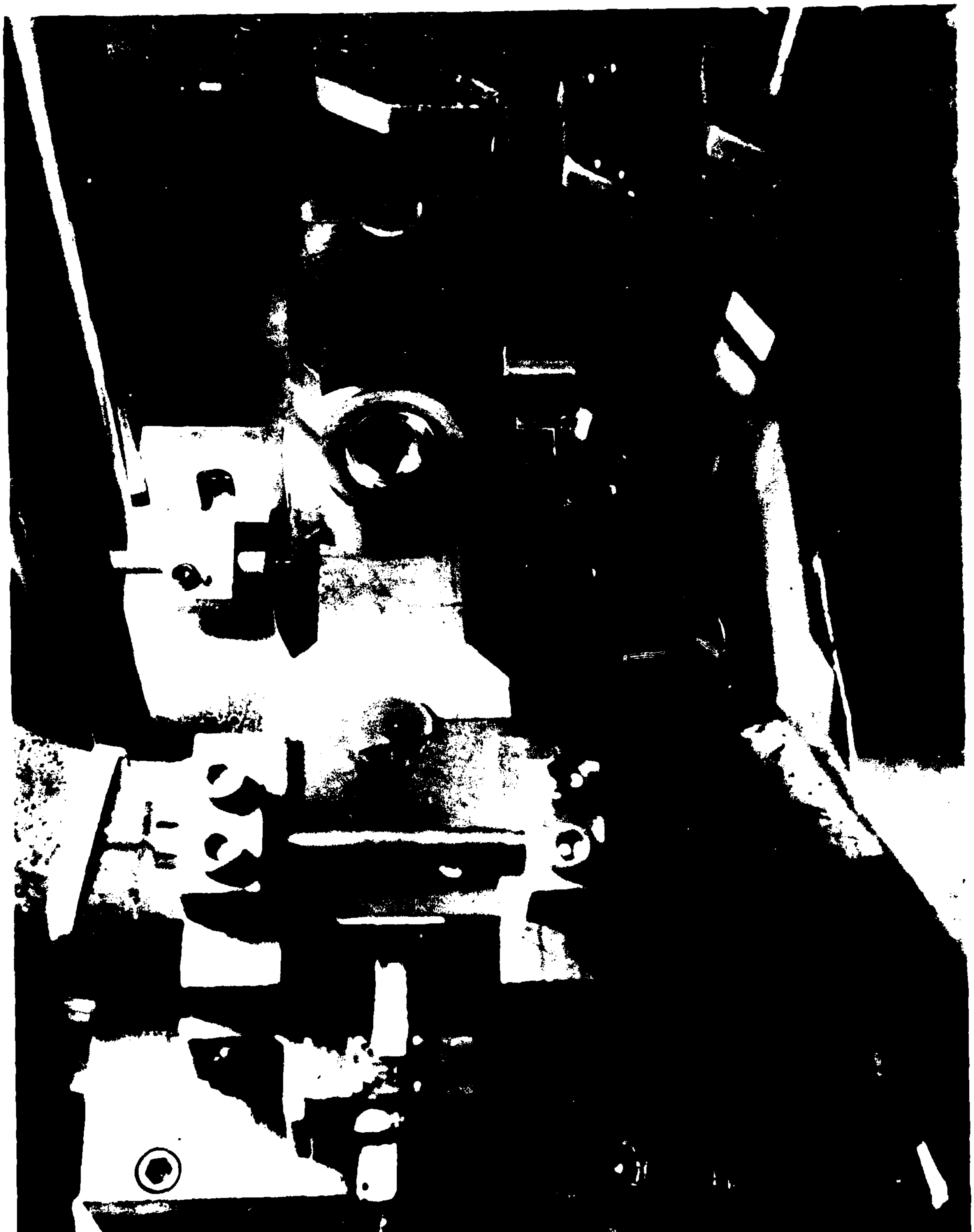

Figure 24

however, accurate prices have been established for the transverse magnetization Rotoflux and Heliflux type machines just described.

A 350 Rotoflux test station, which utilizes transverse magnetization, adapted to the portion of the test requirement it could accomplish, would cost approximately $50,000. As used to inspect the larger diameter, (skirt) only, it could comfortably handle 5,000 pieces per hour by nesting the grenades, one behind the other, along their longitudinal axes. Since the shoulder portion of each grenade would be totally inside the open end of the next piece, what appears as a continuous tube to the RFX is created. Addition of input and output mechanics and sorting would probably cost no more than an additional $25,000. This method will not provide inspection of the shoulder area, however, which is shielded by the material at the end of the adjacent grenade which it has been nested into.

In order to inspect the shoulder, the parts must be separated to expose the shoulder and positioned so that both the shoulder and the skirt can be inspected. This implies an intermittent flow which can be provided by the Heliflux machine which has been described. A machine like this would cost approximately $75,000 adapted to the M-46 grenades. As stated before, a reasonable production rate for this type of machine is 1,800 pieces/hour.

In both cases, for the first machine, of a type, there would be some additional costs for engineering time and the production of drawings, manuals, etc., which would become incidental in subsequent machines of the same type. Also, in the worst case, adding longitudinal magnetization capability might require duplicate test stations and roughly duplicate costs.

There is the hope that once the test parameters are finalized, economies might be realized by combining the basic machine elements in more efficient ways, but this cannot be determined at this time.

VII. CONCLUSIONS AND RECOMMENDATIONS

A. Summary of Results

Experiments conducted upon notched standards indicated that notches of depths in the range of 25% to 50% of the wall thickness can be reliably detected in any orientation and in any portion of the grenade body with signal-to-noise ratios which can accomplish repeatable reject sorting by an automatic machine. The longitudinal notches could be reliably detected at the 25% level or perhaps even less. The most difficult notch would be the 25% transverse E.D.M. I.D. notch in the embossed area, which can be seen in Figure 11 to have a signal-to-noise ratio of approximately 3:2.

Tests were conducted upon approximately 100 production pieces, some of which had shown magnetic particle defect indications. All known defects were detected by the experimental systems as well as three defective pieces which had been missed by the previous inspection method. Known natural defects were easily separated from the normal I.D. embossing.

B. Conclusions

Viewed in a broad sense, the leakage flux method seems an attractive basis upon which to build an automatic M-42 Grenade Body Tester. It has been shown to reliably detect notches in the size range suggested as meaningful, and poses no difficult problems of implementation. Futhermore, there is the acceptance of the method as an inspection technique for critical parts based upon favorable past experience. This past experience has been developed in ordnance applications such as the inspection of gun tubes, as well as in the inspection of high quality steel tubing and critical automotive parts.

C. Recommendations

The writers of this report cannot suggest a level of test which is appropriate, and which would be established by specifying reject reference notches. By the same token, they recognize that this is a difficult determination for those who must ultimately make this decision.

We are left with the dilemma of specifying test parameters which are the overriding determinants of the cost of an automatic machine, based upon this encouraging but limited study.

Rather than suggest a prototype machine immediately, which might result in costly mistakes which may become evident as more parts are inspected, it might be useful to install the experimental apparatus used in this study at a manufacturing plant. This could be done in a few weeks at a modest cost and would enable a comparison of results with present inspection methods, including metallurgical correlation with NDT results. It should be possible, in this plant environment, to determine whether the method lives up to its promise and, if so, what capabilities a full blown production machine should provide.

With this intermediate step, the first machine built would not only be a prototype but, hopefully, a useable production machine.

BIBLIOGRAPHY

THE TECHNICAL COUNCIL OF

THE AMERICAN SOCIETY FOR NONDESTRUCTIVE TESTING, INC.

SUPPLEMENT E - FLUX LEAKAGE TESTING METHOD TRAINING REFERENCES

14. R. S. Sharpe, ed., Research Techniques in Nondestructive Testing, Vol. 2, Ch. 5, Academic Press, New York, 1973.

T. Shiraiwa, T. Hiroshima, and S. Morishima, "An Automatic Magnetic Inspection Method Using Magnetoresistive Elements and Its Application," Materials Evaluation, May 1973.

J. M. Bridges, et al., "Residual and Active Leakage Fields Around Defect", Materials Evaluation, July 1978.

Magnetic Particle Testing Classroom Training Handbook, Ch. 2., General Dynamics/Convair Division, San Diego, 1967.

H. Luz, "The Nondestructive Testing of Bars and Billets for Surface Defects by Magnetic Leakage Methods," Journal of Nondestructive Testing, Vol. 6, No. 1, February 1973.

15. W. J. McGonnagle, Nondestructive Testing, pp. 316-317, Gordon and Breach, New York, 1969.

26. Howard E. Boyer, ed., Metals Handbook, 8th ed., Vol. 12, "Nondestructive Inspection and Quality Control," (1976), pp. 45, 46, 330, 338, 339, 430.

R. C. McMaster, ed., Nondestructive Testing Handbook, Vol. 2, Sec. 30, 32-24, Roland Press Co., New York, 1959.

Marek, J. Bergander, "Application of Integrated Record to Magnetic Testing of Steel Wire Ropes," ASNT Paper Summaries, National Spring Conference, New Orleans, April, 1978.

Marek J. Bergander, "Computerized Magnetic Testing of Steel Ropes," ASNT Paper Summaries, National Spring Conference, San Diego April, 1979.

Dennis N. Poffenroth, "Flaw Detection in Mine Hoist and Elevator Transportation Systems, "ASNT/CSNDT Conference/Show, Niagra Falls, May, 1979.

1978 Annual Book of ASTM Standards, Part II, ASTM, Philadelphia, 1978.

Marek J. Bergander, "Principles of Magnetic Defectoscopy of Steel Ropes," Wire Journal, May 1978.

Marek J. Bergander, Julivaz Stachurski, "A New Device for Magnetic Testing of Steel Ropes," 4th International Congress of Transportation by Rope, Vienna Austria, June, 1975.

Richard A. Egen, "Nondestructive Testing of Wire Rope," Offshore Technology Conference, Houston, May, 1977.

Hymar A. Feldstein, "The Magnetostatic Defectoscope - A Quantitative Characterist of Crack Depth and Width," Seventh World Conference on NDT, Paper No. D-32, Warsaw, Poland, June, 1973.

K. F. Banton, "Characterizing Defects by Determining Magnetic Leakage Fields," NDT International, October 1977, pp. 253-257.

J. Hobson, L. P. Swanepoel, "Some Developments in the NDT of Steel Wire Ropes," The South African Institute of Mechanical Engineering, Johannesburg, Australia, June, 1975.

C. M. Barrett, "Nondestructive Testing of Mine Hoisting Ropes in Ontario," Ontario (Canada) Department of Mines, Toronto, July, 1964.

SUPPLEMENT E - FLUX LEAKAGE TESTING METHOD TRAINING REFERENCES

J. R. Barton and F. M. Kusenberger, "Cible Data Base Acquisition on New and Used Bearings, "Proceedings of the 11th Symposium on Nondestructive Evaluation, San Antonio, April, 1977.

J. R. Barton and F. M. Kusenberger, "Critical Inspection of Bearings for Life Extension 'Cible', Proceedings of the 10th Symposium on Nondestructive Evaluation, April, 1975.

J. R. Barton, "Quantitative Correlation Between Magnetic Perturbation Signatures and Inclusions," ASTM Special Publication 575, 1975.

Robert E. Beissner, "An Investigation of Flux Density Determinations", AFML-TR-76-236 Air Force Materials Laboratory Technical Report.

J. Birchak, et al., "Engineering Appraisal of Southwest Research Institute Magnetic Crack Definer Applied to Ch 47 Rotor Blades," SWRI Report 15-3653, October, 1973.

Richard M. Bozorth, Ferromagnetism, New York, 1953.

F. Brailsford, Magnetic Materials, New York, 1951.

Frank L. Carr, et al., "Metallurgical Examination of 175-MM M113 Gun Tubes," AMMRC Technical Report AMRA TR 62-13, May, 1967.

G. A. Darcy, "Industrial Evaluation and Operation of the Automatic Crack Defector for Tubes, Model II, "Wal No. 732/114-7," June 1, 1951.

Thomas E. Davidson, et al., "The Fatigue Life Characteristics of the 175 MM M113E1 Gun Tube, "Wateruliet Technical Report - WVT6912, March, 1969.

James P. Finfera, "Materials Testing Technology Test of a Magnetic Recording Borescope," A PG-MT-3725, January, 1971.

James P. Finfera, "Special Study Evaluation of Hall Probe Magnetic Recording Borescope for Nondestructive Inspection of Cannon Tubes," APG-MT-4577, February 1975.

F. Forster, "Nondestructive Defect Inspection of Tubing and Round Billets by Means of Magnetic Leakage Flux Probes," Institute Dr. Forster, October, 1975.

F. Forster, "Nondestructive Inspection of Tubing and Round Billets by Means of Leakage Flux Probes," British Journal of NDT, January, 1977.

F. Forster, "New Results of NDT by the Magnetic Leakage Field Method, "Nondestructive Testing, August, 1971.

K. A. Fowler, "Magnetic Detection of Fatigue Cracks in Rifled 175-MM Gun Tubes, "Technical Note AMMRC TN 68-03, April, 1968.

K. A. Fowler, "Proposed Method of Correcting Magnetic Recording Borescope Results for Detection Lift-Off Variations, "Technical Report AMMRC TR68-09, May 1968.

K. A. Fowler, "Magnetic Methods for Crack Detection in Cannon Bores, "Technical Report AMRA TR 67-06, February 1967.

C. H. Hastings, "Crack Depth Measurement in Powder Chambers of Cannon, "WAL Report No. 732/123, July 1953.

C. H. Hastings, "The Development of a Flaw Detection for the Bore Surface of Gun Tubes, "WAL Report No. 732/114-1, August 1946.

Harold P. Hatch, et al., "Magnetic Recording Borescope Inspection Results of the 175-MM M113E1 Gun Tube Special Test for Service Life, "AMMRC TR 70-23, June 1970.

H. Hatch, et al., "Magnetic Recording Borescope Inspection Results of Autofrettaged 175 MM Cannon Tube," Watertown Letter Report APB-2, February, 1969.

H. Hatch, et al., "Preliminary Results of the Magnetic Recording Borescope Inspection of the M113 175 MM Gun Tube for Fatigue Cracks, "Letter Report by AMMRC, July 25, 1967.

H. Hatch, et al., "The Magnetic Recording Borescope - Instrumentation for the Inspection of Cannon Tubes, "AMMRC PTR 71-4, November, 1971.

M. E. Hollan, "Evaluation of the Linalog Pipeline Inspection System for the Detection of Corrosion in Navy POL Pipelines, "Technical Note N-1400 by Naval Facilities Engineering Command, September, 1975.

H. Hoshikawa et al., Suppressing Methods of Lift-Off Effect in Magnetic Defect Detedtion, "Journal of NDI, September 1976.

C. A. Hunt, "Nondestructive Measurements of Cracks in Gun Barrels, "Royal Armmament Research and Development Establishment Rorde Report, 20/75, December 1975.

R. D. Kodis, "Investigation of the Magnetic Field Strength at a Synthetic Crack of Varying Depth in a Magnetized Steel Plate, "WAL No. 732/114-6, January 1950.

R. D. Kodis, "The Development of a Flaw Detector for Gun Tubes, "WAL 732/114-2, January 1950.

R. D. Kodis, "The Application of the Induction Method of Crack Detection to Rifled Tubes, "WAL No. 732/114-5, February 1951.

F. Kusenberger et al., "Magnetic Perturbation Inspection to Improve Reliability of High Strength Steel Compounds," Proceedings Conference ASME Engineering, New York, May 1969.

F. Kusenberger, et al., "Development of Diagnostic Test Equipment for Inspecting Antifriction Bearings," AMMRC CTR-77-13, March, 1977.

W. Lord, et al., "Residual and Active Leakage Fields Around Defects in Ferromagnetic Materials," Materials Evaluation, July 1, 1978.

H. Lux, "The NDT of Bars and Billets for Surface Defects by Magnetic Leakage Methods," NDT, Vol VI, February, 1973.

James K. Stanley, Metallurgy and Magnetism, Cleveland, 1949.

W. Stumm, "Tube Testing by Electromagnetic NDT Methods - 1", NDT, October 1974.

W. Stumm, "Magnetic Stray - Flux Measurement for Testing Welded Tubes or Live," NDT, February, 1976.

R. D. Williams, et al., "Magnetic Perturbation Inspection of Artillery Projectiles," AMMRC-CTR-77-23, September 1977.

L. W. Winn, "Design and Evaluation of Ball and Roller Bearing Analyzers, "AMMRC CTR 76-27, August, 1976.

Donald C. Winters, "Automated Crack Position and Depth Measurements on Cannon Tubes," Wateruliet Technical Report - WVT 7248, Benet Weapons Laboratory, September 1972.

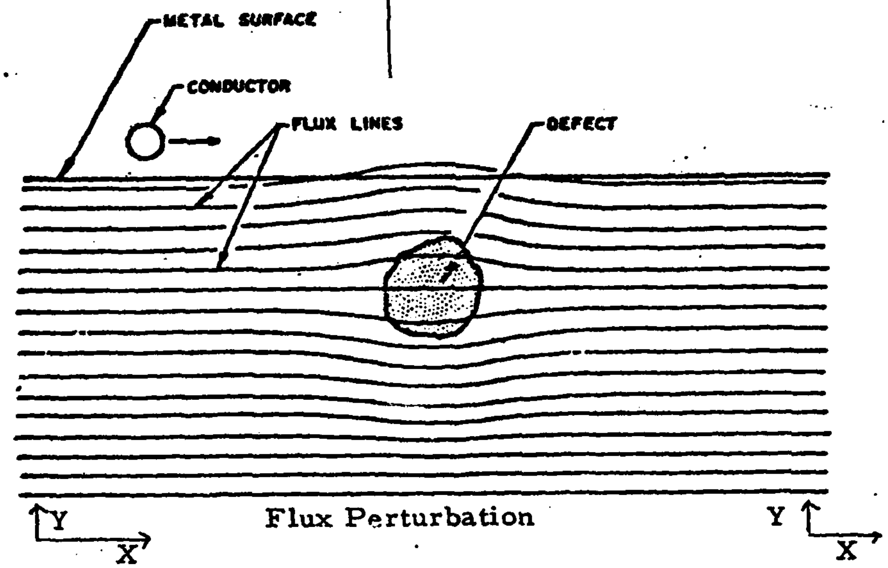

Effect of Inclusion Upon Magnetic Field for Two Depths for an 0.05-in. Inclusion with Applied Field in X-Direction. Scan is in Either X- or Y-Direction.

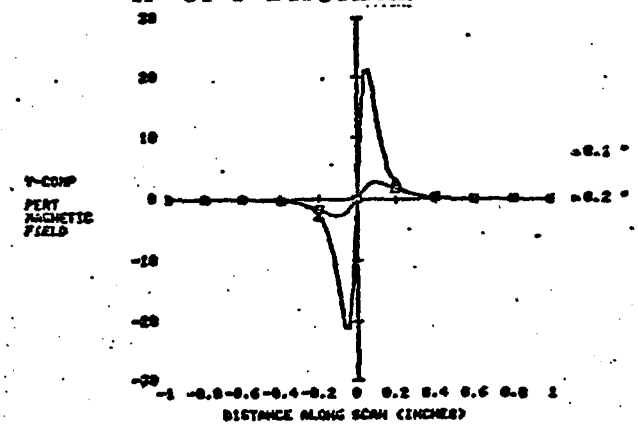

Effect of Inclusion Upon Magnetic Field for Two Depths for an 0.05-in. Inclusion with Applied Field in X-Direction. Scan is in Y-Direction.

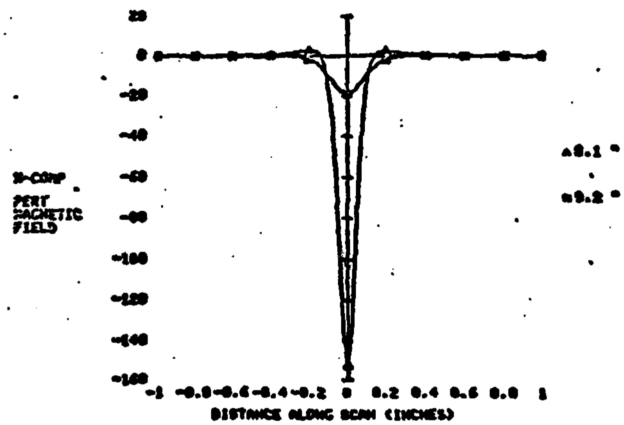

FIGURE 3. SCHEMATIC REPRESENTATION OF MAGNETIC PERTURBATION METHOD AND COMPUTER PLOTS OF SOLUTIONS-SIGNATURES

Appendix II

DATA SHEET NO.RFD-1

Magnetic Analysis Corporation

535 South 4th Avenue, Mount Vernon, N.Y. 10550 Phone 914 699-9450

ROTOFLUX Indicator and Control

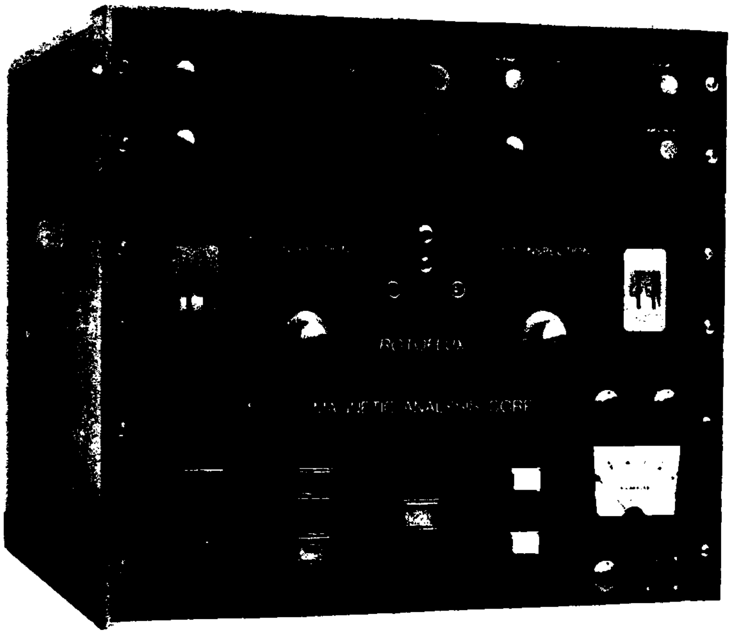

THE ROTOFLUX INDICATOR AND CONTROL:

- Inspects heavy wall magnetic tubing and tubular parts.
- No heavy power requirements, uses permanent magnets.
- Can find and differentiate between O.D. and interior or I.D. defects.
- Unique Multiprobes allow convenient operation at greater speed.
- Detects defects as small as 5% on O.D. and 10% on I.D., depending on general condition of material and manner of equipment utilization.

APPLICATION

The Rotoflux equipment uses flux leakage technology to find defects in magnetic, heavy wall tubing and tubular parts.

This method is highly advantageous in testing heavy wall tubing because it allows detection of surface defects, defects within the wall, and interior diameter defects. Moreover, the test can be run at higher rates of speed than are possible with alternative methods. Defects as small as 5% of the wall thickness on the O.D. and 10% of the wall thickness on the I.D. can be detected, depending on the general condition of the material and the manner in which the equipment is utilized.

DESCRIPTION

For the inspection of tubing, Magnetic Analysis Corp. utilizes a permanent magnet which is capable of saturating the material under test. The detection of any leakage field is accomplished by the use of probes specifically designed to respond to both low and high frequency flux patterns. These probes are utilized in a "multiprobe" configuration having the ability to select the largest instantaneous signal generated by a defect. Uniquely, the system will pass both the largest positive going and largest negative going signals independently. This permits uniform inspection where there are slight variations from the centerline between the product under test and the Multiprobes.

Usually, Multiprobes rotate in unison with the permanent magnet around the test material. (See Figure A). In other cases, the test material can be rotated while the Multiprobes and magnets are held stationary. (See Figure B)

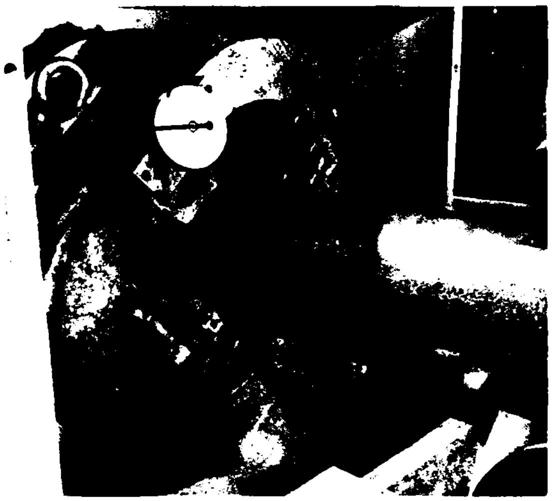

FIGURE A

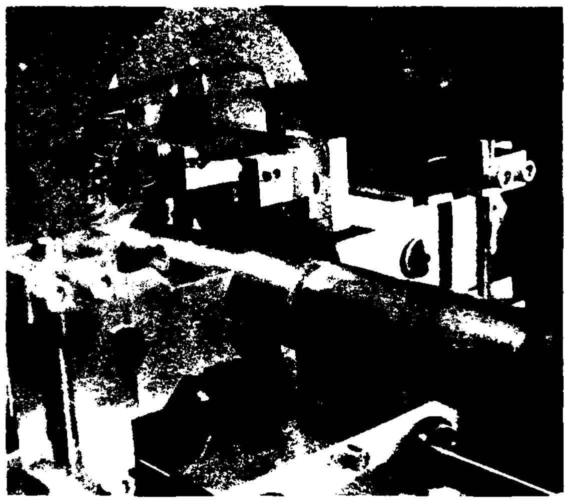

FIGURE B

The Rotoflux Indicator and Control Unit is designed with two separate channels for analyzing the information detected by the Multiprobes. Each of these channels has its own band pass filter, gain control, oscilloscope and readout circuits. The primary difference between them is the range of the band pass filtering available. The frequency generated by a surface defect is higher than that generated by an internal or I.D. defect. Therefore, with proper selection of band pass filters, it is possible to indicate surface defects on one channel and internal defects, including I.D. on the other.

A unique feature of the Rotoflux equipment is the flux measurement circuit which indicates the amount of flux density within the tubing to determine whether the material is properly saturated. This is accomplished with a special flux density detection probe whose output is shown on a meter.

When the Rotoflux unit is used in conjunction with rotating systems supplied by Magnetic Analysis Corp. for testing heavy wall tubing, systems are provided which include the suppression of end signals. (See Data Sheet Aux-9).

Magnetic Analysis Corp. has developed various rotating and drive mechanisms for the inspection of tubing. These are shown in Table I. Also available are custom handling systems for intricately shaped parts. These are usually designed for specific customer applications.

TABLE I

ROTOFLUX ROTARY & DRIVE MECHANISMS

TYPE NO.	SIZE RANGE OF TEST MATERIAL	MAXIMUM WALL THICKNESS	TEST SPEED *
350	1/2" to 3 1/2" (13mm to 90 mm)	.250" (6.4 mm)	50 fpm to 350 fpm (15 m/m to 107 m/m)
750	2 1/2" to 7 1/2" (64mm to 190 mm)	.625" (16 mm)	50 fpm to 350 fpm (15 m/m to 107 m/m)
900	2 1/2" to 8 3/4" (64mm to 222mm)	.625" (16mm)	50 fpm to 350 fpm (15 m/m to 107 m/m)
1600	2 1/2" to 15" (64mm to 381mm)	.750" (19mm)	25 fpm to 250 fpm (8 m/m to 76 m/m)

*Depending on size and wall thickness.

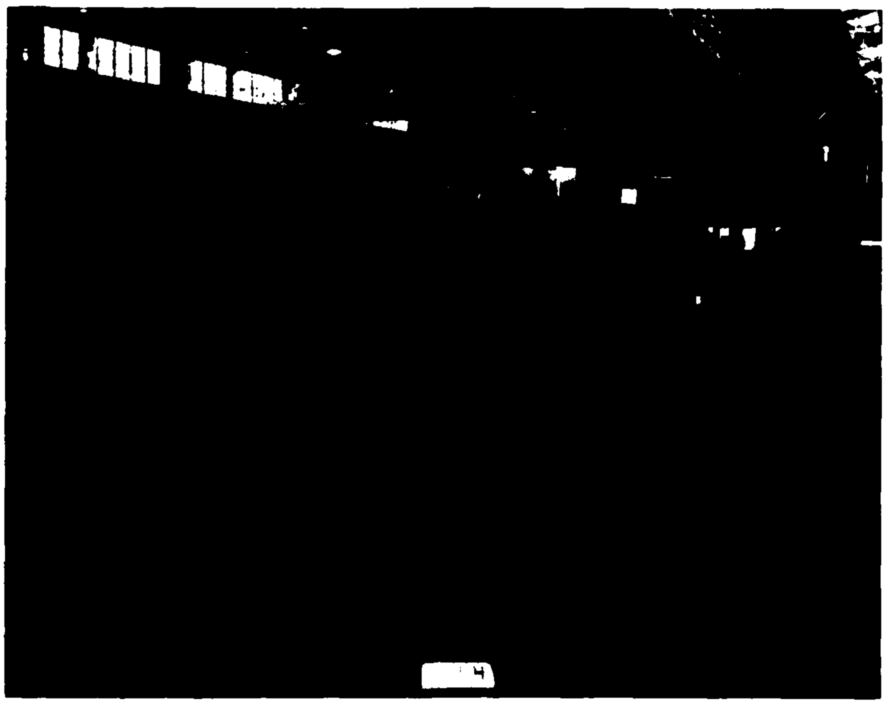

Large wall tubing being tested at a steel mill by MAC's new ROTOFLUX.

SELECTIVE CIRCUITS

Sensitivity	99 position step switch, adjustable in one db increments
Filter	8 steps to minimize unwanted signals - band pass type
Calibration	Built in pulsed signal - checks instrument levels to ± 2% accuracy
	External calibrator checks rotary probes and pre amps
Flaw Threshold	Single level, both O.D. and I.D. channels
Flux Density Meter	Indicates level of flux density in the material under test

DISPLAY & OUTPUTS

Oscilloscope	Two 3" CRT, long persistence phosphor, linear presentation
Alarm Systems	Flaw lights, one for each channel Audible signal, one for each channel
Outputs	Recorder - fast and slow for each channel 4 outputs available Relay - solid state, two for each channel (supplies 110 VAC)
Sweep Control	Automatic synchronization, or adjustable over a wide range

SPECIFICATIONS

Cabinet Dimensions	19" high x 20" wide x 22" deep (48cm high x 51 cm wide x 56cm deep)
Power Requirements	120 VAC, 60 cycles, single phase, 5 amp.
Weight	82 lbs. (38 kg) (electronics only)

For dimension and specifications of rotary installation, drawings are available.

Magnetic Analysis Corporation
535 South 4th Avenue, Mount Vernon, N.Y. 10550
Phone 914 699-9450

"LOCATING INTERNAL AND INSIDE DIAMETER DEFECTS IN HEAVY-WALL FERROMAGNETIC TUBING BY THE LEAKAGE FLUX INSPECTION METHOD"

by

Paul J. Bebick, Project Engineer

Magnetic Analysis Corporation
Mt. Vernon, N.Y.

Presented: October 2, 1973

The state of the art of locating defects in ferromagnetic material by means of leakage flux detection methods has been widely published. Considerable detail interpreting the physics of how a leakage flux occurs and its relationship to the causative defect's properties has been adequately covered by several authors associated with some of the leading organizations in the field of electromagnetic non-destructive testing. The intent of this paper is to circumvent the physics of flux leakage and to elaborate beyond their basic findings. It is hopeful that additional information will be disseminated with regard to the detection of internal and inside diameter (I.D.) defects in heavy wall ferromagnetic tubing, bar stock, and small parts produced from them.

Our leakage flux inspection system utilizes permanent magnets for saturating material, and specially designed low frequency responsive flux sensing probes. The probes are designed to operate as longitudinally adjacent scanners riding just above the surface of a tube specimen. They are utilized in what can be called "Multiprobe" configuration where each of their outputs is sent to individual preamplifiers having a single common output. That output is automatically selective of only the largest instantaneous outgoing signal regardless of which probe it originated from. Uniquely, it will pass both the largest instantaneous positive going signal and the largest instantaneous negative going signal in order to properly cover cases where the tested tube is not perfectly centered with respect to the multi-probes. This off-center condition tends to result in defect signals having mainly one polarity whose excursion depends upon which direction the tube is off center from the multiprobes. Since both types of signal excursions are being passed and further processed, the off center condition poses no threat of missing defects. In addition, since both excursions of any given defect indication are recombined to reconstruct the original signal, sinusoidal in nature, instead of a pulse where only one excursion is passed, it becomes feasible to utilize bandpass filtering techniques for further signal processing. This filtering technique provides some highly desirable system features, as will be seen.

As a result of only one output from all of the probes, only one signal handling instrument is required to process that output signal flow. In addition, because of the possibility of bandpass filtering, that instrument is further subdivided into two processing channels, one designated I.D. and one designated O.D. These two channels are identical, each having its own output signal display scope, flaw light and output alarm-marker relays. Each channel has its own gain control, individually selective, and its own selectable range of bandpass filters. It is the chosen range of filters that really distinguishes one channel from the other. It is also these filters that are the means for separating surface or O.D. defect signals into the O.D. channel and subsurface or I.D. defect signals into the I.D. channel. This separation is made possible because of differences in frequencies between O.D. defect signals and I.D. defect signals. It has already been disclosed in the literature that the leakage flux of an outside surface defect has higher frequency components than does the leakage flux of any internal or inside surface defect when being observed at the outside surface of a piece of ferromagnetic tubing having a heavy wall. In practice, then, the greater the wall, the greater will be those frequency differences between O.D. and I.D. defect signals. These frequency differences can readily be seen in figure 1 as a comparison of a 5% O.D. defect and a 20% I.D. defect in a 7-½" diameter, 5/8" wall piece of seamless #1020 steel tubing. This specimen was chosen on the basis of its large physical dimensions. It turns out that the O.D. defect signal has a major frequency that is more than four times greater than the major frequency of the I.D. defect signal. Simply by providing a low frequency range of bandpass filters for the I.D. channel, and a higher frequency range of bandpass filters for the O.D. channel, the two signals can be separated, for the most part, into two different channels for individual processing.

As can also be seen in figure 1, the amplitude of the 5% outside defect signal is greater than the amplitude of the 20% inside defect for a bandpass filter selected in the center of the frequency range between the two defect frequencies. It is this lack of signal amplitude relationship to defect size when comparing O.D. to I.D. defects that necessitates individual gain controls if the same percentage of defect, regardless of where it occurs in the wall, is to always trip the output alarm and marker. In fact, this criteria can most easily be met, simply by providing at least a dual channel system, with individual output alarms and marking systems.

The utilization of permanent magnets to transversely magnetize the test specimen offers unique simplification of both the energization procedure and the system electronics. Since the magnets require no power for energization, the number of slip rings required on the spinning headplate is reduced and heavy power cabling to the magnets is eliminated. The most advantageous benefit is that the permanent magnets spinning around the test specimen in fixed unison with the multiprobes only establishes a dynamic steady state flux within the specimen. Since no alternating fields are present, no carrier signal is developed from which the defect signals need to be demodulated in a detector. Instead, the resultant defect signals are steady state signals occurring only in true time. Since no detection or demodulation is required to further process the signals the electronics is greatly simplified. Even more significantly, because of the lack of those alternating fields, flux penetration into the tube wall is not so severely limited. The only disadvantage of permanent magnets is that they cannot be deenergized at will to remove foreign magnetic material or a tube that has inadvertently been pulled against a pole piece by the strong magnetic force. However, the pole pieces are made from a soft iron having low retentivity and can be easily removed from the basic magnets. Once removed, all foreign magnetic material will break free and the pole piece cleans easily.

As has also been shown in the literature before, there is a serious limitation that does exist concerning flux penetration into a specimen. As the RPM of the magnets and probes is increased from very slow values, the magnetization rate $\left(\frac{d\phi}{dt}\right)$ of the material increases also. This causes a faster occurring flux change in the material which in turn generates an accompanying large loop unidirectional eddy current flow also in the material. At slow speeds it is insignificant but as the speed is increased, this rotating current also grows in amplitude. In addition, the larger the tube diameter, the faster its outside surface speed for any given RPM and consequently, the greater will be the amplitude of that eddy current. This eddy current in turn produces a magnetic flux which opposes the originally induced flux in the material, thereby reducing the total flux and causing the material to fall out of near saturation. The material must be very close to saturation in order for flux to flow close to the I.D. surface and thereby generate any leakage flux in the presence of an I.D. defect. Any reduction in flux will take place near the I.D. surface first and the I.D. defects will be missed. It is equally important not to fully saturate the test specimen because this tends to cause the flux to jump small O.D. defect gaps, significantly reducing the flux leakage for those O.D. defects.

At the same time that the large eddy current is resulting in a reduction in total flux in the material, it is also causing an undesirable field that is coupled into the test probes. As the RPM or tube diameter is further increased, this field grows with the eddy current and gradually masks out any signal indications gotten from the tube. This phenomena is apparent in figure 2 where the 20% I.D. defect is easily Fig 8 detected at lower speeds, optimized at 60 to 80 RPM, and rapidly deteriorated above 100 RPM. On the basis of these results, it can be surmised that a reciprocal tradeoff between tube diameter and RPM does exist and that on the basis of these two parameters some optimum surface scan speed for the magnets and probes does exist for each different type of conductive material. The loss of defect signals has been termed "Eddy Current Shielding" since an eddy current is the mechanism behind its occurrence.

Since slower RPM is required to inspect large diameter tubing, system throughput declines drastically. Fortunately, throughput for the larger diameter tube mills is considerably slower and any differences between production and testing throughputs can be equalized simply by adding more longitudinal probe scanners to the multiprobe. Another multiprobe can be added 180° away from the original one in the magnet structure to further double the test path and hence double the throughput. As an example, two-four inch multiprobes, 180° apart, containing a total of 16-$\frac{1}{2}$" long probes which yield an 8" long scan path, and spinning at 80 RPM around a 7-$\frac{1}{2}$" diameter tube, offers

100% inspection at 53.5 feet/minute. A throughput of 50 FPM would be feasible here in order to locate defects as small as holes.

The beneficial effects of bandpass filtering of signals emanating from an area of tubing that contains a 10% I.D. defect can readily be seen in figure 3. Without this particular chosen filter, the higher frequency tube noise is passed by the electronics to such an extent that the defect signal to noise ratio (S/N) is only 3 to 1. The switching in of a relatively broadbanded bandpass filter having a rather low center frequency of about 8 HZ sufficiently blocks the system's passage of those higher frequency noise signals while at the same time passes the lower frequency I.D. defect signal without significant attenuation. Its response resulted in a defect signal to noise increase of 11 to 1 at the output scope and recorder. The amount of defect signal attenuation that occurs as a result of this filtering can easily be made up by increasing the selectable gain of the instrument.

In addition two holes were drilled 180° apart on a common circumference line of the tube. The larger hole was approximately double the diameter of the smaller one (.062" & .029"). The effects of using two different filter ranges, one from the O.D. channel and one from the I.D. channel can be seen in figure 4. For the case of the O.D. channel where the chosen filter had a center frequency of about 100 HZ., the ratio of the largest defect signal to the smaller one is just under the actual defects size ratio. For the case of the I.D. channel where the chosen filter had a center frequency of about 15 HZ., the ratio of defect signals is just above the defects size ratio. In both cases, the hole defect signals closely correlated to the diameters of the holes, since both of their depths were completely through the wall. In addition, both cases passed the defect signals with values close to the size ratio value, except for one case being below that value and the other case being above that value. Based on the similarity of signal levels for both cases, it can be assumed that small hole defect signals will appear in both channel outputs with approximately the same signal levels, for normal filter ranges being utilized in each channel. Furthermore, since the signal ratio got larger as the center frequency of the filter was decreased, it is safe to say that the larger the diameter of the hole, the lower will be the frequency components of its corresponding signal. This is expected since the leakage flux path must be broader for larger holes in order to jump over the larger gap involved. Looking at the results from the reciprocal direction tells us that the smaller the hole diameter, the higher will be the frequencies of its corresponding defect signal.

The design of the multiprobe is optimized only when a very large number of pinpoint length probes can be used. This is generally a requirement for designing probes that will create a defect signal that principally correlates to the depth of the defect and ignores its length. However, some electronic limitations do exist concerning the number of probes that can be used in the multiprobe configuration. In order to keep below the maximum number of probes allowed by those limitations, each probe must have some particular length that allows a sufficient multiprobe scan length which compensates for the slow test RPM required. The chosen length of each probe was one-half inch. This meant that accurate signal correlation to defect depth for relatively consistent depth defects could only be guaranteed for defects over one inch in length. This doubling of the defect length over a single probe length is necessary to cover the case when the defect lies centered under two adjacent probes and a one inch defect length is necessary for the defect to lie completely under any single probe. The shortcomings of this multiprobe construction is that the amplitude of signals caused by holes and defect lengths that are shorter than the length of the probe under which they lie, is considerably less than the amplitude of signals caused by equal depth longer length defects. The easiest way around the problem is to reduce the length of each probe to one-half the length of the shortest defect which must be accurately depth correlated to its signal indication. Of course, some sacrifice of testing throughput will occur, but it can be made up with a second set of multiprobes connected in parallel with the first set.

One of the most impressive features of the leakage flux method of test was the accuracy of signal correlation to defect depth once the length factor has been made constant. This was accomplished by producing all defects with a length of two inches and was equally true when comparing O.D. defects or when comparing I.D. defects. A typical example of comparing O.D.

defects can be seen in figure 5. Since these were air abrasive notches made over a two inch length, their depth was not entirely consistent. The depth along the length of each defect had a definite gradient that showed itself in molds made of each defect. The actual depth variation is shown on each recording.

Another impressive point noted when dealing with O.D. defects was that a bandpass filter could easily be chosen to yield signal to noise ratios (S/N) of about 20 to 50 / 1 for a depth range of defects from 5% to 15% of the wall, respectively. In comparing each defect's signal indication, it was assumed that the 6 - 10% depth defect had an average depth close to 10% because of large portions of the two inch long mold being at the 10% value. On that basis, the 3 - 5.5% defect correlates closely as a 5% value, also closely verified by the mold of its dimensions. On the basis of those two defects, the largest 8 - 16% defect correlates as a 13% or a 14% value. Its particular mold had considerable length that measured between 12% and 15% with very little length below or above those values, so a fairly accurate correlation was obtained for that largest O.D. defect also.

The same accurate results were obtained on a tube sample of type 1015 carbon steel electric resistance (E.R.) welded tubing with an outside diameter of 3-¼" (8.25 CM.) and a wall thickness of ½" (1.27 CM.) having a defective length of cold weld within it. In addition to finding longitudinal I.D.

notches ranging from 5% (.025"-.625 MM.) to 20% (.100-2.54 MM.) of the wall, the leakage flux from the defective weld zone was easily sensed with each pass of the multiprobes. Recording the leakage flux signals from each of those passes at a slow recorder speed produced a profile of the extent of that defective weld for slowly changing variations of the weld over a length considerably longer than the length of the multiprobes. If any rapid variations of the weld do occur in a small length under the multiprobes, only a worsening of the weld condition will be acknowledged. If those rapid variations happen to be improvements in the weld, they will go unnoticed because of a portion of adjacent more defective weld line lying under the rest of the multiprobes, the worst of which is only being acknowledged by the system itself. A typical defective weld line profile can be seen on the recording in figure 6. In addition to it, the profile of a long 10% (.050"-1.27 MM. DEPTH) I.D. defect whose beginning depth was more shallow than 10% can be seen. The following full depth indications yielded a signal indication of about one half the amplitude of the defective weld signal indications. Similar results were also obtained from artificial defects and a defective weld line in a length of 4130 alloy steel tube of 3-½ inch O.D. and 3/8 inch (9.5 CM.) wall thickness.

This type of leakage flux inspection system located on a welding line setup some safe distance immediately after the welding operation takes place, could supply the weld line operator with early recognition of any defective weld being produced. Immediate action can then be taken to either manually or automatically correct the conditions of the welding process. In cases where it cannot be installed on the welding line, it can be used to further upgrade the final inspection station of welded product, since it offers a highly reliable and relatively inexpensive testing method.

Considerable success has been attained in applying leakage flux test methods to the inspection of small and medium length ferromagnetic parts for the detection of seams, cracks and non-magnetic inclusions within them. The smaller parts such as fasteners, spacers, and tapered,roller bearings can be sufficiently magnetized with small permanent magnets to effect an adequate leakage flux in the presence of one of those aforementioned defects. Of course, the mechanical feed and parts handling system has to be of a different nature than the long tubular and bar product handling system, but the test methods are identical. Some handling system possibilities are of the rotating disc - fixed rail or rotating support rails nature which can be used to longitudinally advance and simultaneously rotate each part beneath a fixed probe or fixed multiprobe. Larger parts such as drive shafts, torsion bars, fastener stock and gun barrels can be handled as though they were long tubular product, with the magnet assembly and probes rotating around them. To effect a proper test, only relative rotational movement between the test specimen and the magnet assembly and probes is required. The logistics of the mechanical system which produces this relative rotation is left up to the ingenuity of the system designer.

In conclusion, a large variety of circular parts, solid or tubular, having a large range of sizes, lengths, diameters and thicknesses can be adequately inspected with an appropriate leakage flux inspection system. The depth of inspection obtained is greater than that obtained through the use of eddy current, visual, and magnetic fluorescent particle inspection systems. In addition, since it is easily automated and relatively inexpensive to install, the system should be highly competitive with Ultrasonic inspection systems for ferromagnetic tubular product of almost any diameter having wall thicknesses up to three-quarters of an inch (1.91 CM.), as well as for bar product up to one and one-half inch (3.82 CM.) in diameter. A most desirable feature of the system is the avoidance of the liquid couplants and numerous seals associated with watertight integrity that are required for an ultrasonics system. The leakage flux system is further simplified with the usage of permanent magnets for specimen magnetization eliminating the need for both heavy power requirements and magnet coil cooling water. Having such a simplified inspection system, where output signals are well correlated to the depth of their defects, the user can be reasonably certain of not missing any meaningful level of defects in his product. On the basis of those correlations, it should be easy for him to classify defective parts according to their degree of defectiveness. He should then be able to set up simpler, more meaningful rejection levels to suit his product's end usage as well as to meet the product safety requirements of each of his customers and to ensure the final consumer of a safe and reliable product.

SYSTEM DESCRIPTION

This particular leakage flux inspection system has been designated "ROTOFLUX" which is an abbreviation of the "rotating magnetic flux" set up in the specimen. The spinning mechanism contains the multiprobes, each of their preamplifiers and the signal recombination adder as well as a sync reference point relative to the tube specimen that generates a triggering pulse in a sationary mounted sync generator which is used to start each adjustable sweep of the scopes. As designed, the single output of the multiprobes is supplied to two channels simultaneously which are used to separate incoming signals on the basis of their frequency differences. The chosen Bandpass Filter is responsible for that separation. Each channel then has identical components after its filters. An attenuator or sensitivity control is provided to reduce the high incoming levels of signals to a workable level. They are capable of individual DB gain selectivity out of a possible 100 DB available. (100,000/1 ratio). A high voltage amplifier is provided to bring signals up to levels necessary to display them on the oscilloscope. At the same time they are used to trigger an adjustable threshold output which is used to control a decision switch, if a specified level of defect signal is surpassed. Each channel threshold triggers the flashing of an independent alarm light and any external horns and paint markers that may be connected to each decision switch. This feature provides completely independent channel marking and sorting facilities that may be used to immediately determine whether the defect is on the surface or within the material.

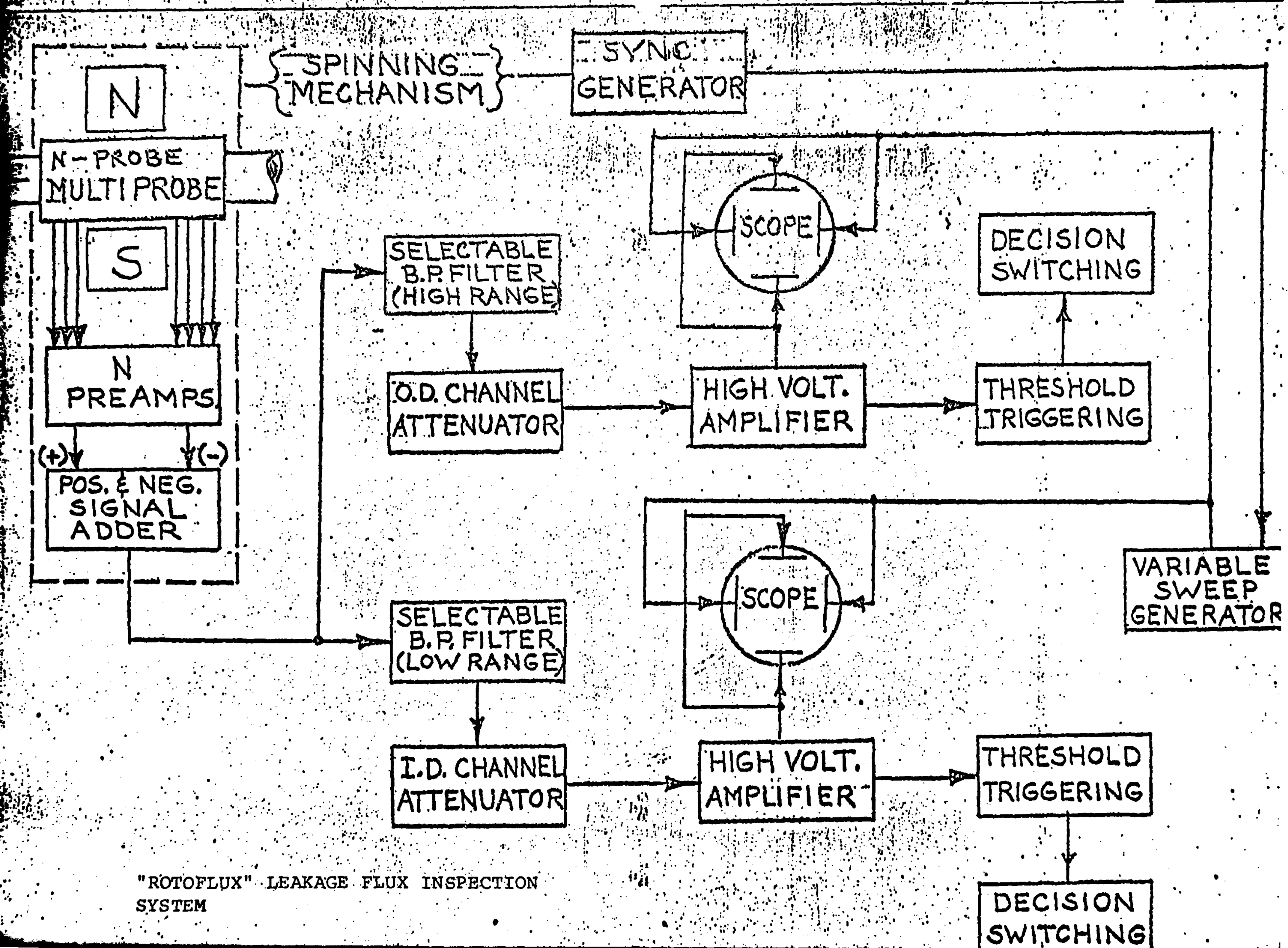

"ROTOFLUX" LEAKAGE FLUX INSPECTION SYSTEM

AT'L. O.D. – $7\frac{1}{2}$" (19 cm.) WALL THICKNESS – .625" (1.59 cm

NOTCHES: O.D. – .035" (.89 mm.); I.D. – .125" (3.17 mm.)

BANDPASS FILTERED: f_c = 40 to 60 HZ.
B.W. – 100 HZ.

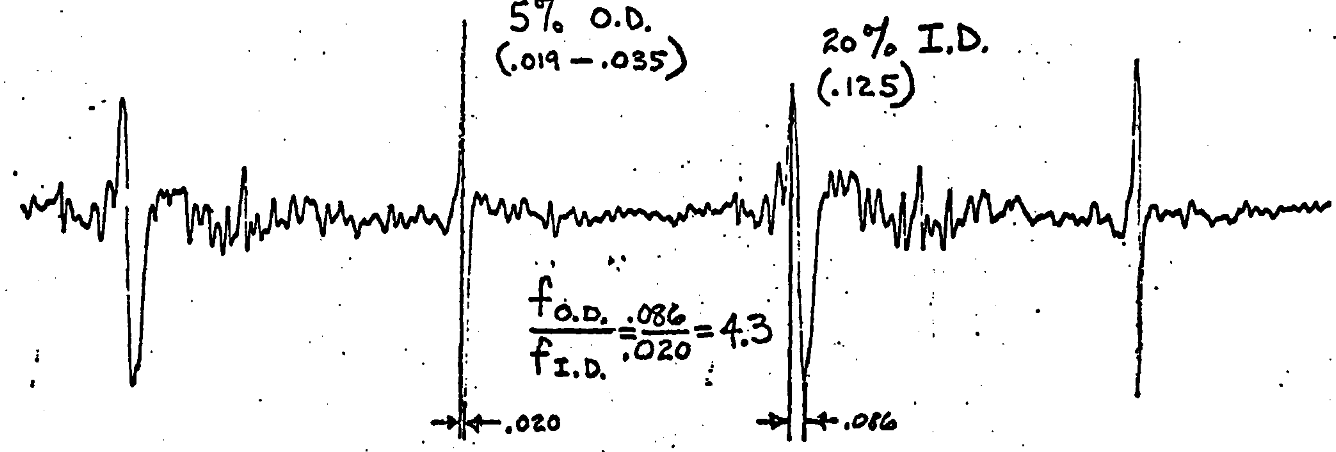

FIG. 1

FREQUENCY RELATIONSHIP – O.D. & I.D. DEFECTS

AT'L O.D. – $7\frac{1}{2}$" (19 CM.) WALL THICKNESS – .625" (1.59 CM

FECT: .125 (20%) – 3.18 MM. I.D.

EFFECT OF HIGH RPM CAUSED E.C. SHIELDING OF I.D. DEFECT

FIG. 2

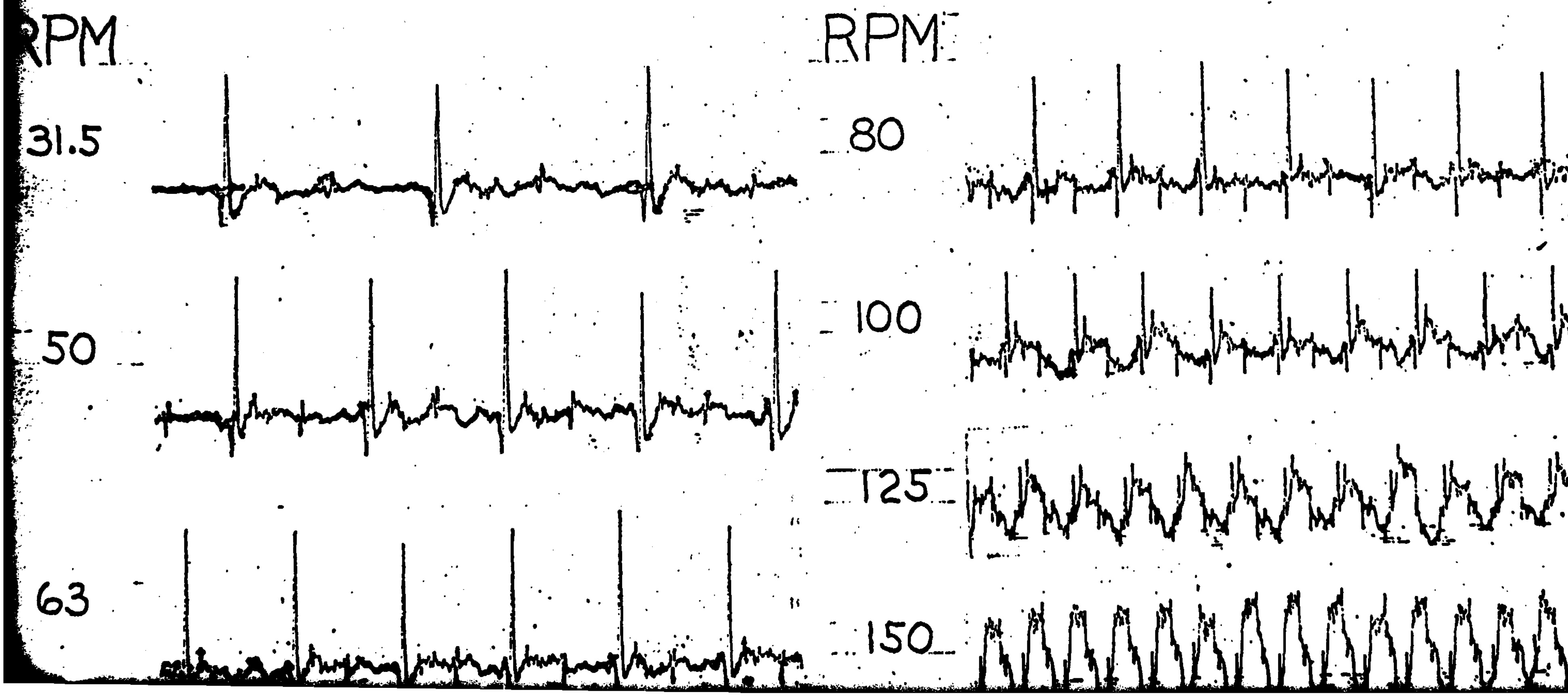

MATL: 1020 SEAMLESS
RPM: 63
SURFACE SCAN: 125 F.P.M.

TYPE NOTCH – AIR ABRASIVE

.064" = 1.625 MM. $7\frac{1}{2}$" = 19 CM. .625" = 1.59 CM.

.064 (10%) I.D. DEFECT IN 7-1/2" O.D. - .625 WALL TUBE

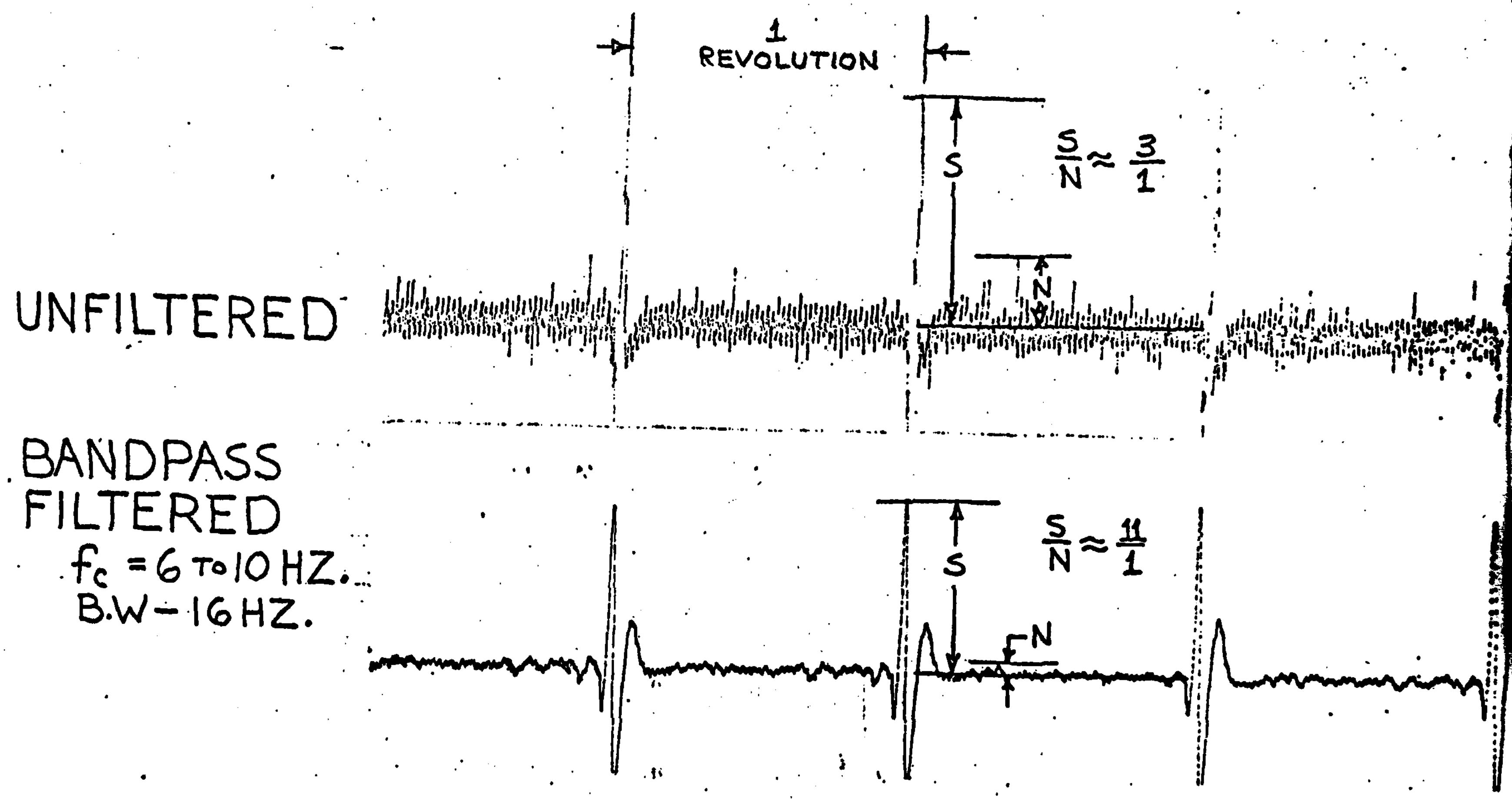

FIG. 3

.062" (1.57 mm.) & .029" (.735 mm.) HOLES IN 7-1/2" O.D. - .625" WALL
7-1/2" = 19 cm. .625" = 1.59 cm.

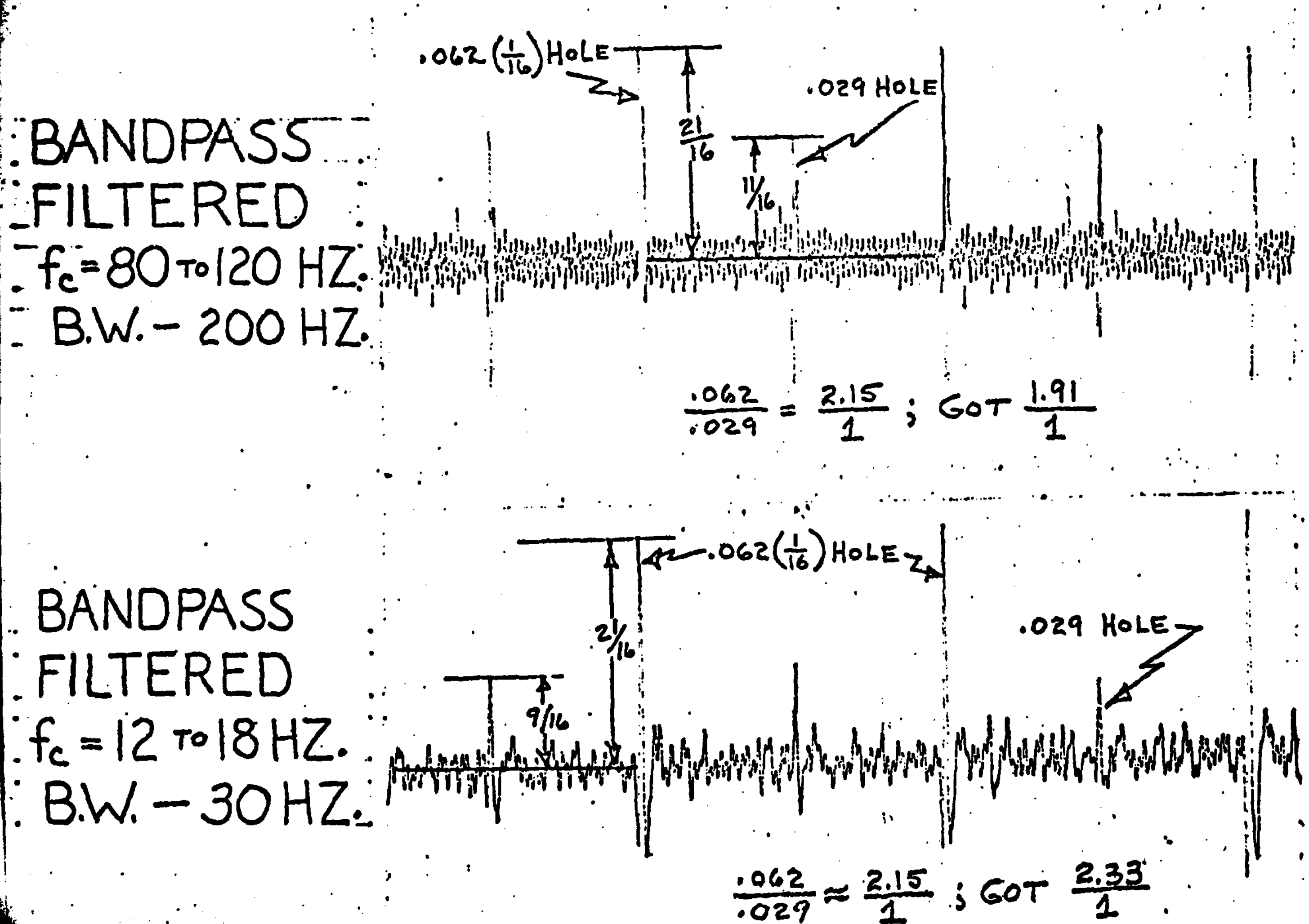

FIG. 4

DEFECT LENGTH: 2" (5.08 CM.)

INSTRUMENT SENSITIVITY: 60 of 100 DB (GAIN DOWN $\frac{100}{1}$)

DEPTH RELATIONSHIP - O.D. DEFECTS - 1/2" (1.27 cm.) WIDE PROBE

BANDPASS FILTERED

f_c = 80-120 HZ. B.W. - 200 HZ.

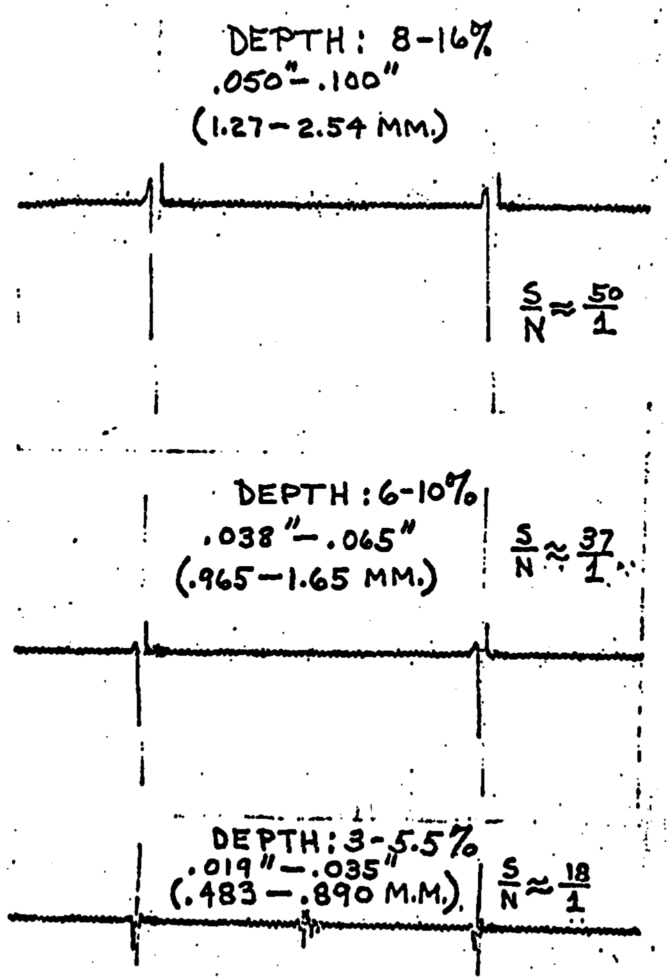

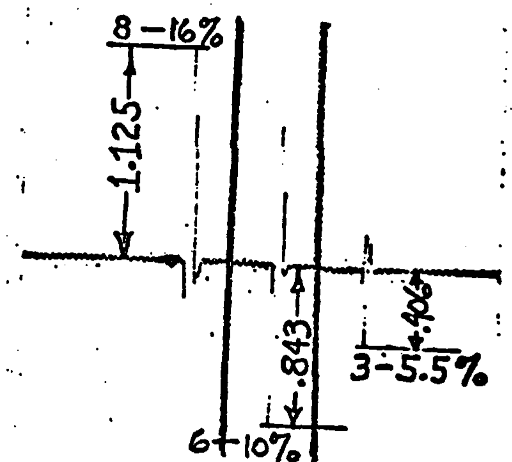

ASSUMING .843 IS 10%:

$\frac{.843}{.406} = \frac{2.07}{1} \approx \frac{10\%}{5\%}$

$\left.\begin{array}{l} \frac{1.125}{.843} = \frac{1.34}{1} \approx \frac{13\%}{10\%} \\ \frac{1.125}{.406} = \frac{2.77}{1} \approx \frac{14\%}{5\%} \end{array}\right\}$ 1.125 HA[S] A 13-14% AVG. DEPTH

FIG 5

MAT'L: 1015 CARBON STEEL — $3\frac{1}{4}$"(8.25 CM.) O.D. — $\frac{1}{2}$"(1.27 CM.) WALL

RPM: 200 10% - .050" - 1.27 MM.

MULTIPROBE PROFILE OF 10% I.D. & WELD LINE DEFECTS

UNFILTERED

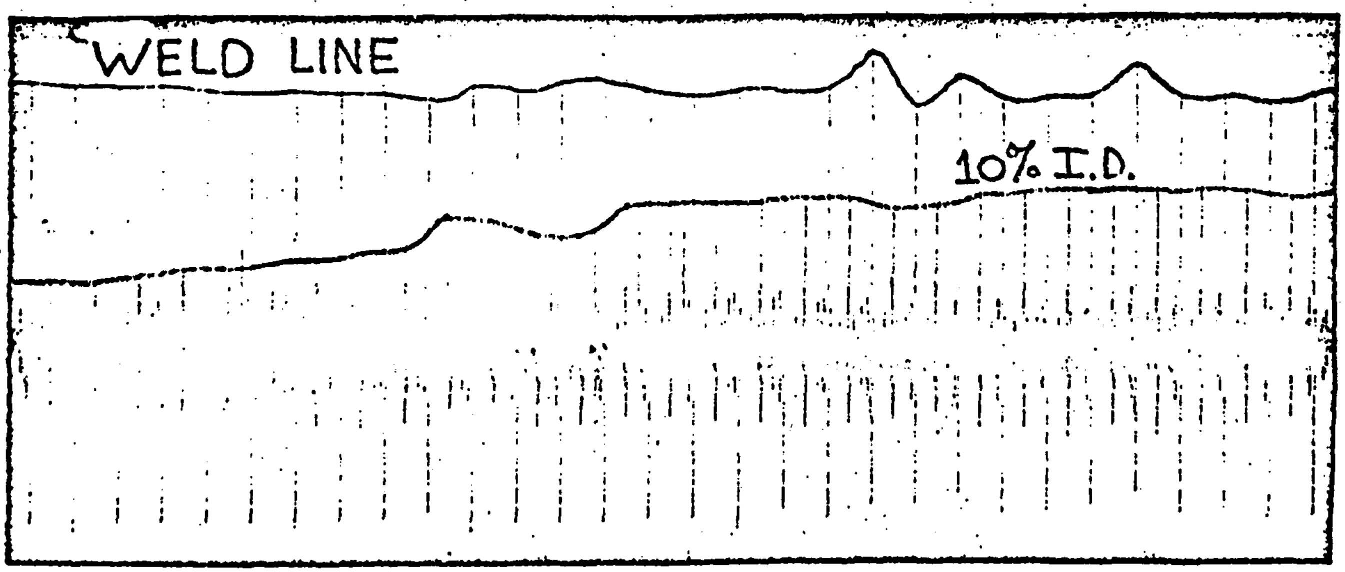

FIG. 6

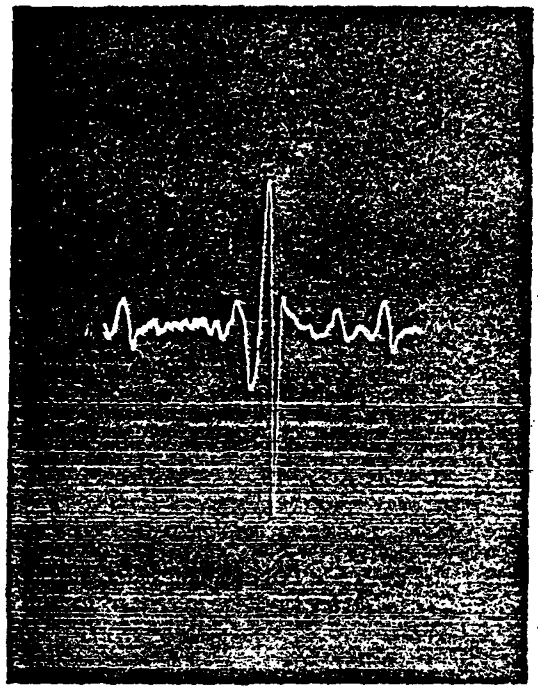

TYPICAL WELD LINE DEFECT SIGNAL OBTAINED WITH "ROTOFLUX" LEAKAGE FLUX INSPECTION SYSTEM

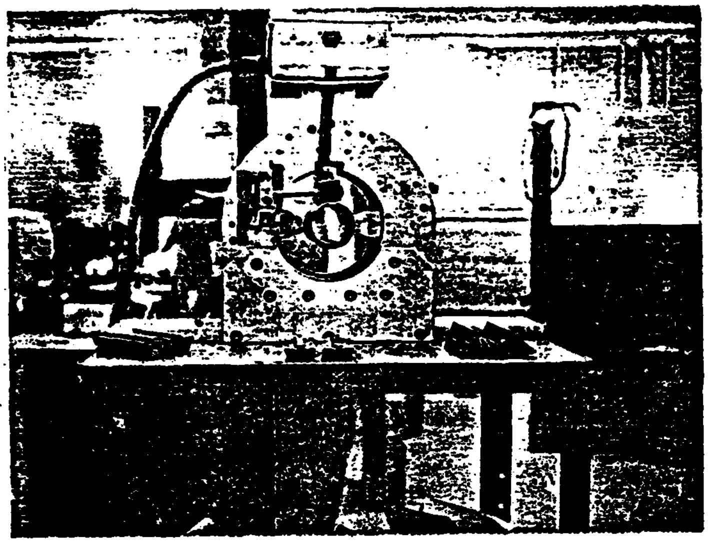

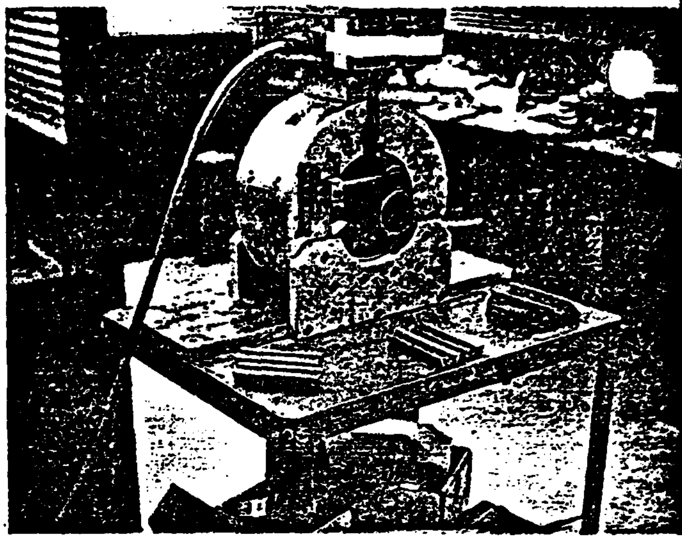

VIEWS of FIXED MAGNET & MULTIPROBE ASSY.

WITH INTERCHANGABLE POLE PIECES, ADJUSTABLE PROBE RIDE, AND MAGNET DISTANCES & NON-ROTATING PREAMPLIFIERS

ROTATING TEST SPECIMEN SYSTEM

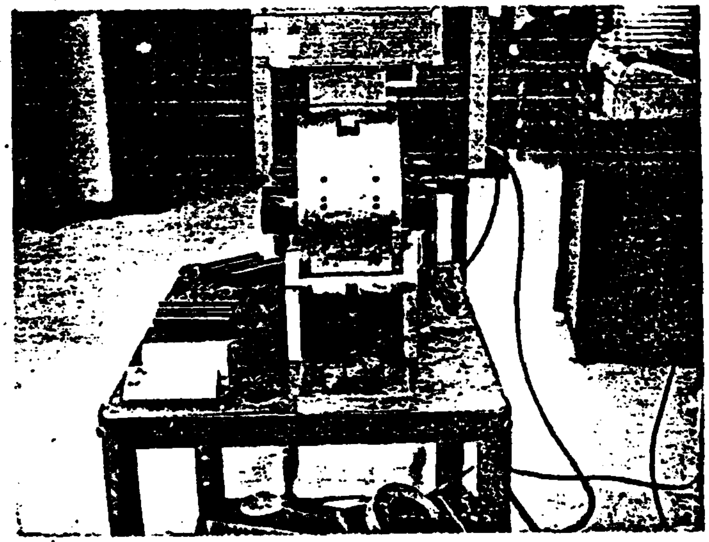

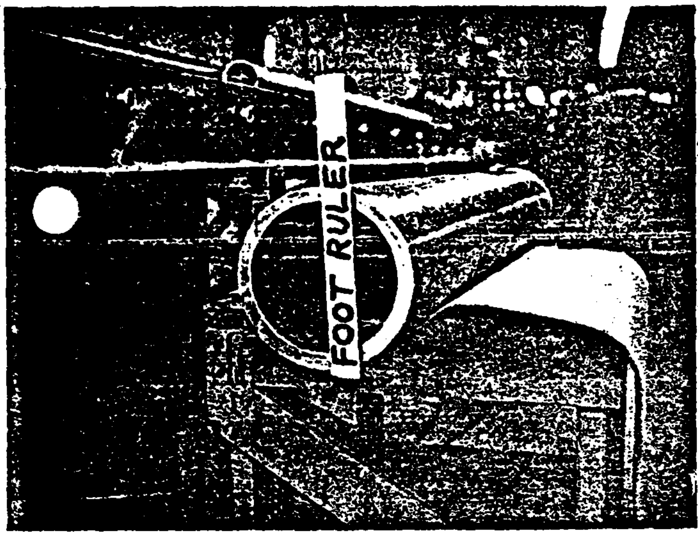

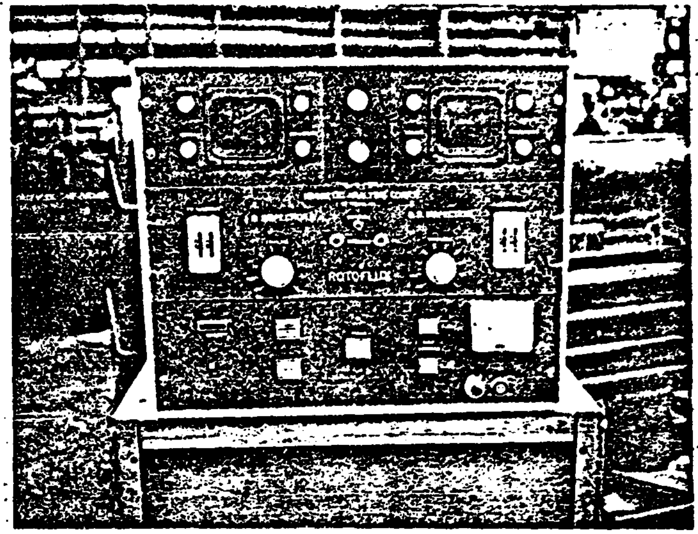

$7\frac{1}{2}$"(19 CM.) O.D. × $\frac{5}{8}$"(1.59 CM.) WALL TYPE 1020 SEAMLESS
&
"ROTOFLUX" TEST INSTRUMENT CABINET

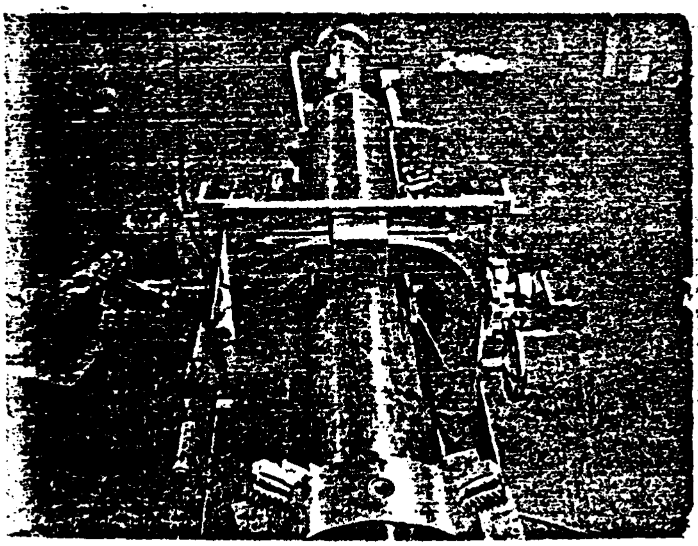

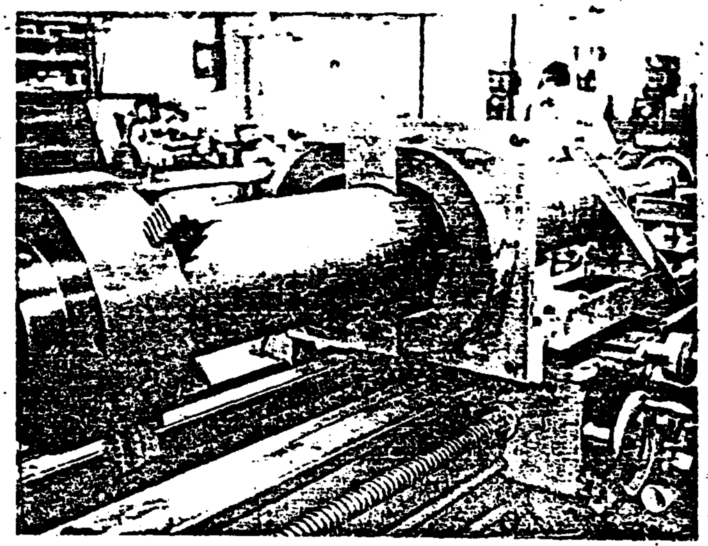

TEST SETUP VIEWS of MAGNET ASSY. & PROBE
FNCOMPASSING THE ROTATING TUBE

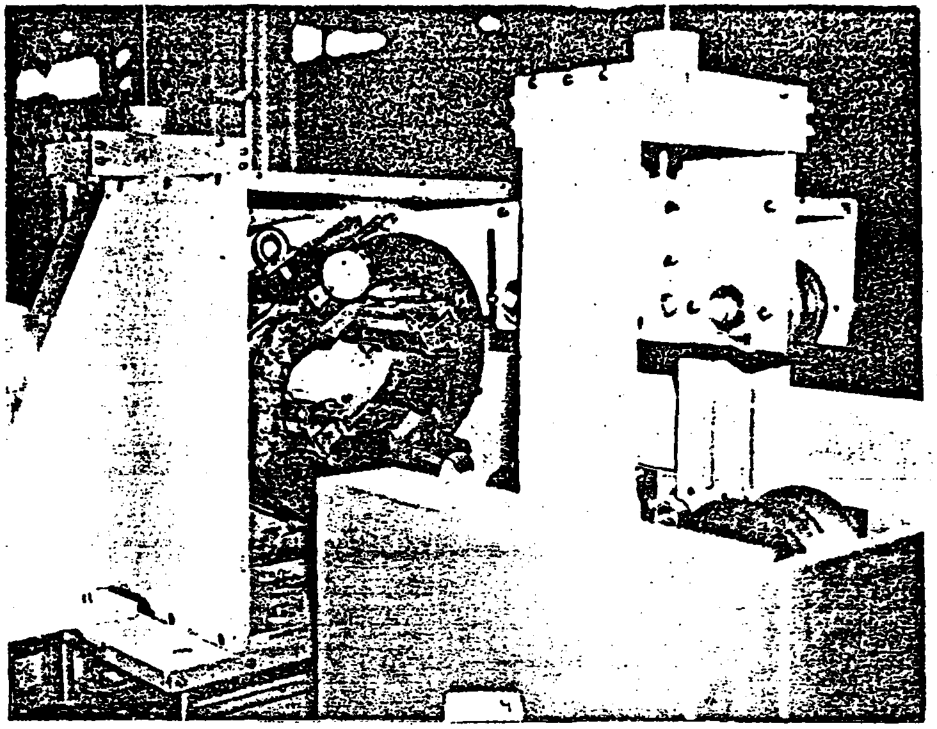

Closeup view of steel tubing passing through rotating magnet and probe assembly.

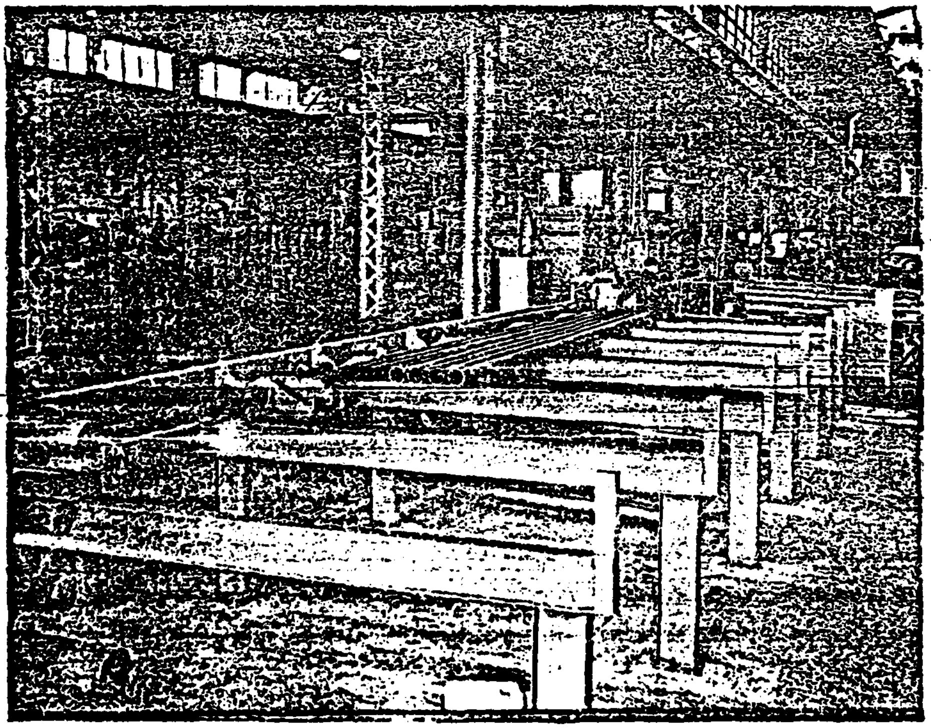

Large wall tubing being tested at steel mill by MAC's new ROTOFLUX.

Appendix IV

DISPOSITION FORM

For use of this form, see AR 340-15, the proponent agency is TAGCEN.

REFERENCE OR OFFICE SYMBOL	SUBJECT
DRDAR-SCM-P	Metallographic Examinations of M42 Grenades Previously Examined by Magnetic Flux Leakage

TO G. Zamoot, PAD-ATSD-IEB
Bldg. 62

FROM J.V. Rinnovatore

DATE 31 Jul 79 CMT 1
JVRinnovatore/md/5751

1. Subject grenades, identified as A, D, E, were delivered to this laboratory by W. Naguszewski for metallographic examination of areas suspected of containing cracks.

2. Cracks on the order of 40% depth were found in the unembossed suspect sections of grenades A and E. Cracks were also found in grenade D but these were in the embossed section which is known to contain cracks. The resulting micrographs are inclosed in Figures 1, 2, and 3.

3. If any additional information is required please contact J.V. Rinnovatore, ext. 5813.

J.V. Rinnovatore

J.V. Rinnovatore

1 Incl
as

DA FORM 1 FEB 62 2496 REPLACES DD FORM 96, WHICH IS OBSOLETE.

...TION FORM

DRDAR-SCM-P

Metallographic Examinations of M42 Grenades Previously Examined by Magnetic Flux Leakage

G. Zamoot, PAD-ATSD-IEB
Bldg. 62

J.V. Rinnovatore

31 Jul 79
JVRinnovatore/md/5751

1. Subject grenades, identified as A, D, E, were delivered to this laboratory by W. Naguszewski for metallographic examination of areas suspected of containing cracks.

2. Cracks on the order of 40% depth were found in the unembossed suspect sections of grenades A and E. Cracks were also found in grenade D but these were in the embossed section which is known to contain cracks. The resulting micrographs are inclosed in Figures 1, 2, and 3.

3. If any additional information is required please contact J.V. Rinnovatore, ext. 5813.

1 Incl
as

J.V. Rinnovatore

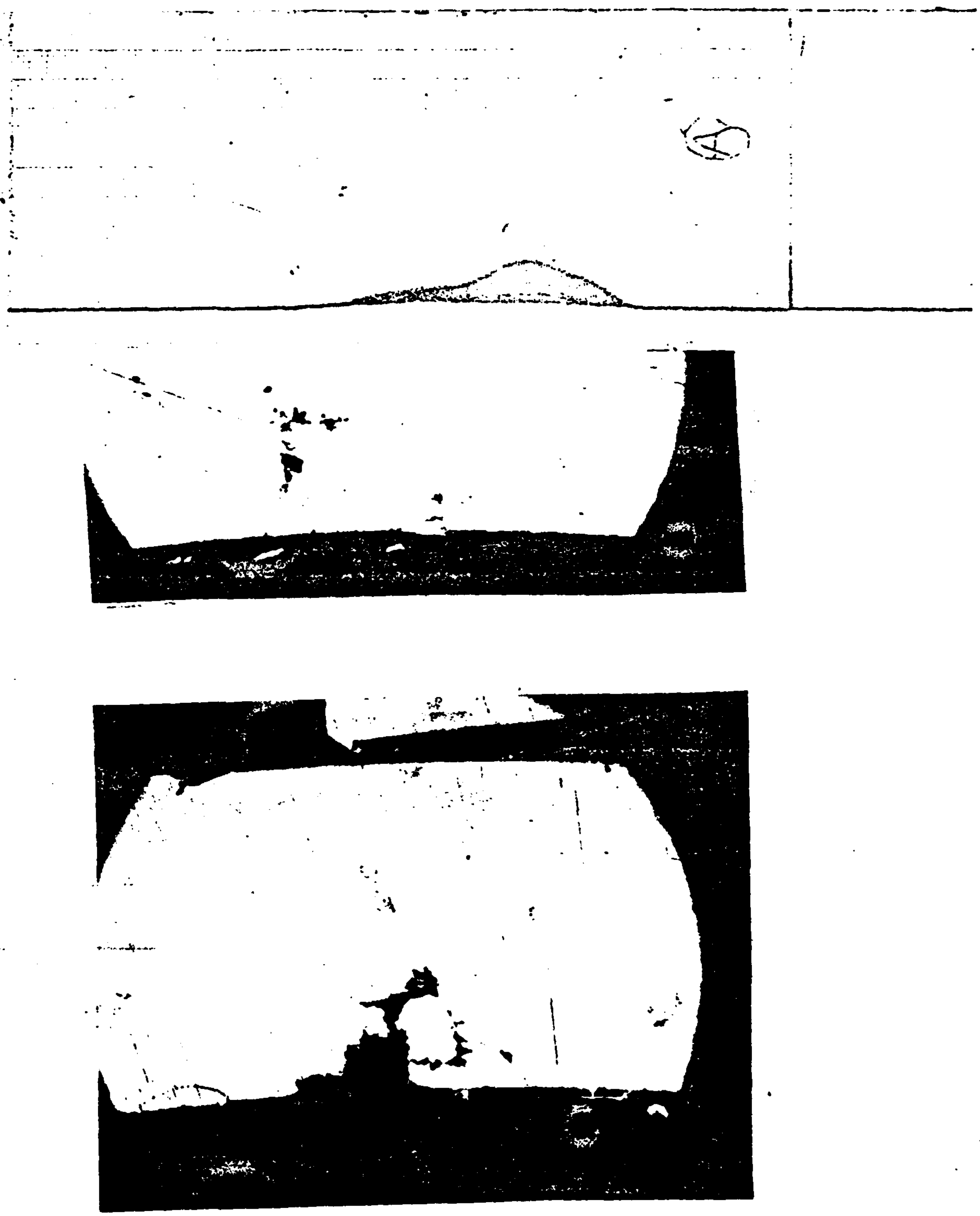

Figure 1. Micrographs of suspect areas of grenade A. Cracking is about 40% thru-the-wall. 25X.

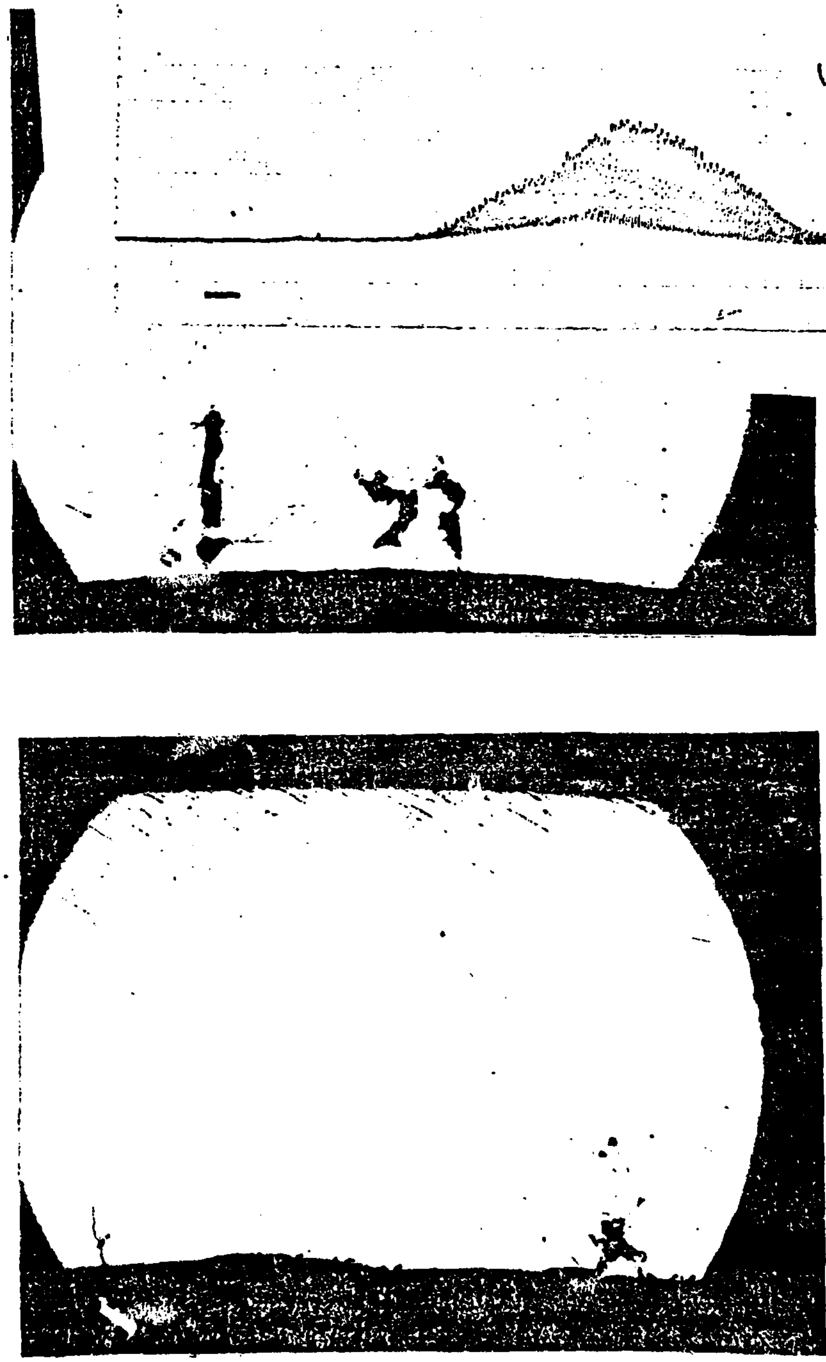

Figure 2. Micrographs of suspect areas of grenade E. Cracking is about 40% thru-the-wall. 25X.

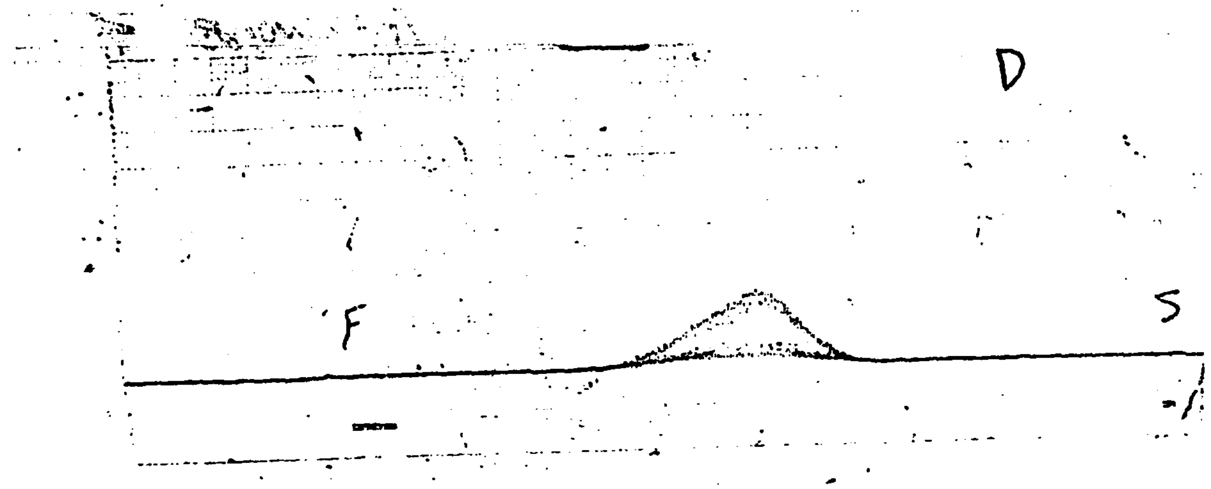

Figure 3. Micrograph of suspect area of grenade D. This is typical of cracking that is normally found in embossed section. 25X.

A

MAGNETIC ANALYSIS CORPORATION	
M-42 GRENADE	TOL. FRAC: ± 1/64 DEC: ± .005 OR OTHERWISE AS SPEC
UNLOADED	
10 % O.D. LONGITUDINAL	
SCALE: 4:1	DATE: 7-9-79
DRAWN: ML	CHECKED:

1 pc

EDM NOTCH O.D.
.250L x .011 D x .005W

WESTERN PROFESSIONAL, INC.
645 9th Street, N.W.
Salem, OR 97304

ACTUAL DIM.
.250L x .010D x .004W

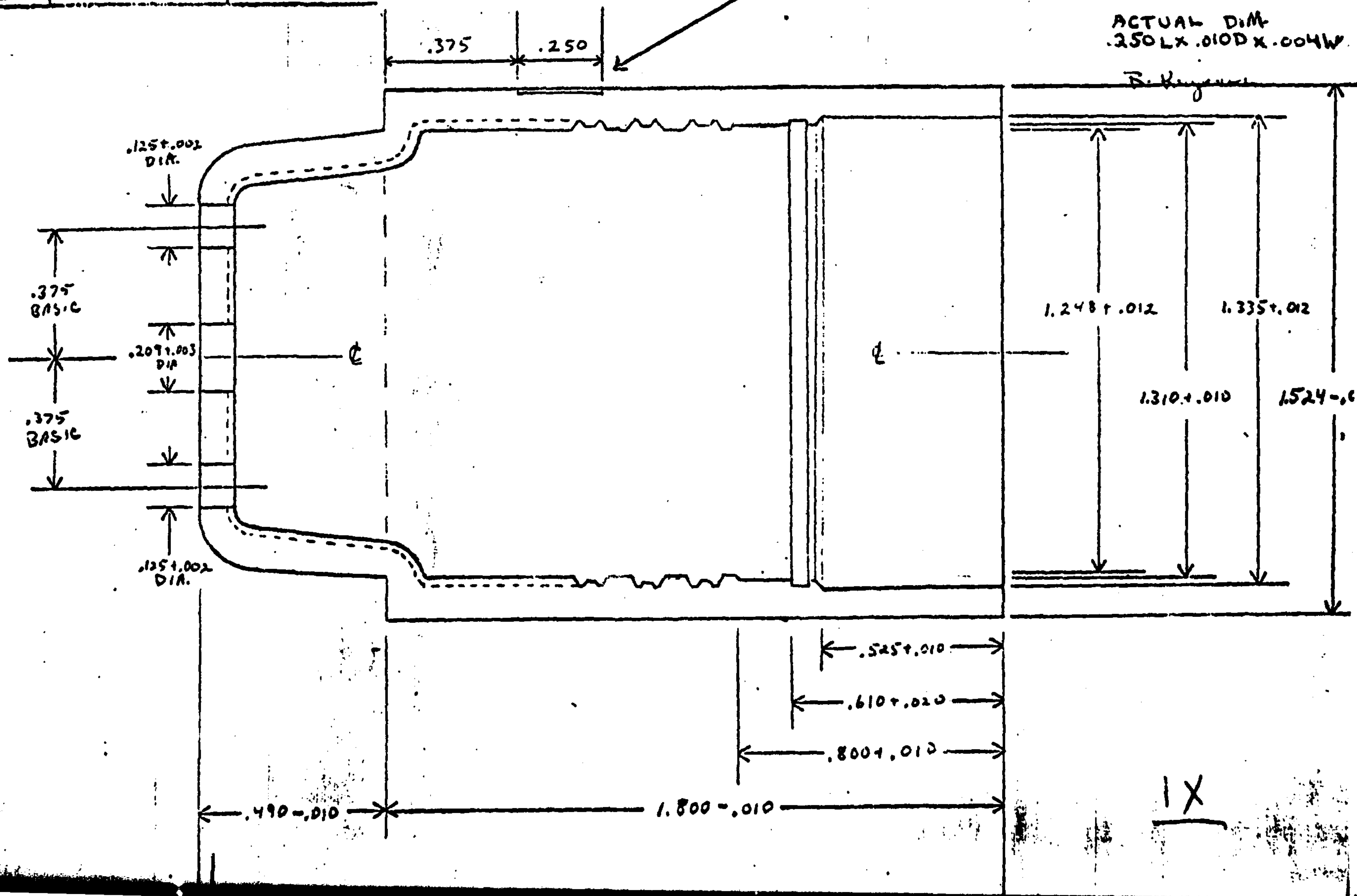

1X

Appendix V

M-42 GRENADE ·		TOL. FRAC: ± 1/64 DEC: ± .005 OR OTHERWISE AS SPEC
UNLOADED		
25% O.D. LONGITUDINAL		
SCALE: ~~[illegible]~~	DATE: 7-9-79	
DRAWN: ML	CHECKED:	

1 pc.

WESTERN PROFESSIONAL, INC.
645 9th Street, N.W.
Salem, OR 97304

ACTUAL DIM.
.250 L X .029 D X .005 W

R. Kingsmith

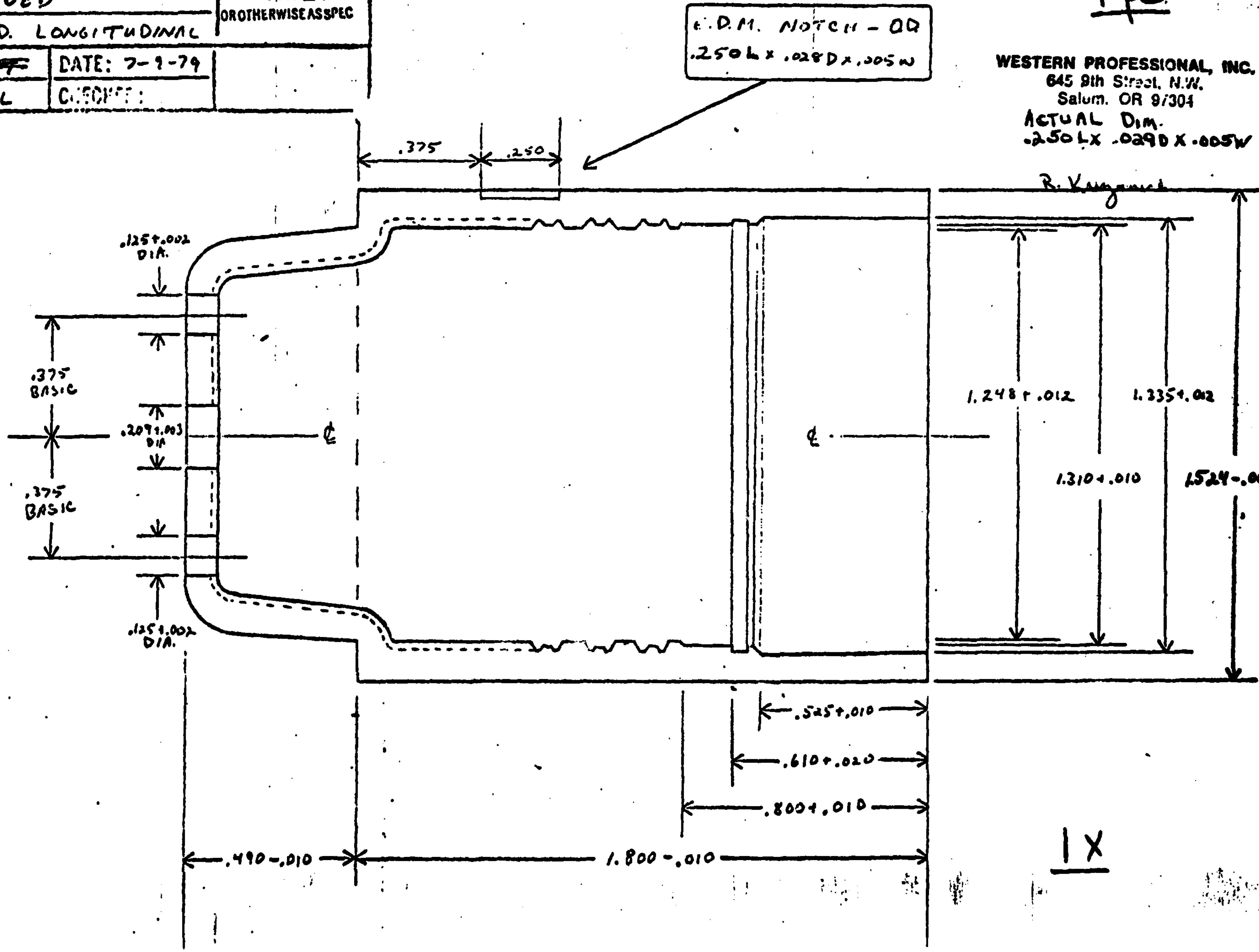

1X

MAGNETI ANALYSIS CORPORATION

M-42 GRENADE UNLOADED 5% ID LONGITUDINAL	TOL. FRAC: ± 1/64 DEC: ± .005 OR OTHERWISE AS SPEC
SCALE: ~~4/7~~	DATE: 7-9-79
DRAWN: ML	CHECKED:

C1 & C2

Req'd 2 pcs

WESTERN PROFESSIONAL, INC
645 9th Street N.W.
Salem, OR 97304

ACTUAL DIM.
C1 .250L x .027D x .005W
C2 .250L x .028D x .005W

R. K

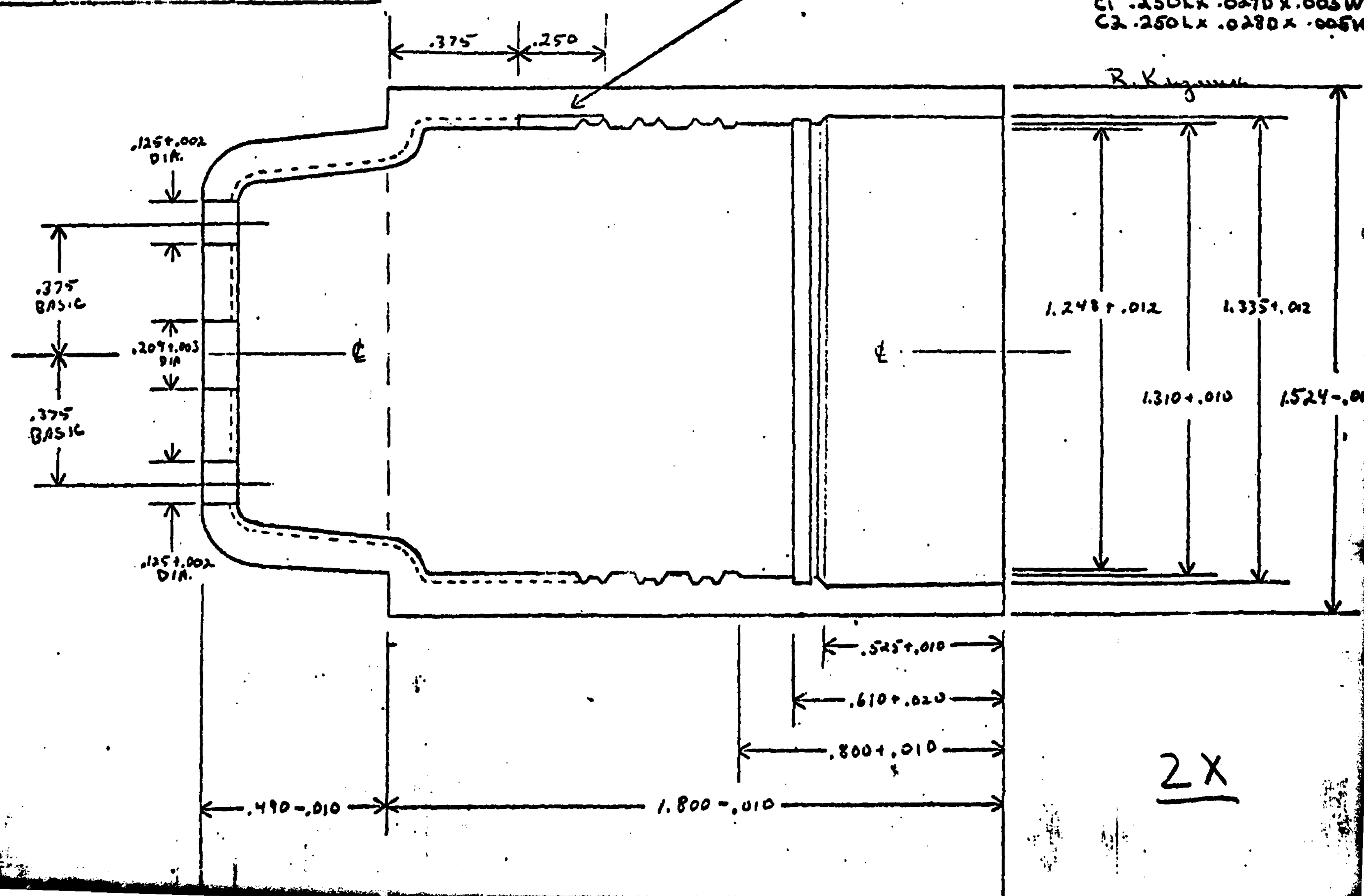

2X

D.

1 pc.

MAGNETIC ANALYSIS CORPORATION	
M-42 GRENADE	TOL. FRAC: ± 1/64 DEC: ± .005 OR OTHERWISE AS SPEC
UNLOADED	
25% OD TRANSVERSE	
SCALE: ~~4/1~~	DATE: 7-9-79
DRAWN: ML	CHECKED:

WESTERN PROFESSIONAL
64.. 9.h Street, N.W.
Salem, OR 97304

ACTUAL DIM.
.250L X .028D X .005

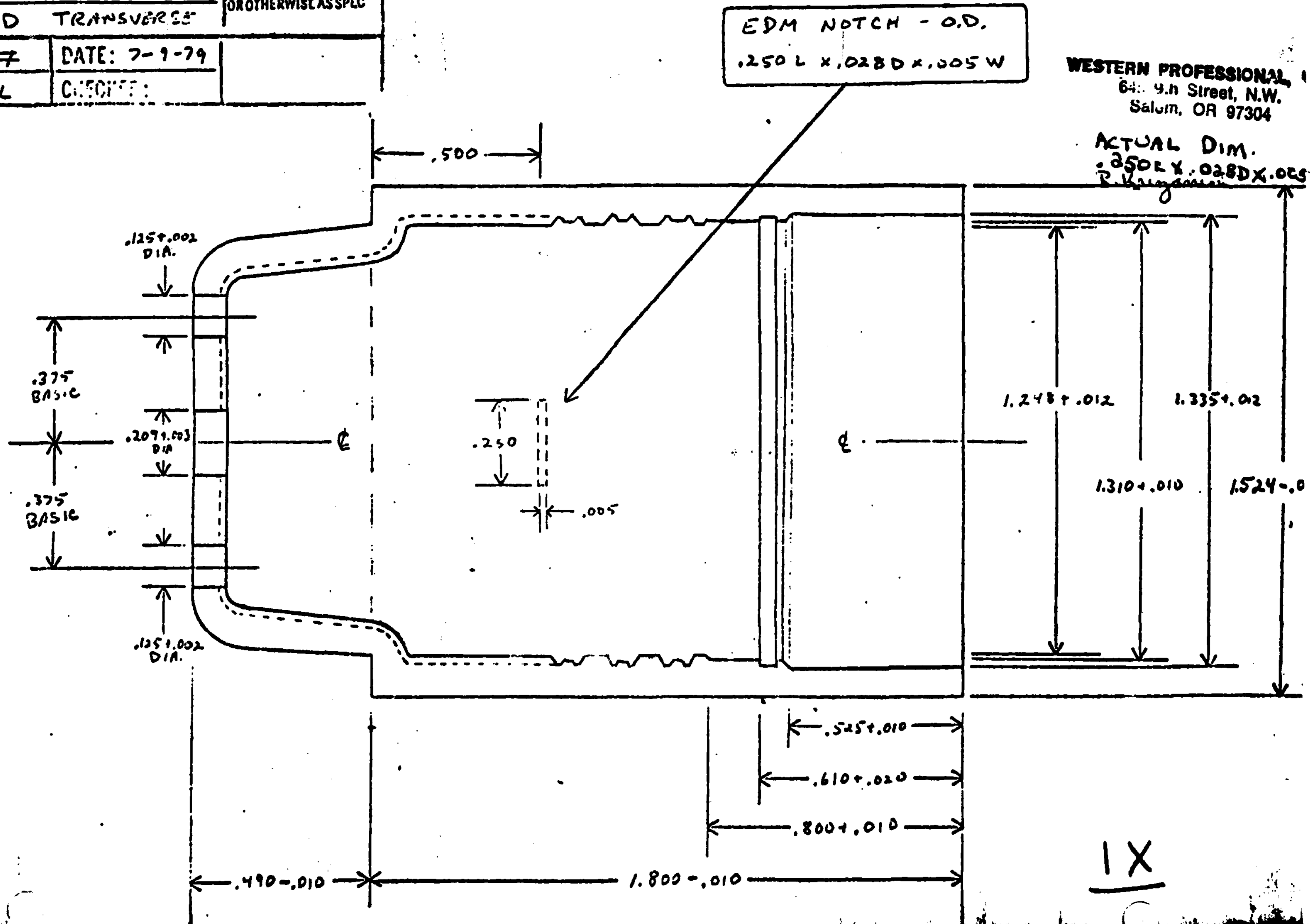

1X

MAGNETIC ANALYSIS CORPORATION	
1-42' GRENADE	TOL. FRAC: ± 1/64
UNLOADED	DEC: ± .005
5% I.D. TRANSVERSE	OR OTHERWISE AS SPEC
SCALE:	DATE: 7-9-79
DRWN: ML	CHECKED:

E1 & E2

2 pcs.

WESTERN PROFESSIONAL, INC.
645 9th Street, N.W.
Salem, OR 97304

ACTUAL DIM.
E1 .250L x .028D x .004W
E2 .250L x .029D x .004W

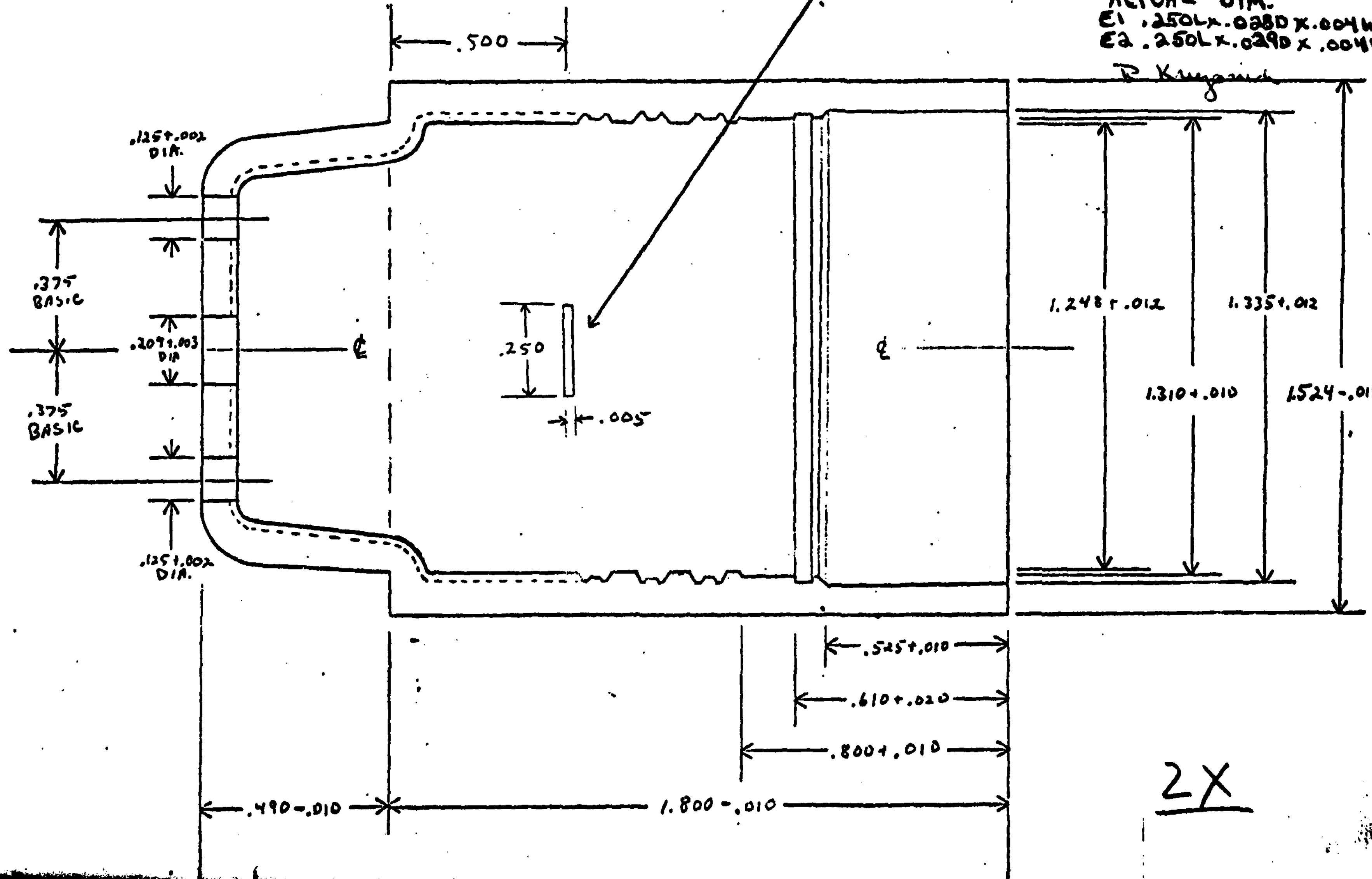

2X

M-42 GRENADE,
UNLOADED
50% O.D. LONGITUDINAL

TOL. FRAC: ± 1/64	DEC: ± 1/16
OR OTHERWISE NOTED	
SCALE: ~~ST~~	DATE: 7-9-79
DRAWN: ML	CHECKED:

1 pc.

EDM NOTCH - OD
.250 L x .056 D x .005 W

WESTERN PROFESSIONAL, INC
645 9th Street, N.W.
Salem, OR 97304

ACTUAL DIM.
.250 L x .054 D x .005 W

R Kuyama

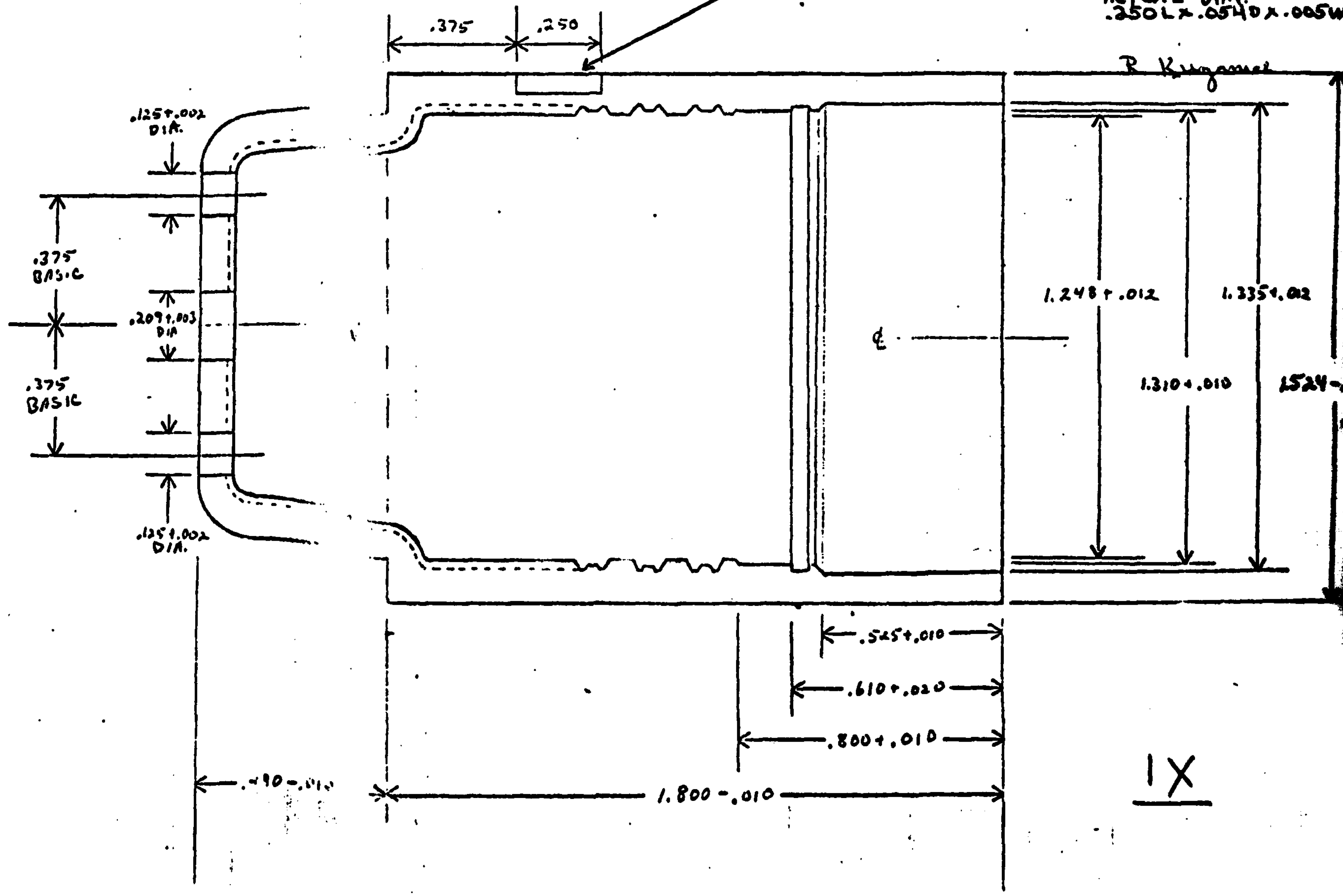

1X

MAGNETIC ANALYSIS CORPORATION

-42 GRENADE	TOL. FRAC: ± 1/64 DEC: ± .005 OR OTHERWISE AS SPEC
UNLOADED	
% ID TRANSVERSE	
SCALE: ~~2:1~~	DATE: 7-9-79
DWN: ML	CHECKED:

G1 & G2

2 pcs.

EDM NOTCH, - I D
.250 L x .05 D x .005 W

WESTERN PROFESSIONAL INC
645 9th Street. N.W.
Salem, OR 97304

ACTUAL DIM.
G1 .250L x .055D x .004W
G2 .250L x .058D x .004W

R. K...

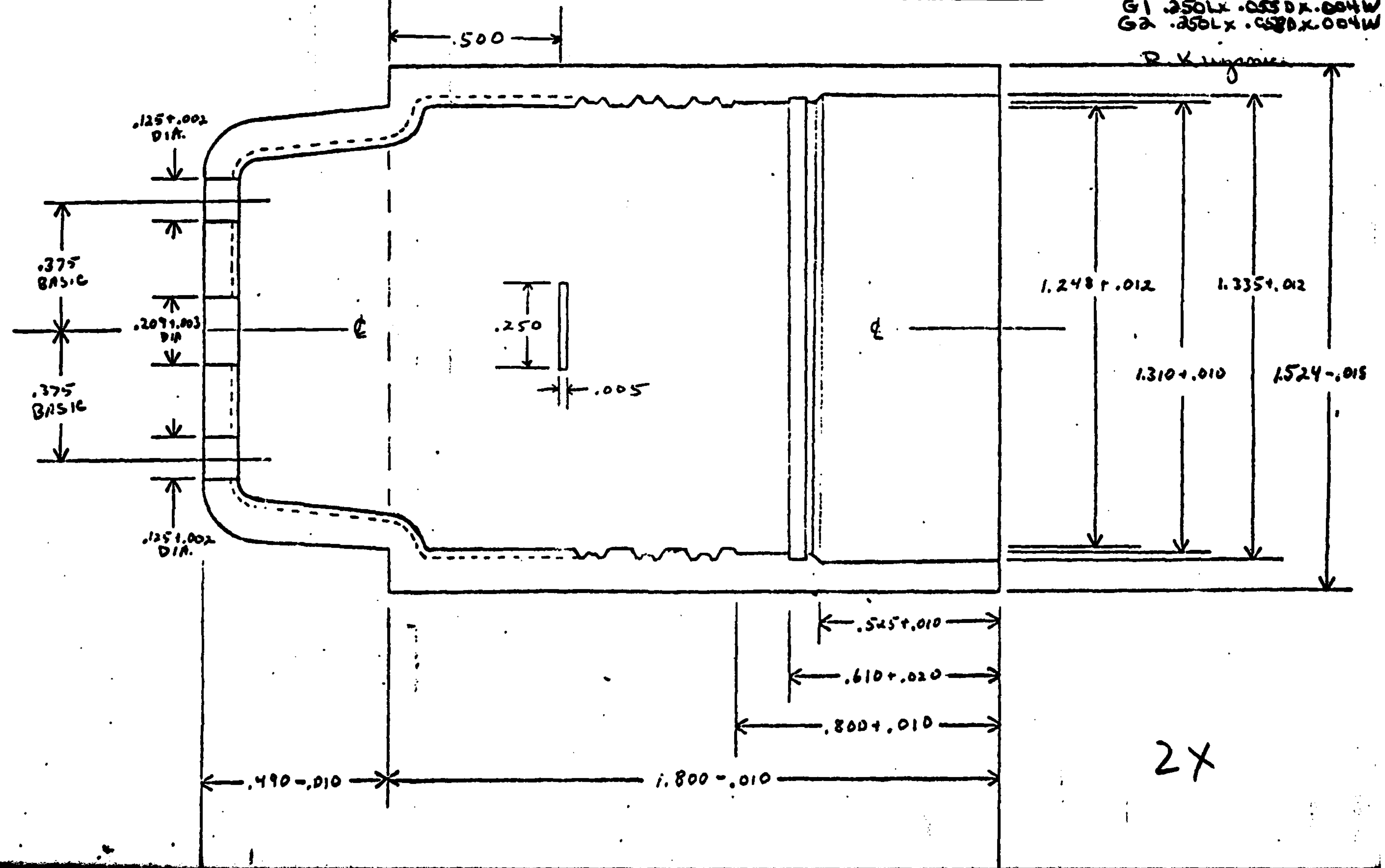

2X

MAGNETIC ANALYSIS CORPORATION

M-42 GRENADE	TOL. FRAC: ± 1/64 DEC: ± .005 OR OTHERWISE AS SPEC
UNLOADED	
5% OD LONGITUDINAL	
SCALE: ~~SAT~~	DATE: 7-9-79
DRAWN: ML	CHECKED:

1 pc.

WESTERN PROFESSIONAL, INC.
645 9th Street, N.W.
Salem, OR 97304

ACTUAL DIM.
.250L x .029D x .004W

R. Kruzynski

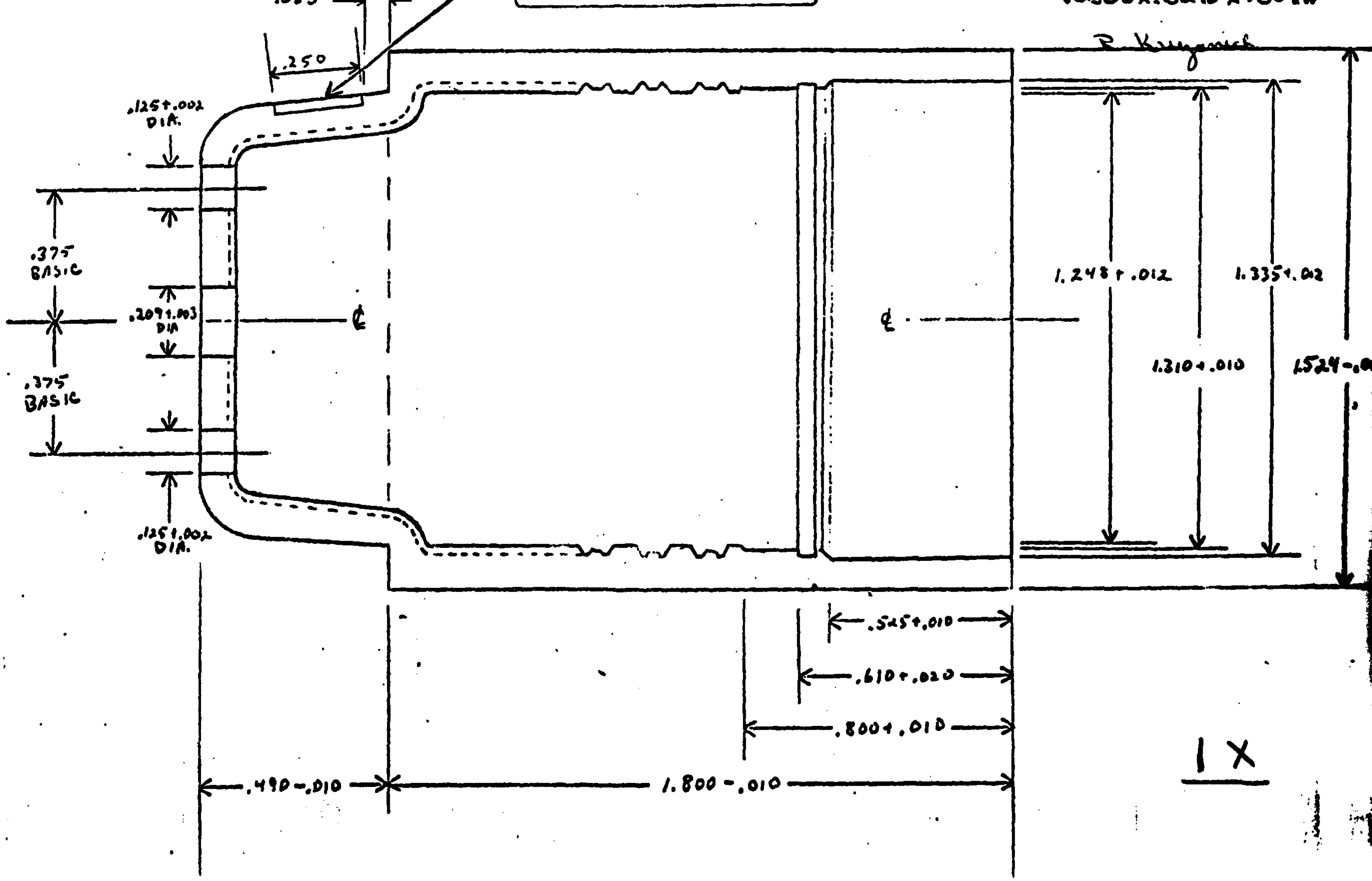

I1 & I2

2 pcs.

1-42 GRI DE	TOL. FRAC: ± 1/64 DEC: ± .005 OR OTHERWISE AS SPEC
ANL ON DED	
5% ID LONGITUDINAL	
LE:	DATE: 7-9-79
DWN: ML	CHECKED:

WESTERN PROFESSIONAL, INC.
645 9th Street, N.W.
Salem, OR 97304

ACTUAL DIM.
I1 .250L x .028D x .005W
I2 .250L x .028D x .004W

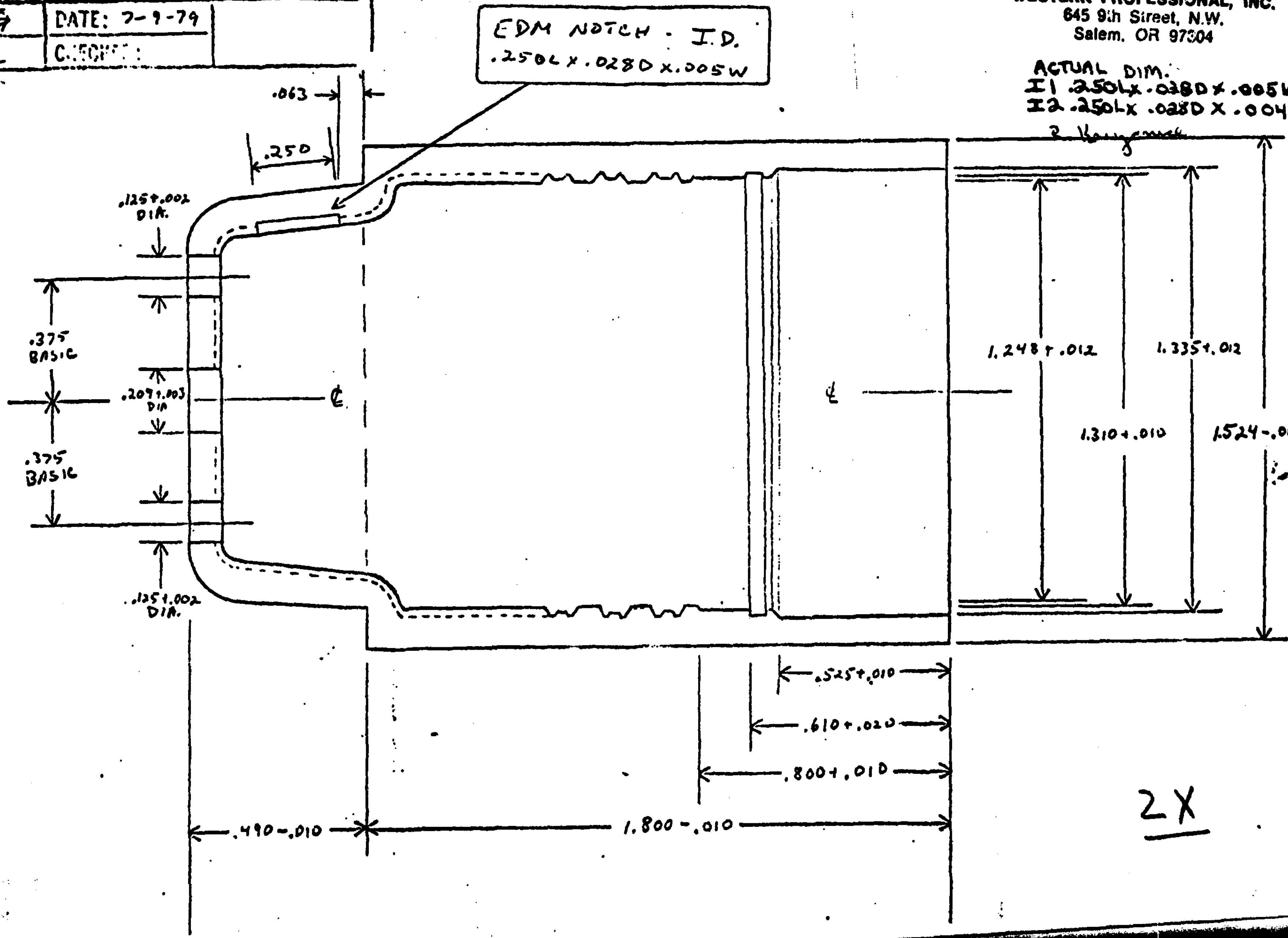

2X

MAGNETIC ANALYSIS CORPORATION

M-42 GRENADE UNLOADED 5% OD TRANSVERSE		TOL. FRAC: ± 1/64 DEC: ± .005 OR OTHERWISE AS SPEC
SCALE: ~~1x1~~	DATE: 7-9-79	
DRAWN: ML	CHECKED:	

1 pc

WESTERN PROFESSIONAL, INC.
645 9th Street, N.W.
Salem, OR 97304

ACTUAL DIM.
.250L x .029D x .004W

R. Kruzemics

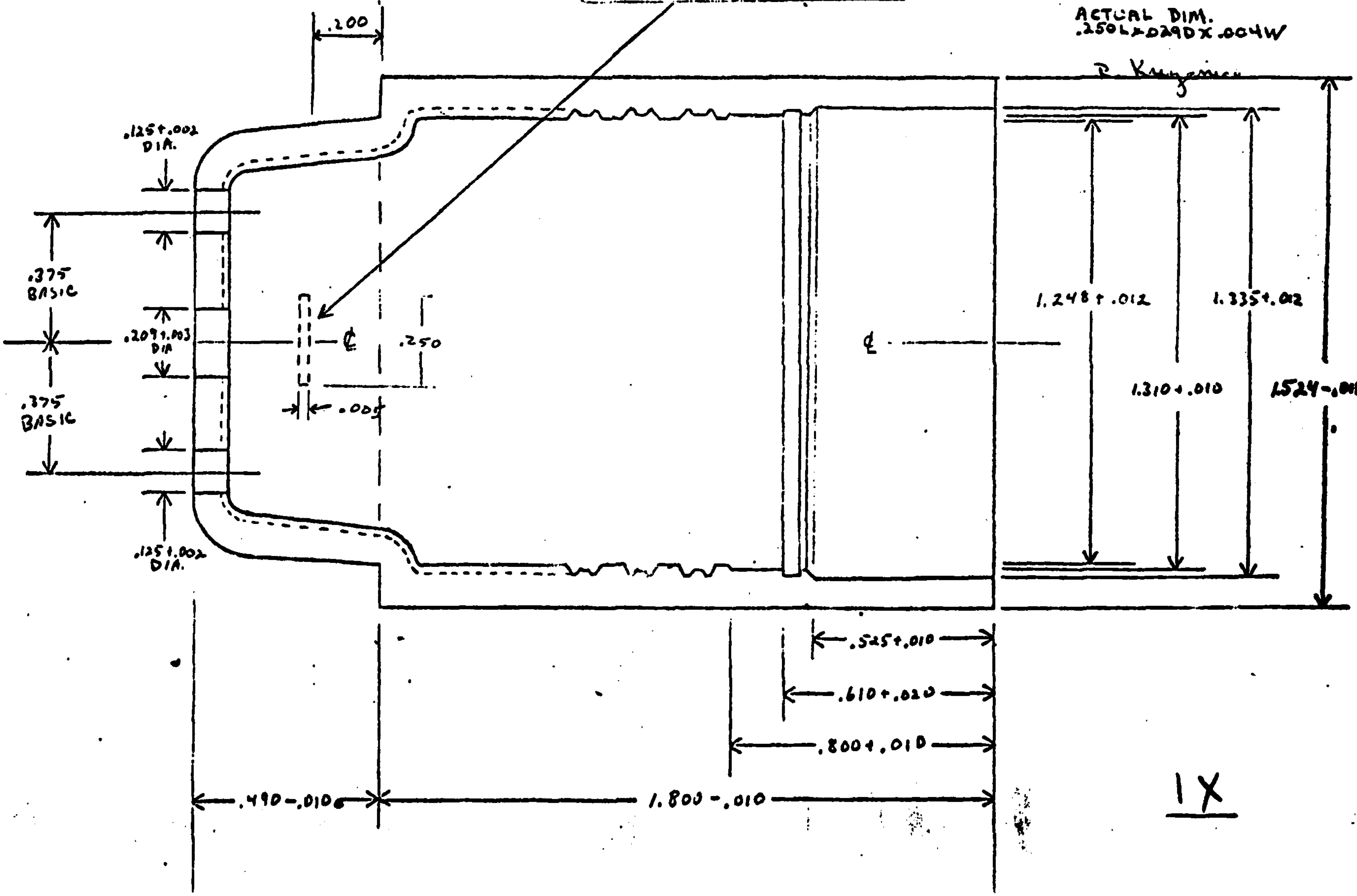

1X

KINETIC ANALYSIS CORPORATION

M-42 GRENADE	TOL. FRAC: ± 1/64
UNLOADED	DEC: ± .005
5% ID TRANSVERSE	OR OTHERWISE AS SPEC
SCALE: ~~4/1~~	DATE: 7-9-79
DRAWN: ML	CHECKED:

K1 & K2

2 PCS.

WESTERN PROFESSIONAL, INC.
645 9th Street, N.W.
Salem, OR 97304

ACTUAL DIM.
K1 .250L x .027D x .004W
K2 .250L x .028D x .004W

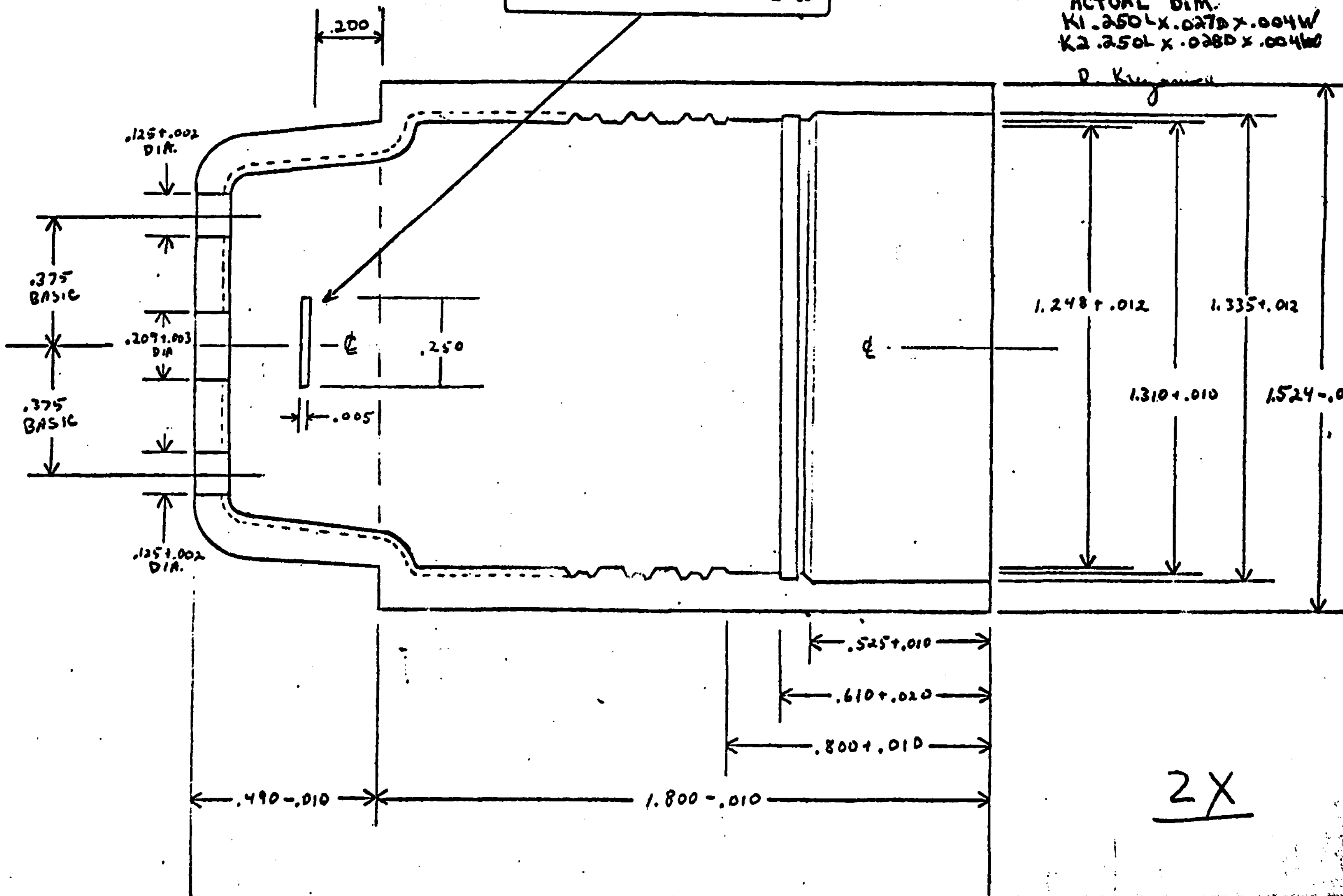

2X

XM-42 GRENADE		TOL FRAC: ± 1/64 DEC: ± .005 OR OTHERWISE AS SPEC
UNLOADED		
.020" hole		
SCALE 4:1	DATE 7-9-79	
DRAWN ML	CHECKED	

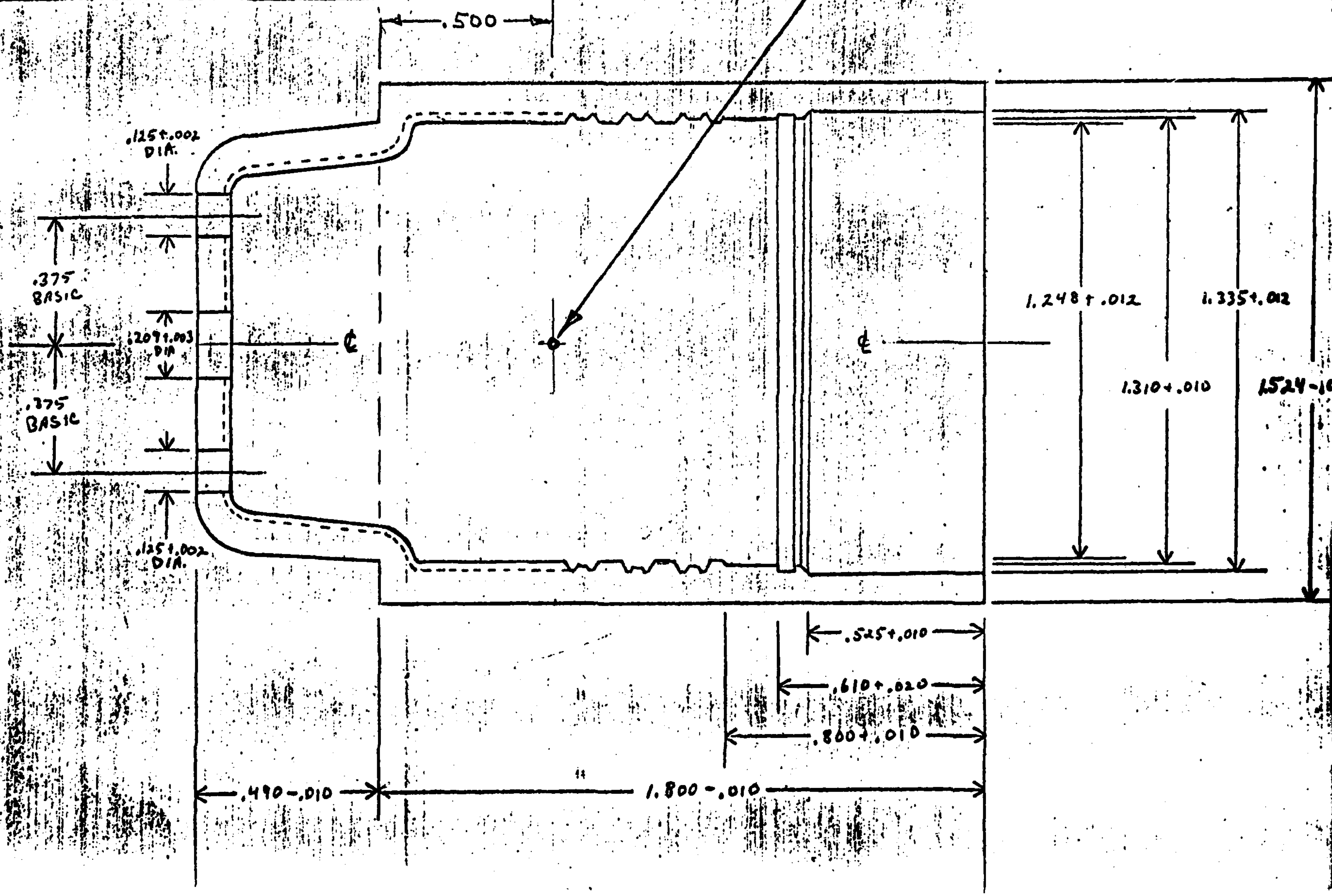

AD-A079 864 MAGNETIC ANALYSIS CORP MOUNT VERNON NY F/G 19/1
FEASIBILITY STUDY ON THE USE OF LEAKAGE FLUX NDT METHODS FOR AU--ETC(U)
1979 E SPIERER, D BUGDEN, M LUPERO

UNCLASSIFIED NL

2 OF 2
AD A079864

END
DATE
FILMED
2 — 80
DDC

MAGI[illegible]C ANALYSIS CORPORATION

M-42 - GRENADE	TOL. FRAC: ± 1/64 DEC: ± .005 OR OTHERWISE AS SPEC
UNLOADED	
.031" hole	
SCALE: [illegible]	DATE: 7-9-79
DRAWN: ML	CHECKED:

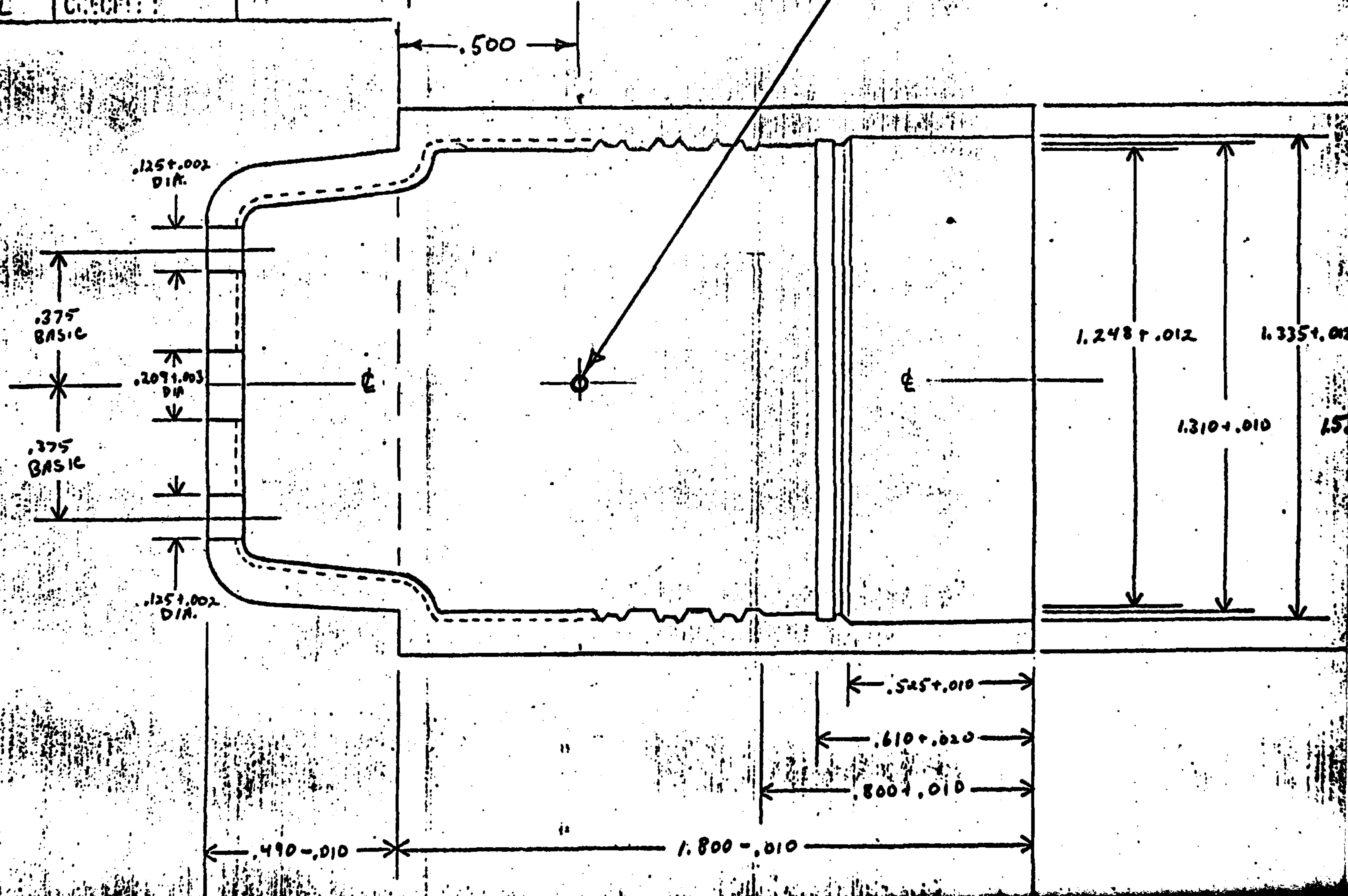

M-42 GRENADE	TOL. FRAC: ± 1/64 DEC: ± .005 OR OTHERWISE AS SPEC

SCALE: 4:1	DATE: 7-1-79	
DRAWN: ML	CHECKED:	

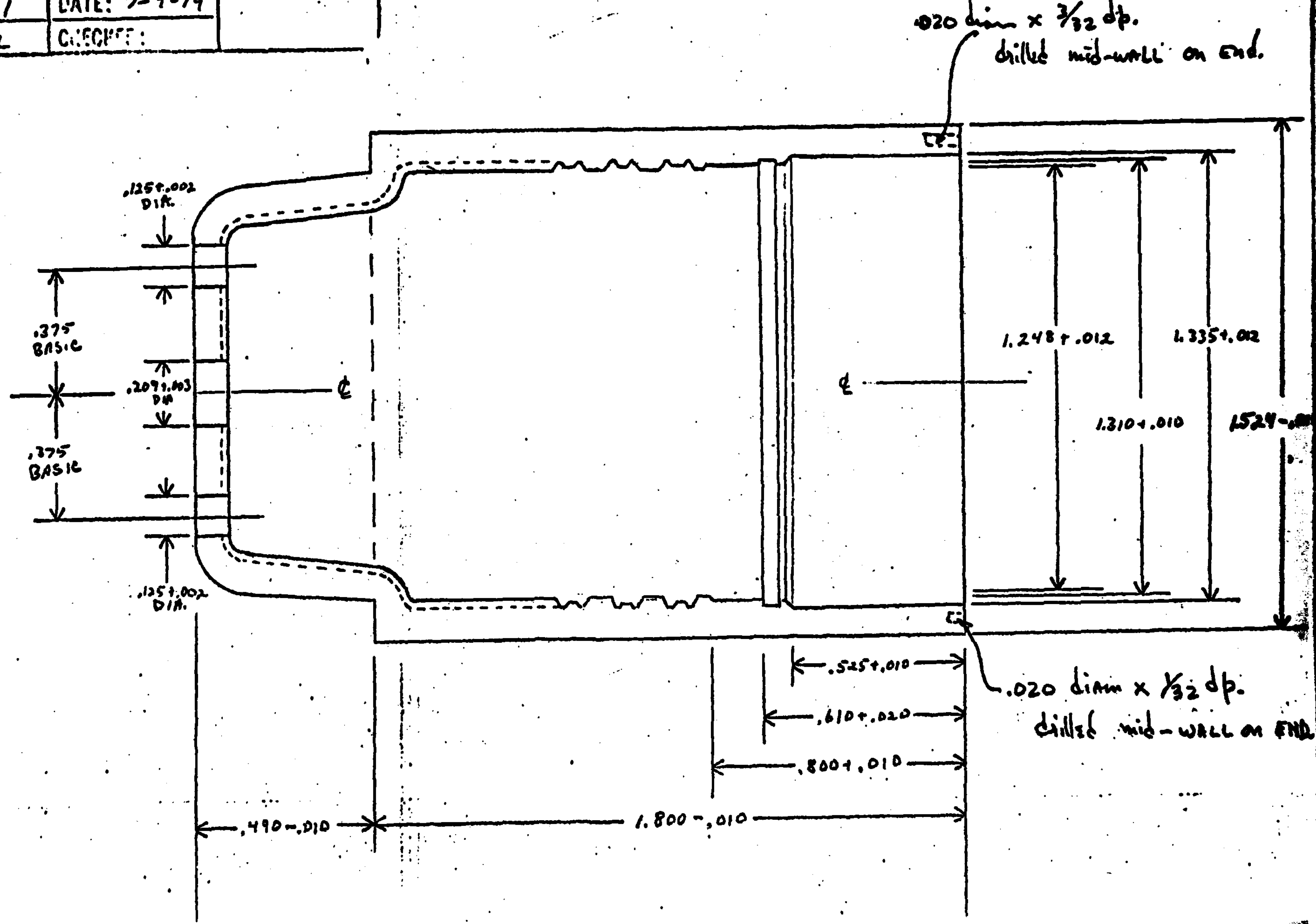

MAGNET ANALYSIS CORPORATION	
M-42 GRENADE	TOL. FRAC: ± 1/64 DEC: ± .005 OR OTHERWISE AS SPEC
SCALE: 4:1	DATE: 8-24-79
DRAWN: ML	CHECKED:

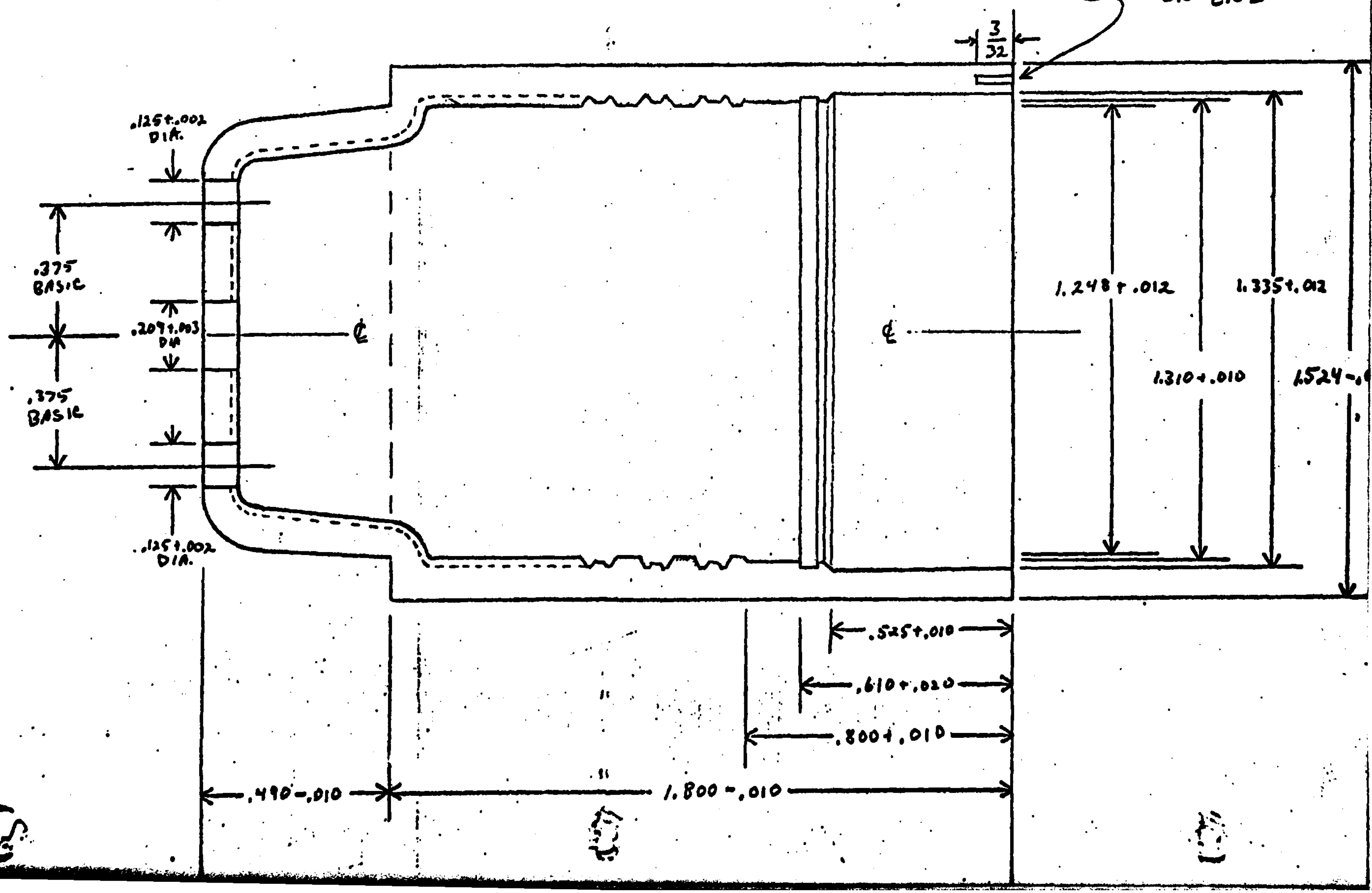

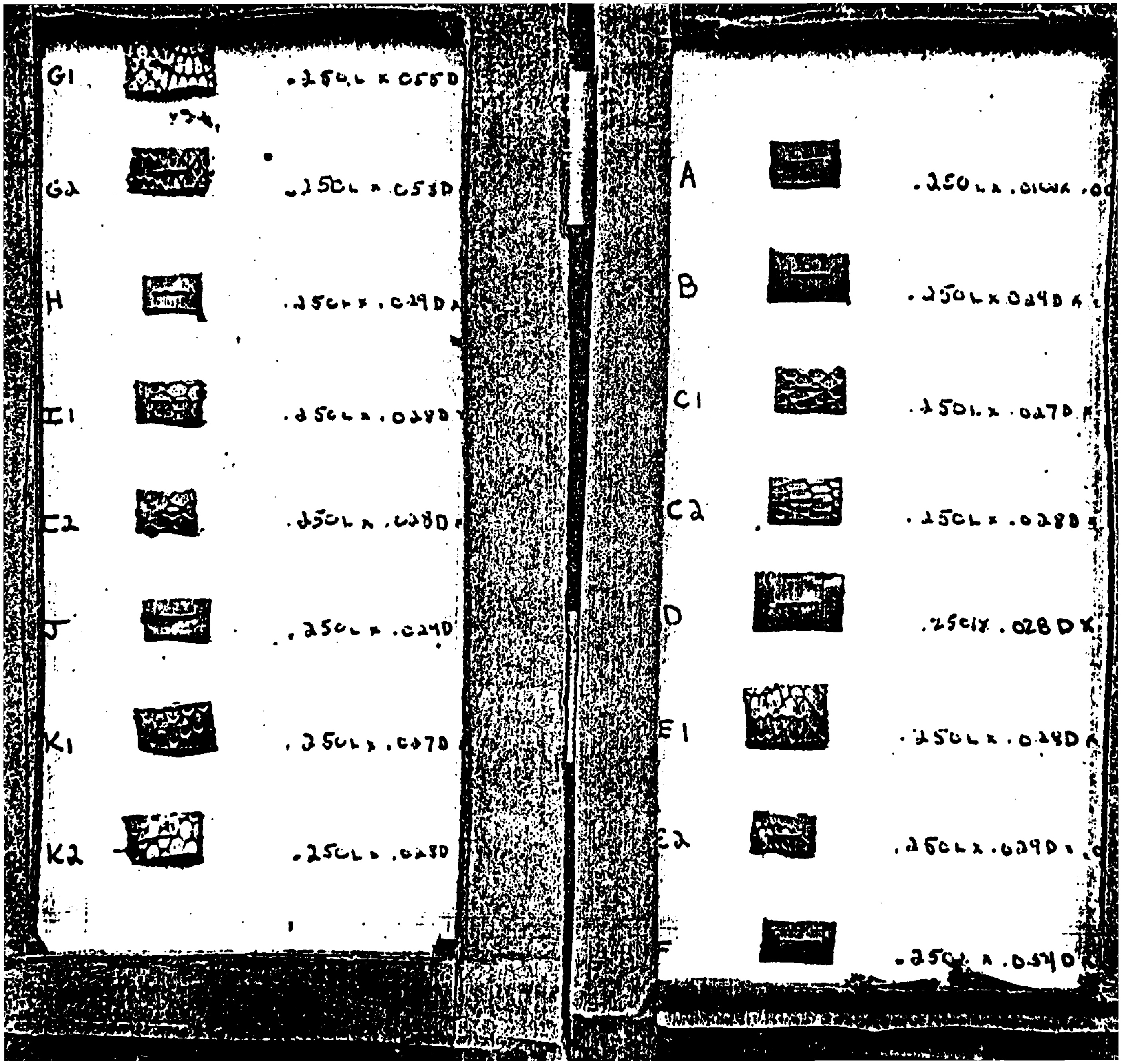
G1
.250L x .055D
G2
.250L x .053D
H
.250L x .029D
I1
.250L x .029D
I2
.250L x .028D
J
.250L x .029D
K1
.250L x .027D
K2
.250L x .028D
A
.250L x .016W
B
.250L x .029D
C1
.250L x .027D
C2
.250L x .028D
D
.250L x .028D
E1
.250L x .028D
E2
.250L x .029D
.250L x .029D